NEUTRONS FOR SCIENCE

ANNUAL REPORT

Institut Laue-Langevin

2015

The world's leading facility in neutron science and technology.

ANNUAL REPORT

Institut Laue-Langevin

2015

PUBLISHING INFORMATION

Editors:
Giovanna Cicognani and Helmut Schober

Production team:
Giovanna Cicognani, Virginie Guérard, Alison Mader, Robert Corner and Susan Tinniswood

Design:
Morton Ward Limited

Photography:
ILL (unless otherwise specified)

Further copies can be obtained from:
Institut Laue-Langevin
Communication Unit
CS 20156, F-38042 Grenoble Cedex 9

communication@ill.eu
www.ill.eu

CONTENTS

DIRECTOR'S FOREWORD

It is absolutely clear to me that Europe's scientific community needs the ILL's unsurpassed reactor source and instruments.

A slight modification of the old English proverb *March comes in like a lion and goes out like a lamb* nicely sums up 2015 for the ILL. The year started dramatically, with a proposal in January by the AREVA-CERCA company for huge price increases in fuel elements; the monopoly position of this company reinforced the gravity of the situation for the future operation of the ILL. However, following difficult negotiations we embark on 2016 with a contract signed for a small number of fuel elements sufficient for operation until 2017, and encouraging progress towards a longer term, more comprehensive contract. In general, after two years that have been challenging as far as finance has been concerned, the new year of 2016 promises to be somewhat calmer on the budget front. The costs of the post-Fukushima reinforcement programme are being absorbed in the long term financial plan of the institute, the Steering Committee has agreed to a budget increase of 2 % compared to that of 2015, and, most significantly, we have been given the go-ahead for the essential Endurance modernisation programme.

In the following pages of this report you will find many examples of the excellent scientific investigations carried out by the ILL's user community and in-house scientists. For the spring 2015 round, the ILL received just over 600 proposals, in line with the average over the last few years. Of these almost 400 were accepted for beamtime by the Subcommittees, again in line with usual levels. To avoid a large backlog of accepted experiments arising from the long shut-down of 2014-2015, Management decided to take the unusual step of cancelling the autumn proposal round. Normal business will be resumed with the spring round of 2016. To date, notification has been received by the library of some 557 publications on work at the ILL during 2015. It is interesting to note that over the last ten years the number of recorded "ILL publications" has remained more or less constant, lying between 500 and 600, while the number of cycles has varied. I acknowledge gratefully the efforts of the ILL's user community, whose publications are the principal product of the ILL.

On the reactor operation side, this was a relatively routine year albeit with some particular features. After the winter shutdown, the reactor was started as planned in April. Unfortunately this cycle was terminated mid-May due to a fault in the cooling circuit of the control rod. The second cycle ran as scheduled, with all available instruments participating in the external user programme. The third cycle of the year was short (two weeks, to "burn up" a partially used element), followed by a full cycle terminating mid-December; I believe that this was the first 60-day cycle (operated at 42 MW) in the ILL's history. After the Xenon "poisoning" period, lasting about 48 hours, the reactor was restarted and ran at nominal power for more than a day and a half; this additional time can be used for future internal experimental work on the instruments, and for commissioning and testing.

The Millennium Programme is coming to an end, with the commissioning of the majority of the instruments in guide hall ILL22 now completed. Work on the last Millennium project, the wide-angle spin-echo spectrometer WASP, has continued with the completion of the civil engineering design and realisation; a very large hole in the guide hall ILL22 is now equipped with its a-magnetic, reinforced-concrete infrastructure to host the spectrometer.

At the December 2015 Steering Committee meeting our Associates gave us the authorisation to initiate the first phase (2016-2019) of the Endurance modernisation programme, which is designed to open up new avenues of science in the directions of smaller samples, weaker signals, and higher resolution or faster kinetic processes. New capabilities for currently emerging scientific areas will be complemented by techniques that have not yet been fully developed within the Millennium Programme. The first new science is planned for delivery in 2018.

In the context of advanced preparations for Endurance, representatives of the Scientific Members met in June to discuss their future involvement with the ILL. Among the issues discussed was their longer term commitment to the ILL and the ILL's central role in preparing the scientific community for the European Spallation Source over the next ten years. Representatives of the Scientific Members expressed their clear intention to continue their partnerships with the ILL beyond 2018 on a similar financial basis to that currently in place.

As advanced medical technologies become increasingly important world-wide, there is an ever-increasing demand for high quality radioisotopes, used in various types of cancer therapies. Due to the exceptionally high neutron flux, the ILL's reactor is capable of producing high specific activity radioisotopes. A funding proposal (to the French *Banque Publique d'Investissement*) has been successful and so the ILL can now construct and operate an automated radiation facility, producing mainly two radioisotopes, Tungsten-188 and Lutetium-177. The first of these is for use in the treatment of liver cancer and therapies for gliomas and skin cancers, while several ^{177}Lu products are already in clinical use or in clinical studies, for example in the treatment of neuroendocrine tumours or prostate cancer. I consider this project to be an exciting opportunity for the ILL to contribute to the important societal issue of health while generating income to enhance our scientific programme.

The current isotope pilot programme has produced a bonus in the form of a major contribution to a long-standing question of major fundamental significance, namely the mass of the neutrino. This can be obtained by studying the decay of the (artificial) isotope ^{163}Ho, and independently, the difference in mass between this isotope and its daughter nucleus ^{163}Dy. An international team (German-Russian-Swiss-ILL) is working on this problem using ^{163}Ho produced by irradiation of enriched ^{162}Er in the ILL reactor. This project aims to determine the neutrino mass at the sub-eV level.

A new management team will take over later in 2016, so this is the last introduction I will write at the ILL. I take this opportunity to thank all those who, together, have contributed to the continued success of the ILL. New science and new knowledge resulting from experiments at the ILL are the result of the innovative ideas and careful preparation of our users from around the world, the superb level of service of our scientists and technicians on the instruments and the excellent "back-room boys" of the reactor, the technical services and the administration. The ILL is not just another neutron laboratory – it is special. It grew out of the post-war reconciliation between France and Germany. The shared European vision materialised in the ambitious project to build the world's most advanced laboratory for neutron science, based on an exceptional high-flux reactor. This spirit of excellence in an open international scientific atmosphere is at the heart of the ethos of the ILL. As we know, the UK became the third Associate in 1973 a few years after its establishment in 1967.

The next few years will be testing times for neutron users, as some first-class reactor sources (BER II at HZB and Orphée at LLB) are closed and the ILL's long-term future remains unclear. I have seen and experienced the ILL as a young scientist and instrument responsible, as a user and committee member and, finally, as Director. It is absolutely clear to me that Europe's scientific community needs the ILL's unsurpassed reactor source and instruments, operated with the ILL's special attitude towards service, well into (and beyond) the decade of the 2020s. In the past, on several occasions the ILL's Associates have taken the long-term view in their governance of the ILL: the *Deuxième souffle* in the early '80s, the replacement of the reactor vessel in the '90s, the refit programme at the beginning of this century and the Millennium and Endurance Programmes, all demonstrate the long-term commitment made by the governments of France, Germany and the UK with the support of the Scientific Members. As the date for the renewal of the ILL's Convention (2023) approaches I am confident that our Associates will once again demonstrate the same level of wisdom and confidence in the future of the ILL.

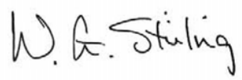

W.G. Stirling
Director of the ILL

About the Institut Laue-Langevin

The Institut Laue-Langevin (the ILL) is an international research centre at the leading edge of neutron science and technology, where neutrons are used to probe the microscopic structure and dynamics of a broad range of materials at molecular, atomic and nuclear level.

The ILL is owned by the three founding countries – France, Germany and the United Kingdom. These three Associate countries contributed a total of about 62 M€ to the institute in 2015, a sum enhanced by significant contributions from the ILL's Scientific Member countries of Austria, Belgium, the Czech Republic, Denmark, Hungary, Italy, Poland, Spain, Slovakia, Sweden and Switzerland. The ILL's overall budget in 2015 amounted to approximately 81 M€.

The Institut Laue-Langevin operates the most intense neutron source in the world, based on a single-element, 58.3 MW nuclear reactor designed for high brightness. The reactor normally functions round-the-clock during four 50-day cycles per year, feeding neutrons to a suite of 40 high-performance instruments that are constantly upgraded.

As a service institute, the ILL makes its facilities and expertise available to visiting scientists. Our user community is world-wide: every year, about 2 000 researchers from close to 40 countries visit the ILL to perform over 800 experiments selected by a scientific review committee. The ILL monitors the papers published as a result of the use of our facilities, of which there are between 550 and 600 per year. We pay particular attention to papers published in high-impact journals. About one quarter of such papers are published per year from data taken on ILL instruments.

The ILL has a Director and two Associate Directors who represent each of the Associate countries and are appointed on short-term contracts, normally for five years. The scientific council, comprising external scientists from the member countries, advises the Directors on scientific priorities for the institute and how to develop the instrument suite and technical infrastructure in order to best meet the needs of the user research programme. It also assesses the scientific output of the institute. Our governing body is the Steering Committee, which meets twice yearly and is made up of representatives of the Associates and the Scientific Members together with the Directors and staff representatives. Within the framework of the Intergovernmental Convention between our Associate countries, the Steering Committee has ultimate responsibility for determining operational and investment strategies for the institute.

NEUTRONS FOR SOCIETY

The scope of the research carried out at the ILL is very broad, embracing condensed matter physics, chemistry, biology, materials and earth sciences, engineering, and nuclear and particle physics. Much of it impacts on many of the challenges facing society today, from sustainable sources of energy, better healthcare and a cleaner environment to new materials for information and computer technology. For example, neutron scattering experiments have given us new insights into the structure and behaviour of biological and soft condensed matter, important in designing better drug delivery systems and for improving polymer processing. They also provide a unique probe into the phenomena that underpin high-temperature superconductivity as well as the molecular magnetism that may provide the technology on which the computers of the future are based.

PREPARING FOR THE FUTURE

In 2001, the ILL launched an ambitious programme to modernise its instruments and infrastructure. Called the ILL Millennium Programme, its aim was to optimise the ILL's instrument suite (Phase M0: 2001-2008; Phase M1: 2008-2014). We are now looking forward to and setting the scene for – in the framework of our Endurance Programme – developments still further into the future, in order to maintain the institute's world-leading position for another 20 years.

Why neutron scattering is useful

When used as a probe for small samples of materials, neutron beams have the power to reveal what is invisible using other radiations. Neutrons can appear to behave as particles, waves or microscopic magnetic dipoles, and it is these specific properties which enable them to uncover information that is often impossible to access using other techniques.

WAVELENGTHS OF TENTHS OF NANOMETERS

Neutrons have wavelengths varying from 0.01 to 100 nanometers. This makes them an ideal probe of atomic and molecular structures ranging from those consisting of single atomic species to complex biopolymers.

ENERGIES OF MILLI-ELECTRONVOLTS

The associated energies of milli-electronvolts are of the same magnitude as the diffusive motions of atoms and molecules in solids and liquids, the coherent waves in single crystals (phonons and magnons) and the vibrational modes in molecules. An energy exchange between the incoming neutron and the sample of between 1 μeV (even 1 neV with spin-echo) and 1 eV can easily be detected.

MICROSCOPICALLY MAGNETIC

Neutrons possess a magnetic dipole moment which makes them sensitive to magnetic fields generated by unpaired electrons in materials. Precise details of the magnetic behaviour of materials at the atomic level can be investigated. In addition, the scattering power of a neutron by an atomic nucleus depends on the orientation of the spin of both the neutron and the atomic nuclei in a sample, thereby providing a powerful tool for detecting the nuclear spin order.

ELECTRICALLY NEUTRAL

Neutrons are electrically neutral and so can penetrate deep into matter while remaining non-destructive. This makes them an ideal probe for studying, for example, biological samples or engineering components under extreme conditions of pressure, temperature or magnetic field, or within chemical-reaction vessels.

HIGH SENSITIVITY AND SELECTIVITY

The scattering power from nucleus to nucleus in a sample varies in a quasi-random manner, even in different isotopes of the same atom. This means that light atoms are visible in the presence of heavy atoms and atoms that are close to one another in the periodic table may be distinguished from each other. This introduces the possibility of using **isotopic substitution** (for example deuterium for hydrogen or one nickel isotope for another) to allow contrast to be varied in certain samples, thereby highlighting specific structural features.

In addition, neutrons are particularly sensitive to hydrogen atoms and therefore they are a powerful probe of hydrogen storage materials, organic molecular materials and biomolecular samples or polymers.

© ARTECHNIQUE

SCIENTIFIC HIGHLIGHTS

The scientific highlights presented in this year's annual report demonstrate how research with neutrons continues to push back the frontiers of science.

One of the defining features of complex systems is that they display an enormous number of intricate dependencies. In such systems, it is far from easy to identify the dominant driving forces, and no more so than when dealing with human societies. If we are to believe mainstream opinion, it is the political and economic actors who occupy centre stage. Science is granted the secondary, albeit noble, role of providing support in the form of knowledge necessary for maintaining competitiveness. This popular view ignores two important facts. Firstly, scientific method has permeated all corners of our societies and thus directly influences all aspects of our lives. Secondly, it is scientific progress which shapes (in part, at least) the course of our cultural development and not the opposite. Science can no longer be relegated to the role of providing a means to satisfy human aspirations. By instilling into our cultures the belief in unlimited access to knowledge, and hence the thirst for discovery and invention, it is science which creates these aspirations in the first place. If not yet recognised as occupying centre stage, science must surely be considered the *"Éminence Grise"* of societal evolution.

By providing unique tools for investigating materials at the atomic level, the ILL is at the heart of scientific endeavour. 2015 was a particularly prolific year for the institute, producing a plethora of outstanding results, as I hope you will see from the selection of highlights presented in this year's report.

In the section on materials science, for example, you will read about the discovery of a new phase of ice. This phase, which happens to be the least dense of all ice forms, was obtained from a neon clathrate by pumping at temperatures close to the point of instability. This allowed the neon atoms to be extracted while leaving behind a scaffold of empty cages. Depending on how we look at them, clathrates in the form of methane clathrates can be considered as either a blessing or a curse for humanity. While they constitute an immense but equally fragile fossil fuel reserve, they could also lead to ecological disasters if released in an uncontrolled way. The experimental proof of the existence of empty clathrates is important for predicting the stability of clathrate systems and, as such, has a direct impact on questions related to energy and the climate.

In the section on magnetism, you will find several articles demonstrating how polarised neutron scattering, with its high information content, gives insight into the fascinating world of electronic correlations. In one example, it was possible to determine correlations of tiny magnetic moments in high-temperature superconductors that may originate from current loops on the nanometer scale. In another example, polarised neutrons were used in conjunction with Reverse Monte Carlo modelling to unveil the origin of a hitherto "hidden" phase transition. The order responsible for the transition emerges at the level of spin clusters and can be described by "spin directors", a concept well known from liquid crystals.

I will leave it you to discover more about these and all the other fascinating examples of research that has been carried out recently at the ILL. These highlights are a testimony not only to the excellence of the ILL's instrumentation but also to the vitality of its user community. I am convinced that they contribute their share of momentum to moving science to the centre of public attention. I hope that you enjoy reading about them as much as I have done.

These highlights are a testimony not only to the excellence of the ILL's instrumentation but also to the vitality of its user community.

Helmut Schober
Associate Director

SCIENTIFIC HIGHLIGHTS

COLLEGE INTRODUCTIONS

COLLEGE 1 – APPLIED METALLURGY, INSTRUMENTATION AND TECHNIQUES

A. Stunault (College 1 Secretary)

The activities of College 1 are extremely varied and have a clear applied focus. About half of the proposals submitted concern very practical problems in the field of metallurgy, which are investigated primarily by strain scanning or texture analysis using the SALSA instrument. This is very nicely illustrated in the work described on p.22, where the strain imaging on SALSA was used most effectively to study aluminium casting. This also demonstrates how metallurgy has progressed far beyond trial and error, as models have now been developed and can be efficiently tested by performing neutron experiments on strain scanners such as SALSA.

Other applications cover a wide variety of fields and instruments, although a number of proposals are obviously on the borderline with other colleges, such as studies on dental cements using powder diffraction (p.16) or back scattering (p.18).

College 1 noted an increasing number of proposals related to solar cells, a topic shared with Colleges 5A and 9 (p.26). Such studies make wide use of neutron reflectometry and grazing-incidence small-angle neutron scattering. Our College also hosted a small number (about 10 %) of cultural heritage-related experiments aimed at studying the structures of archaeological artefacts.

Finally, about 25 % of the proposals submitted to College 1 were related to developments in neutron instrumentation and techniques, particularly concerning the use of polarised neutrons: separation of the coherent and spin-incoherent scattering contributions in hydrogenous liquids (p.50) and developments in 3-dimensional polarisation analysis on time-of-flight instruments (PASTIS project) or under high pressure (D7).

COLLEGE 2 – THEORY

M.B. LePetit (ILL Theory Group)

In 2015, the ILL Theory College saw its first PhD student graduate since the reorganisation of the College three years ago. Samuel Hanot, now a post doctoral researcher at the Institut Pasteur in Paris, successfully defended a PhD in soft matter on molecular dynamics modelling of ionic surfactants in explicit aqueous solutions. He specifically focused on the influence of the water content on morphological aspects and dynamical features. A unique framework rationalising the existence of dynamical heterogeneities in fluids, adsorbed in soft confining environments was provided. The different structures, found theoretically, were characterised in terms of diffraction patterns and neutron scattering structure factors. They were successfully compared to experimental quasi-elastic neutron scattering (QENS) data measured at the ILL.

The ILL Theory College has a strong tradition of hosting visiting scientists for a few months. This year we were delighted to host Pavel Grigoriev from the Landau Institute, Konstantin Kikoin from Tel Aviv University, and Mariya Gvozdikova and Ghassen Yahia from the University of Paris-Sud. Their work while at the ILL covered a broad range of subjects, including the scattering mechanisms of ultra-cold neutrons on a liquid helium surface (PG), the tunability of the impurity bandwidth in superconductor-dilute ferromagnetic semiconductor-superconductor junctions (KK), and magnetic excitations, magnetic phase diagram and magnetic spectrum of multiferroic compounds (MG and GY). Their visits were a success in terms of their collaboration not only with the ILL Theory College but also with ILL instrument groups and users.

Amongst the many subjects, we would like to attract attention to the strong activity that has taken place around the subject of spintronics this year. Of the many challenges faced in this area, we would like to focus on the conversion of spin currents to and from conventional charge ones, and the design of magnetic materials free of the so-called 'dead layer' hindering the spin and transport properties at the interface. Work is in progress on the latter, and *ab initio* calculations allowed us to design promising super-lattices with the desired properties. In the highlight on p.76 we will see how one can use resonances to enhance the skew scattering of electrons from impurities. It allows the electrons to spend more time in regions of strong spin-orbit potential, and thus convert efficiently spin currents into conventional charge ones.

COLLEGE 3 – NUCLEAR AND PARTICLE PHYSICS

M. Jentschel (College 3 Secretary)

Although neutrinos were experimentally discovered in the middle of the 20th century, many of their fundamental properties are still rather uncertain. The Standard Model predicted them to have zero mass, which has since turned out to be wrong. The 2015 Nobel Prize in physics was awarded to T. Kajita and A.B. McDonald for "the discovery of neutrino oscillations, which shows that neutrinos have mass". The NPP group of the ILL is heavily involved in the preparation of the experiment STEREO, which will search for a new type of neutrino oscillation and is expected to deliver its first data in 2016. In the meantime, the ILL has made an important contribution to efforts to determine the neutrino mass. By measuring the energies and masses of all decay products of the electron capture process of ^{163}Ho to ^{163}Dy, it should become possible to extract the neutrino mass. One particular problem is the availability of ^{163}Ho for this experiment, which U. Köster and his colleagues solved using the ILL's high neutron flux to 'breed' this isotope from a ^{162}Er target. As a result, a new and more precise determination of the decay energy is now possible.

The neutron as an object of study also continues to challenge our experimental efforts. One particularly important quantity is the lifetime of the free neutron, since its value has an impact on several fields: it is of relevance to the weak interaction, it impacts on the elemental abundance in the universe, which interferes with nuclear structure, and it is also of importance for neutrino oscillation measurements. On the ultra-cold neutron source PF2, a new lifetime measurement was carried out by storing ultra-cold neutrons in a storage volume (p.74). A particular effort was made to eliminate all systematic errors experimentally and the accuracy of the experiment itself was compatible with the world average of all recent storage experiments. However, the results obtained differ substantially from the values measured using so-called in-beam experiments, prompting the question as to whether there is a fundamental difference between these two types of experiment.

The understanding of nuclear structure is another field of research of the NPP group. In recent years, significant progress has been made due to the development of nuclear shell-model calculations. This model makes considerable use of closed shells and treats additional nucleons as valence particles on top of a closed shell core. However, the validity of magic numbers and the associated closed shells in extreme neutron-rich nuclei might be uncertain. In a recent experiment (p.72), the unique features of the PN1 fission fragment separator and the EXILL spectrometer were used to study isotopes close to the doubly magic ^{78}Ni core and compare them to the shell model calculations. These measurements, fascinating in themselves, also give us a glimpse of possible future research exploring the potential of the NPP's Endurance project FIPPS (p.82).

COLLEGE 4 – MAGNETIC EXCITATIONS

J. Ollivier (College 4 Secretary)

In our never-ending quest to understand the origin of high-Tc and more generally of unconventional non-BCS superconductors, inelastic neutron scattering with the aid of efficient instruments is still at the forefront.

Sometimes this technique leads to a surprising "simplification" of the observations, such as in the heavy fermion superconductor $CeCoIn_5$ (p.46), where high-resolution measurements on the powerful, upgraded three-axis spectrometer IN12 led to a perfect matching of the field-induced magnetic ordering with the spin resonance associated with the superconducting state, and both occurring at the same incommensurable wave vector. This reinforces confidence in a strong relationship between the superconducting state and the magnetic fluctuations (replacing the phonons in a conventional BCS picture) that was called into question by previous measurements reporting a spin resonance located at the antiferromagnetic point, whereas the field induced Q-phase was reported at the incommensurate position in this system.

Of the zoo of exotic magnetic excitations that accompany non-conventional superconductors, the hourglass excitation was expected to be of importance. Measurements on cold and thermal three-axis spectrometers (p.44) have confirmed that the hourglass-shaped magnetic excitation is not specific to superconductors and, contrary to previous findings, suggest that it is not related to fluctuating stripes but rather to the effect of the superposition of domain-like magnetic contributions due to a phase separation at the nanometer scale. These results, which are valid for a cobaltate, need to be confirmed on a larger family of superconductor parents.

Compared with the above results, the physics of "dirty bosons" seems like a quiet haven in the turbulent realm of quantum magnetism. Taking advantage of a modern time-of-flight spectrometer (p.40), it was quite straightforward to obtain a detailed picture of a wide portion of the reciprocal space of a chemically substituted disordered quantum magnet. These measurements made a reliable comparison with the undoped parent system possible, revealing a renormalisation of the excitations. The results could also be easily matched against the theoretical models, albeit with a negative conclusion as far as the appearance of localised states in the energy gap was concerned.

And finally, what is the relation between a simple square lattice and the Higgs boson? A possible answer may be found on p.42, which describes how polarised-neuron spectroscopy measurements were performed on a quantum square-lattice antiferromagnet (QSLHAF). The extra intensity identified at certain wave vectors may be interpreted as scattered by two-magnon states, with the magnon-magnon interaction inducing a Higgs resonance. As the QSLHAF is a model for undoped layered cuprates, we can see that superconductivity is never far from the preoccupations of scientists in the magnetic community.

COLLEGE 5A – CRYSTALLOGRAPHY

E. Mossou (College 5A Secretary)

The activities of College 5A are aimed at obtaining detailed atomic-level structural information from well-ordered solid-state materials, in other words from single crystals and polycrystalline-powder materials. College 5A focuses on the study of the nuclear non-magnetic part of the structure, while magnetic structures are covered by College 5B and biological structures are College 8's area of expertise.

At a time when techniques such as synchrotron X-rays, Electron Microscopy (EM) and Free Electron Laser (FEL) capabilities are developing rapidly in crystallography, it is important to note that neutron diffraction is still a unique tool and continues to occupy a central role alongside the other techniques. The highlight published in last year's annual report on the real-time diffraction study of electrode materials for lithium ion batteries illustrates perfectly the power of the technique. As lithium is a light element, it is not readily visible with X-rays. However, one of the many advantages of neutrons is their ability to visualise atoms with low atomic numbers, even in the presence of heavier ones. The neutron study was therefore able to give us unique insight into the dynamics of this charge/discharge process. This study has since been awarded a number of prizes, including the Materials Research Society Graduate Student Silver Award 2015 and the Electrochemical Society Battery Division Student Research Award 2015 (Dr Matteo Bianchini).

With the current emphasis on renewable energy, several studies have been conducted at the ILL which lie at the forefront of this field, as illustrated by the D20 highlight on the new high-performance hybrid lead-perovskite photovoltaic material (p.26). This detailed neutron study as a function of temperature provided a unique understanding of this material and its use in solar cells. Another notable study reports a new phase of ice (Ice XVI) characterised by its symmetrical cage-like structure capable of trapping gas hydrates (p.24). The discovery of this new type of empty clathrate could offer new solutions for the transport and storage of energy.

Another highlight illustrates how neutron powder experiments on human tooth enamel made it possible to localise hydrogen atoms, providing a more detailed knowledge of its structure (p.16). These results will undoubtedly help to improve our understanding of the demineralisation processes. Other examples of the types of materials that have been studied with powder diffraction over the last few years include molecular hydrides for hydrogen storage, oxides and multi-ferroelectric materials.

Finally, single crystals of organic compounds are attracting a lot of interest, with questions directly relating to the hydrogen positions and hydrogen-bonding interactions, as can be seen from the high number of proposals submitted by users from this community.

COLLEGE INTRODUCTIONS

COLLEGE 5B – MAGNETIC STRUCTURES

N. Qureshi (College 5B Secretary) and **C. Dewhurst** (vice-Secretary)

The creation of a focus group which deals with proposals related to small-angle scattering and reflectivity has proved to be very successful, both in terms of dividing the heavy workload College 5B experiences during the proposal rounds and in terms of the division of dedicated expertise between the main college and the focus group. Thanks to the lightened workload, there can now be a full and lively scientific discussion of all proposals during the subcommittee meetings.

In comparison to the previous proposal round in autumn 2014, 2015 saw a slight increase in College 5B proposals, underlining the continuing interest in magnetic properties. In the field of diffraction, there has been an increased interest in spin-orbit coupling systems (containing Os, Ru, Ir). The study of these systems is challenging due to their very low magnetic moments. There has also been continued interest in quantum magnetism, and frustrated and multiferroic systems. Competing interactions lead to a rich variety of magnetic structures. One of our highlights is a perfect example of this: using polarised neutrons with spherical polarisation analysis on D3, a magnetic stripe phase was discovered in the β-$TeVO_4$ compound which appears at the transition between a collinear and a spiral magnetic order (p.30).

Multiferroicity has been observed in many transition metal oxides, but the occurrence of this effect in molecular-based magnets remains rare. A highlighted example of the latter is deuterated ammonium pentachloroaquaferrate(III), which was studied by using single crystals on D9 and powders on D2B. While the sequence of magnetic phase transitions and the microscopic origin of multiferroicity were similar to those observed in common multiferroics, the change of the electric polarisation under an applied magnetic field differed from what had been observed so far (p.36).

Compared with the previous proposal round, there has been a significant increase in the number of reflectivity proposals, coinciding with the returned availability of SuperADAM along with its upgraded neutron guide and instrumentation in the ILL22 guide hall.

Small-angle scattering has continued to enjoy the usual level of interest for the study of flux-line lattices. There has also been a marked increase in the number of proposals involving skyrmion systems. So-called Bloch-type skyrmions have been observed in materials with a chiral crystal structure. Using small-angle neutron scattering on D33, a new type of skyrmion – the Néel-type skyrmion – was discovered in GaV_4S_8, a material originally theoretically predicted to host skyrmions (p.38).

COLLEGE 6 – LIQUIDS AND GLASSES

G. Cuello (College 6 Secretary)

The complexity of disordered systems requires the combined use of various experimental techniques, usually in conjunction with computer simulations, in order to obtain a deeper insight into the structural and dynamical properties of such materials. This is the reason why in our College the neutron scattering experiments are performed on a broad set of instruments and contribute to a wide range of scientific fields. The areas of activity include liquid and glassy dynamics of ionic and metal liquids, polymers, water and molecular liquids, as well as the dynamics of nano-confined molecules. A trend currently observed in this field is the use of complex experimental techniques in order to attain extreme conditions of temperature or pressure, and the injection of gases in porous materials.

In recent years, the demand for beamtime to perform pair distribution function (PDF) analysis has been constantly increasing. The high proportion (about one third) of experiments requested on the hot neutron diffractometer D4 is a clear indication of the increasing interest in this kind of study, which is useful for the structural characterisation of partially disordered materials or materials with ordering only at the nanoscale. Liquids are generally considered as complex systems, since they do not have the full disorder of a gas or the full order of a crystalline solid. Of these, monoatomic liquid metals are usually considered as quite simple liquids. However, a recent study performed on BRISP (p.48) has broken down this paradigm, showing the existence of a complex pattern of excitations in liquid zinc which could be ascribed to anisotropic contributions in the atomic interaction potential (see also College 7 below).

The other College 6 highlight in this year's report deals with the separation of coherent and incoherent scattering in hydrogenated systems, particularly in molecular liquids (p.50). The structural determination of disordered materials containing substantial amounts of hydrogen is always problematic when using neutron diffraction techniques. With the help of neutron diffraction with polarisation analysis, the spin-incoherent scattering can be isolated and subtracted from the total scattering. In the case of hydrogenated materials, this is the main contribution to the incoherent scattering. The experiment – performed on D3 – made it possible to properly determine the structure factor for several mixtures of heavy and light water, including pure light water. The same technique has also been used to determine the structure factor of normal propanol, opening up the possibility of conducting diffraction experiments without the need for deuteration.

COLLEGE 7 – SPECTROSCOPY AND MODELLING

A. Piovano (College 7 Secretary)

Spectroscopy experiments in the fields of solid-state physics and chemistry, which are covered by College 7 activities, have been clearly moving in two distinct directions in recent years. On the one hand, we see many studies dealing with the fundamental aspects of solid-state physics, while, on the other hand, more and more work is being devoted to the investigation of challenges facing society concerning the environment, energy and life sciences.

The proposals accepted for College 7 during the most recent proposal rounds were all high ranked, demonstrating the quality of the projects produced by users and reflecting the healthy and attractive scientific image of the College. The requests for instruments, with only a few exceptions, were well balanced over most of the ILL spectrometers, and were occasionally accompanied by a parallel request for a diffractometer when both structure and dynamics needed to be analysed. Our highlights include studies of both single-crystal and polycrystalline materials and cover principally materials physics and materials chemistry, with a particular emphasis on materials for energy-related applications. Increasingly, a non-negligible proportion of interesting spectroscopic results come from the biophysics and life sciences fields.

The importance of neutron spectroscopy and its versatility in different fields ranging from fundamental research and materials for technological applications to biophysics is clearly illustrated by three highlights in this year's report. A study of fundamental interest, conducted on the BRISP spectrometer on liquid zinc (p.48), revealed that even monoatomic liquid metals can show unexpectedly complex dynamics at the atomic scale. The spectra collected clearly showed the existence of a complex pattern of excitations, breaking the paradigm that monoatomic metal liquids are the prototype of simple liquids.

The topic of ionic conduction also took centre stage this year with a study performed on the IN6 spectrometer on a Nd_2NiO_{4+d} system (p.20). Comparing experimental data with MD simulations, the team carrying out the study was able to investigate the microscopic mechanism of diffusion at moderate temperatures. In particular, they identified that excess oxygen has a strong impact on behaviour in low energy modes, favouring diffusion events. This work also highlights the synergistic way in which modelling activities assist spectroscopy experiments to enable full interpretation of the data collected.

Finally, we must mention work with both fundamental and potential societal impact which has been carried on IN16B and which focused on gaining an understanding of the dynamics of protein hydration water (p.60). More details on this study can be found in the College 8 section below.

COLLEGE 8 – BIOLOGY

B. Demé (College 8 Secretary)

Once again this year, highlights in the field of Biology and Health illustrate a wide range of neutron techniques for probing structures and dynamics: spectroscopy techniques (IN5 and IN16B), single-crystal diffraction (LADI), SANS on macromolecular solutions (D22), and membrane diffraction (D16).

Using the neutron backscattering technique, work on the tau protein illustrates the benefits of using neutrons in combination with deuterium labelling to probe the dynamics of biological samples (p.60). The study performed on IN16B made it possible to measure the mobility of water molecules at the surface of tau protein with high accuracy. The set of results obtained suggest that methodologies sensitive to the diffusion of water could be used to detect increased water mobility in Alzheimer-diseased brains.

Neutron spectroscopy was also used to investigate the dynamics of alcohol dehydrogenase on a broad range of time scales to obtain a coherent picture of the molecular motions in solution (p.70). The study performed at the ILL (IN5) and MLZ-Munich demonstrated the potential of combining neutron spin-echo spectroscopy and high-resolution neutron time-of-flight and backscattering spectroscopy.

Data collected on D22 provided new insights into the molecular details and control mechanisms of protein degradation pathways in hyperthermophilic organisms and suggested strategies to optimise the performance of macromolecular complexes for biotechnological applications (p.64).

A joint X-ray/neutron study was performed to visualise hydrogen bonding in a protein kinase (PKG) complex with a cyclic nucleotide-binding domain activator (p.62). Crystallographic evidence revealed crucial hydrogen-bond interactions between the nucleotide and the protein, shedding light on the atomic details of the nucleotide-binding domain selectivity. The results obtained on LADI will assist the structure-guided design of PKG activators in the treatment of hypertensive disease.

Finally, experiments performed on D16 revealed novel details about the dimension, asymmetry, organisation and water permeability of myelin (p.68). Beyond elucidating the structure of myelin, neutron diffraction holds much promise for analysing the function of myelin and provides a direct and focused measurement of myelin function and integrity that could be exploited to measure the permeability of myelin from transgenic animals modelling human myelinopathies.

COLLEGE 9 – SOFT CONDENSED MATTER

O. Czakkel (College 9 Secretary) and **Y. Gerelli** (vice-Secretary)

Soft matter studies once again represented the second largest share of submitted proposals. In 2015, College 9 proposals increased both in percentage terms and in absolute numbers. As in previous years, both fundamental and applied science were represented in the work conducted and the topical distribution among the proposals was reasonably balanced.

As instrumentation improves year by year, complex studies become feasible. For example, the *in situ* combination of rheology and neutron reflectivity on D17 investigated the interactions of ferrofluids (colloidal suspensions of magnetic particles) with a solid interface under the influence of both magnetic field and shear. This experiment sets the stage for a wide range of studies into fundamental magnetic interactions on the nanoscale, highlighting that understanding the rheology and surface interactions of ferrofluids will help extend the range of ferrofluid applications (p.52).

Another interesting finding concerns the dynamics of ring polymers, which, owing to their unique topology, have recently been the subject of intensive investigations and are being used to produce polymer materials with new properties. Results from neutron spin-echo spectroscopy measurements on IN15 revealed directly that in long chain matrices the entanglement spacing was unaffected by local reptation of the host molecules. In addition, secondary relaxation processes were also quantified for shorter entangled matrices (p.58).

Small-angle neutron scattering experiments conducted on D11, combined with DLS and rheology results, made it possible to establish a generalised view in terms of the structure–property relationship and equilibrium dynamics of soft colloids. Excellent agreement was also observed between theory and experiment, in particular with respect to the location of the liquid-solid phase boundary (p.54).

Last but not least, a fascinating showcase study of the complementarity of neutron and X-ray scattering is presented. Combining the results from the two techniques obtained during experiments on D11 and ID02 (ESRF), a statistical model was proposed explaining why, in particular, the smallest nanoparticles cause efforts to elucidate the chain structure of polymer nanocomposites by small-angle neutron scattering to fail. These results are expected to pave the way for strategies to circumvent this problem (p.56).

Finally, the Partnership for Soft Condensed Matter (PSCM, p.106) continues to offer a wide range of complementary techniques for soft matter studies, such as light scattering, ellipsometry, film balances, calorimetry and many others. In 2015, the laboratories hosted more than 1 000 experiments with an average of 70 neutron proposals submitted per cycle requesting access to PSCM facilities. In 2015, new partners also joined the PSCM and we are therefore delighted to welcome Paderborn University, Imperial College London and TU-Berlin!

SCIENTIFIC HIGHLIGHTS

ILL IN THE PRESS

1. Published in *Geoscientist* in March 2015
2. Published in *Medical Press* on 28 April 2015
3. Published in *Nuclear Engineering* in June 2015
4. Published in *Materials Today* on 6 August 2015
5. Published in *Physics Org* on 6 August 2015

1.

NEUTRONS
FOR GEOLOGY

RECENT STUDIES HAVE ALLOWED GEOSCIENTISTS TO STUDY OUR PLANETS INTERNAL WORKING, AS WELL AS THOSE OF WORLDS FURTHER AFIELD, AT NEW FUNDAMENTAL LEVELS

The humble neutron is becoming a valuable tool to model the internal workings of our planet, says **Martin Dove***

With the ability to analyse the properties of the Earth's internal environment under the atomic scale it conditions only found kilometres below our feet, recent studies have allowed geoscientists to study our planet's internal working, as well as those of worlds further afield, at new fundamental levels. And all from the relative comfort of the laboratory! Only last year, for example, researchers from Bath University used neutron techniques to map structural changes within oxide glasses and liquids - research that could provide a new tool to investigate the environmental conditions that melt the Earth's interior and produce volcanoes at the surface.

With instruments able to recreate extreme pressure conditions up to 9.7 GPa and 1500 K, neutron sources such as

Neutrons as a tool

Forecasting melts

2.

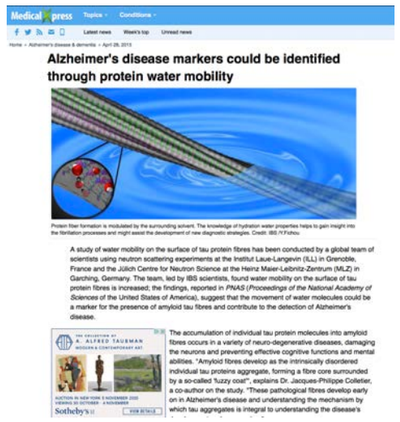

Medical Xpress

Alzheimer's disease markers could be identified through protein water mobility

A study of water mobility on the surface of tau protein fibres has been conducted by a global team of scientists using neutron scattering experiments at the Institut Laue-Langevin (ILL) in Grenoble, France and the Jülich Centre for Neutron Science at the Heinz Maier-Leibnitz-Zentrum (MLZ) in Garching, Germany. The team, led by IBS scientists, found water mobility on the surface of tau protein fibres is increased; the findings, reported in *PNAS (Proceedings of the National Academy of Sciences of the United States of America)*, suggest that the movement of water molecules could be a marker for the presence of amyloid tau fibres and contribute to the detection of Alzheimer's disease.

The accumulation of individual tau protein molecules into amyloid fibres occurs in a variety of neuro-degenerative diseases, damaging the neurons and preventing effective cognitive functions and mental abilities. "Amyloid fibres develop as the intrinsically disordered individual tau proteins aggregate, forming a fibre core surrounded by a so-called 'fuzzy coat'", explains Dr. Jacques-Philippe Colletier, a co-author on the study. "These pathological fibres develop early on in Alzheimer's disease and understanding the mechanism by which tau aggregates is integral to understanding the disease's

3.

Upgrading & Uprating | Fukushima improvements

Investing in ILL

Post Fukushima upgrade work is nearing completion at the Institute Laue-Langevin in France where a research reactor provides neutrons for science, materials research, and radioisotope production.

Nestled between two mountain ranges in the Rhône-Alpes region of France, the high-flux research reactor at the Institute Laue-Langevin in Grenoble is one of about a dozen facilities worldwide that produces neutrons for science. It is also one of the most powerful. The 58.3MW$_{th}$ heavy-water cooled reactor produces the most intense continuous neutron flux in the world in the moderator region: 1.5x10^{15} neutrons per second per cm^2. Once the neutrons produced by the reactor have been slowed to lower energies, they are guided to a suite of around 40 instruments installed in experimental halls. A hot source and two cold sources enable the neutrons to be produced over a broad range of wavelengths. Over a thousand experiments are carried out at the facility each year and it is in high demand.

The HFR typically operates for 200 days a year – four 50-day cycles – after which it is shut down to change the single 99kg fuel element. Each year there is a longer shutdown to enable necessary maintenance work to be carried out.

Fukushima response

4.

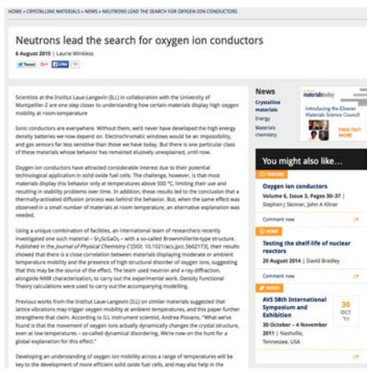

HOME » CRYSTALLINE MATERIALS » NEWS » NEUTRONS LEAD THE SEARCH FOR OXYGEN ION CONDUCTORS

Neutrons lead the search for oxygen ion conductors

6 August 2015 | Laurie Winkless

Scientists at the Institut Laue-Langevin (ILL) in collaboration with the University of Montpellier 2 are one step closer to understanding how certain materials display high oxygen mobility at room-temperature.

Ionic conductors are everywhere. Without them, we'd never have developed the high energy density batteries we now depend on. Electrochromatic windows would be an impossibility, and gas sensors far less sensitive than those we have today. But there is one particular class of these materials whose behavior has remained elusively unexplained, until now.

Oxygen ion conductors have attracted considerable interest due to their potential technological application in solid oxide fuel cells. The challenge, however, is that most materials display this behavior only at temperatures above 500 °C, limiting their use and resulting in stability problems over time. In addition, these results led to the conclusion that a thermally-activated diffusion process was behind the behavior. But, when the same effect was observed in a small number of materials at room temperature, an alternative explanation was needed.

Using a unique combination of facilities, an international team of researchers recently investigated one such material – Sr_2SiGaO_5 – with a so-called Brownmillerite-type structure. Published in the *Journal of Physical Chemistry C* (DOI: 10.1021/acs.jpcc.5b02175), their results showed that there is a close correlation between materials displaying moderate or ambient temperature mobility and the presence of high structural disorder of oxygen ions, suggesting that this may be the source of the effect. The team used neutron and x-ray diffraction, alongside NMR characterization, to carry out the experimental work. Density Functional Theory calculations were used to carry out the accompanying modelling.

Previous works from the Institut Laue-Langevin (ILL) on similar materials suggested that lattice vibrations may trigger oxygen mobility at ambient temperatures, and this paper further strengthens that claim. According to ILL instrument scientist, Andrea Piovano, "What we've found is that the movement of oxygen ions actually dynamically changes the crystal structure, even at low temperatures – so-called dynamical disordering. We're now on the hunt for a global explanation for this effect."

Developing an understanding of oxygen ion mobility across a range of temperatures will be key to the development of more efficient solid oxide fuel cells, and may also help in the

You might also like...

5.

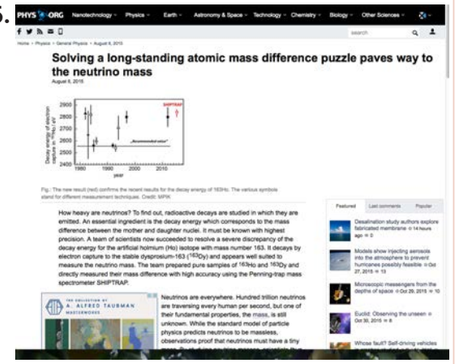

PHYS.ORG

Solving a long-standing atomic mass difference puzzle paves way to the neutrino mass

August 6, 2015

How heavy are neutrinos? To find out, radioactive decays are studied in which they are emitted. An essential ingredient is the decay energy which corresponds to the mass difference between the mother and daughter nuclei. It must be known with highest precision. A team of scientists now succeeded to resolve a severe discrepancy of the decay energy for the artificial holmium (Ho) isotope with mass number 163. It decays by electron capture to the stable dysprosium-163 (^{163}Dy) and appears well suited to measure the neutrino mass. The team prepared pure samples of ^{163}Ho and ^{163}Dy and directly measured their mass difference with high accuracy using the Penning-trap mass spectrometer SHIPTRAP.

Neutrinos are everywhere. Hundred trillion neutrinos are traversing every human per second, but one of their fundamental properties, the mass, is still unknown. While the standard model of particle physics predicts neutrinos to be massless, observations proof that neutrinos must have a tiny

6.

IOP Physics World - the member magazine of the Institute of Physics

physicsworld.com

Home | News | Blog | Multimedia | In depth | Events

Neutrino-mass measurements could benefit from holmium-trapping result

Aug 12, 2015 3 comments

Weighing up: team member Michael Block at SHIPTRAP

Physicists in Europe have resolved a long-standing puzzle regarding the energy released when an isotope of the rare-earth element holmium decays via electron capture. They say that their extremely precise measurement of the mass difference between mother and daughter nuclides will be crucial in helping to pin down the unknown and very small mass of the neutrino. Other experts, however, insist that this measurement will not help to significantly reduce the upper limit on neutrino mass.

Experiments in the late 1990s and early 2000s showed that neutrinos oscillate from one flavour to another as they travel through space, and that therefore they have mass – in contradiction with the Standard Model of particle physics. However, such experiments can only establish the difference in mass between the three flavours, and not their absolute masses. But establishing the absolute value could point scientists to new physics beyond the Standard Model and identify the role of neutrinos in galaxy formation. A number of experiments including the Electron Capture ^{163}Holmium experiment (ECHo) at the University of Heidelberg in Germany have therefore been developed to try and pin down that mass.

ECHo will begin in 2016 with the aim of measuring neutrino mass using the phenomenon of electron capture in holmium-163. The neutron-deficient isotope absorbs an electron from its inner shell, so converting one of its protons into a neutron and thereby changing into stable dysprosium-163. This results in the emission of an electron neutrino, as well as X-ray photons and Auger electrons – as an outer electron drops to fill the hole left by the absorption – and sometimes a gamma ray from the excited nucleus.

7.

Features

Physics World October 2015

Life as an instrument scientist

Estelle Mossou is an instrument scientist on the D19 instrument at the Institut Laue-Langevin in Grenoble, France, e-mail mossou@ill.fr

Estelle Mossou explains how she balances the demands of users while carrying out her own research

Local knowledge Estelle Mossou uses her knowledge of neutron scattering and instrumentation to help users at the Institut Laue-Langevin in Grenoble, France. (Serge Claisse/ILL)

The intimate atmosphere of the university campus at Bath University in the UK where I studied physics reminded me of Libreville, the small town I had left behind in Gabon. After completing a year-long placement at the Institut Laue-Langevin (ILL) in Grenoble, France, in 2004, which contributed to my Master's degree in physics, I felt that same atmosphere where everybody knows everybody else.

I enjoyed the experience of my placement so much that I came back to the ILL

8.

Physics World October 2015

Planning for the future

Helmut Schober is associate director of the Institut Laue-Langevin, e-mail schober@ill.eu

Neutrons are increasingly being used by scientists in a variety of disciplines. **Helmut Schober** warns that more funding will be required to meet the demand of more users

Looking ahead Helmut Schober (ILL)

Neutrons bring unique capabilities in a wide range of scientific disciplines from probing the Standard Model of particle physics and understanding the behaviour of HIV drugs to testing the strength of aircraft turbine blades. Neutrons continue to provide answers to many of society's pressing questions, and with demand for sources still high, that looks set to continue.

To maintain an outstanding level of service, we need to anticipate the wider trends that shape research in the field. Most significant of these has been the drive in recent years for researchers to move beyond a general understanding of broad scientific concepts towards ever more specific analyses of samples with technological applications. This push in materials science towards the particular, and away from the universal, is only set to grow as the global scientific community comes under pressure to provide solutions for societal challenges. Neutron science is already playing an important role in that respect in energy storage and computing performance.

Another area where neutron science is likely to grow is in soft-matter research – notably in the life sciences where the research community has just

9.

DDW

Drug Design

How neutron science has enabled innovation in drug design and delivery

Meeting global health challenges, from cancer to viral infections, requires a profound understanding of living processes – not just at the level of cells but right down at the molecular level. And designing the most efficient therapeutics requires an in-depth understanding of the disease. Most diseases result from biomolecular processes going wrong. Viruses invade cells and take over their molecular machinery, eventually killing the cells and bacteria may release toxins that block a vital molecular interaction. The ambitious aim of biologists today is thus to observe the structure and behaviour of biological molecules at the atomic scale, as they function in their natural, physiological environment. Understanding the complex biological processes that regulate our bodies requires insight into structure and dynamics at the molecular scale. And for that we need particularly potent analytical weapons. While x-rays are well-known to most, the use of neutrons in health-related research is not common knowledge. The Institut Laue-Langevin (ILL), the world's flagship centre for neutron science, is using its vast array of instruments to piece together the huge biological puzzle of life.

The molecules of life

By Dr Giovanna Fragneto

6. Published in *PhysicsWorld* on 12 August 2015
7. Published in *PhysicsWorld* in October 2015
8. Published in *PhysicsWorld* in October 2015
9. Published in *Drug Discovery World* in Autumn 2015

MATERIALS SCIENCE

SCIENTIFIC HIGHLIGHTS

Localisation of hydrogen atoms in human tooth enamel

High resolution diffractometer D2B

Dental enamel is the hardest biological and mineralised tissue. Its main constituent is a mineral of 96 wt% associated with 3 wt% water and 1 wt% of organic matter. The mineral is non-stoichiometric calcium hydroxyapatite $Ca_{10}(PO_4)_6(OH)_2$ with partial substitution with, for instance, carbonate and fluoride ions. The stability or instability of biological apatites has been associated with the presence of minor substitutions. For example F^- is thought to promote caries resistance, while CO_3^{2-} is associated with caries susceptibility. The anionic impurities such as F^- or Cl^- are known to substitute for OH^- and CO_3^{2-}, and HPO_4^{2-} to substitute for PO_4^{3-} [1]. Knowledge of the detailed crystal structure of biological apatites is therefore of great importance in order to understand the physico-chemical properties of tooth and bone, and also to explain formation and calcification processes, such as caries in human teeth.

AUTHORS

B. Ouladdiaf and **J. Rodriguez-Carvajal** (ILL)
C. Goutaudier (Université de Lyon, UMR CNRS 5615, France)
S. Ouladdiaf and **B. Grosgogeat** (Université de Lyon, Faculté d'Odontologie de Lyon and Hospices Civils de Lyon, France)
N. Pradelle and **P. Colon** (Université de Lyon and Faculté d'Odontologie de Paris Diderot, France)

REFERENCES

[1] R.A. Young, J. Dent. Res. 53 (1974) 193
[2] R.A. Young and S. Spooner, Arch. Oral Biol. 15 (1969) 47
[3] A. Vyalikh, R. Mai and U. Scheler, Bio-Med. Mater. Eng. 23 (2013) 507
[4] M.J. Bottero, J. Yvon and J. Vadot, Eur. J. Mineral. 4 (1992) 1347

The main apatite structure (general formula $Ca_{10}(PO_4)_6X_2$, where X can be F (fluorapatite), Cl (chlorapatite, ClAp) or OH (hydroxyapatite, HAp)) is hexagonal, with space group $P6_3/m$. The calcium atoms occupy two non-equivalent sites, namely Ca_I and Ca_{II} at sites 4f and 6h respectively; the phosphorous atoms also occupy a 6h site, while the oxygen atoms are on three non-equivalent sites, $6h_1$, $6h_2$ and 12i; and the X ions partially occupy the 4e site. The network of PO_4 tetrahedrons forms the basic framework of the apatite's structure and ensures its great stability. Although intensive investigations using various techniques have been performed on the crystal structure of biological apatites, and of human enamel in particular, several ambiguities remain as regards the actual structure of human tooth enamel.

To answer these questions and obtain deeper insight into the crystal structure of human tooth enamel, a high-resolution neutron diffraction experiment was performed at the ILL using the D2B diffractometer. The human enamel was prepared from the non-carious portion of a tooth extracted from an informed patient aged 21. The neutron diffraction pattern collected over seven hours is shown in **figure 1**. It is characterised by well-defined Bragg peaks and a relatively high background, as previously reported [2].

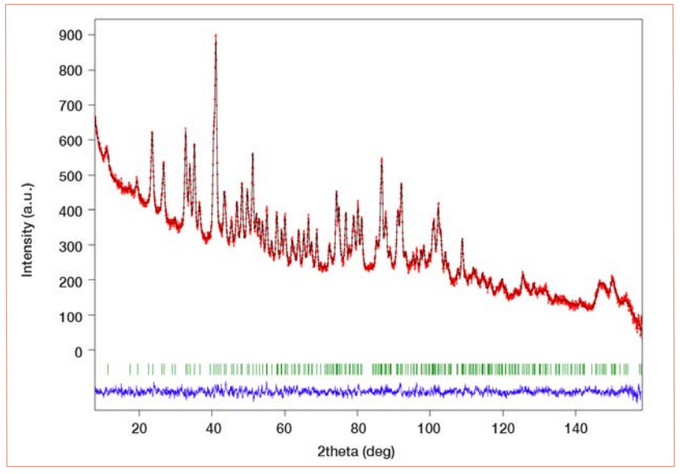

Figure 1
Plot of the observed (red circles) and calculated (black line) neutron powder diffraction pattern of human enamel.

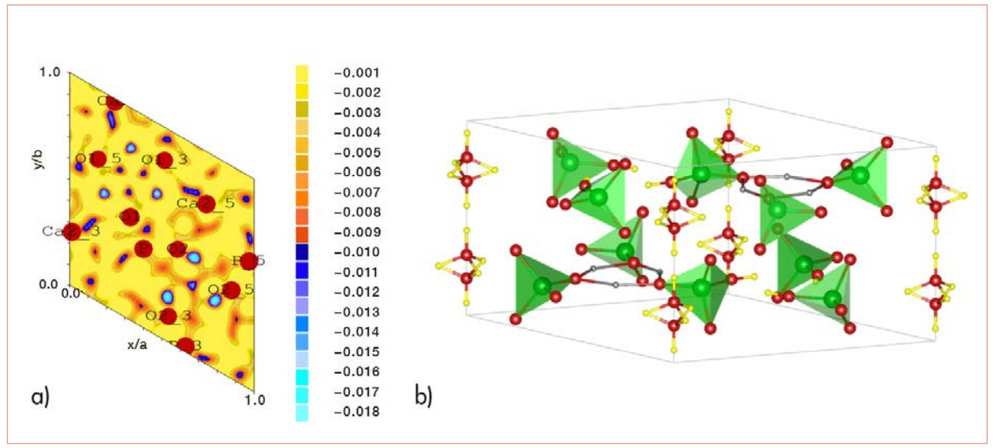

Figure 2
a) Difference Fourier maps of the section z = 1/4, showing the positions of H-atoms; **b)** View of the crystal structure of human enamel refined from the neutron data. Hydrogen atoms are yellow and bound always to oxygen atoms (in red). The configuration of hydroxyl groups is statistically disordered.

The refinement of the neutron data was performed using the FullProf software based on the Rietveld method. The complex background was well modelled by Chebyshev polynomials of the first kind. The refinement of the data using the theoretical OH^- content leads to relatively good refinement. However, when refining the OH^- occupancy factor the agreement between calculation and observation is much improved. The refined OH^- normalised occupancy factor is 0.47(5), indicating large hydroxyl deficiency in agreement with hydroxyl content determined recently by spectroscopic techniques [3].

In contrast to X-rays, neutron diffraction is well adapted for studying the structure of biological apatites because of its sensitivity to the presence of hydrogen. This is evidenced in the scattering density Fourier difference maps, as shown in **figure 2a**. The scattering density sections parallel to the (001) plane show clearly weak negative scattering next to oxygen at the mirror planes located at z = 1/4 and 3/4. This site corresponds to hydrogen atoms because of their negative scattering length. These atoms are located at the 6h Wyckoff site (x, y, 1/4) with x = 0.5244 and y = 0.2088. The hexagonal structure model used for tooth enamel is therefore not very accurate and H-atoms should be included. The refinement of the neutron data with additional hydrogen atoms at the 6h site is significantly improved, leading to excellent agreement between the observed and calculated patterns. The refined crystal structure of the enamel is shown in **figure 2b**, where we can see clearly that the H-atoms located at the 6h site correspond indeed to HPO_4^{2-} anions. The refined occupancy factor of the H-atoms of HPO_4^{2-} reaches 0.43(6), indicating about 4 wt% of HPO_4^{2-} content in agreement with the reported figure of 5 wt%.

The high background observed in the neutron diffraction pattern is associated with the incoherent scattering of hydrogen, not only from hydroxyl but also from excess hydrogen in the tooth enamel, which is shown from this study to be structurally incorporated and associated with PO_4 groups and water molecules.

The slight preferred orientation of the crystallites seems to be related to their nanometric sizes, which certainly contribute to the mechanical properties of teeth. The refined global apparent size of the crystallites is 18.2 nm, in agreement with previous results. Indeed it was found that the average crystallite size in human dental apatites diminishes with tooth age, from 38 nm for younger age teeth (five years) to 12 nm for older (87 years) [4]. This affects the mechanical properties of the enamel for most people.

These new insights into the crystallographic structure of enamel will help us to understand in more detail the demineralisation process that is deeply connected to hydroxyl ion substitutions.

MATERIALS SCIENCE

Neutrons help assess proton mobility in dental cements

Backscattering spectrometer IN10

Among the materials used for dental fillings, glass ionomer cements are an interesting restorative option due to their good biocompatibility, release of fluoride and ability to bond to the teeth. One of their drawbacks, however, is their limited strength. A better understanding of their structure and time-dependent hydration using neutrons could contribute to future improvements.

AUTHORS

A.R. Benetti (Department of Odontology, University of Copenhagen, Denmark)
J. Jacobsen and **H.N. Bordallo** (Niels Bohr Institute, University of Copenhagen, Denmark, and ESS, Sweden)
B. Lehnhoff and N.C.R. Momsen (Niels Bohr Institute, University of Copenhagen, Denmark)
D.V. Okhrimenko (Department of Chemistry, University of Copenhagen, Denmark)
M.T.F. Telling (ISIS Facility and University of Oxford, UK)
N. Kardjilov and **I. Manke** (Helmholtz-Zentrum Berlin, Germany)
M. Strobl (ESS, Sweden)
T. Seydel (ILL)

REFERENCES

[1] United Nations Environment Programme [Minamata Convention on Mercury] Text and annexes presented at the Conference of Plenipotentiaries. Kumamoto: UNEP (2013)
[2] M.S. Baig and G.J.P. Fleming, J. Dent. 43 (2015) 897
[3] A.R. Benetti *et al.*, Sci. Rep. 5 (2015) 08972
[4] J. Jacobsen *et al.*, Sci. Rep. 3 (2013) 02667

With dental amalgam being phased out as a dental replacement material [1], tooth-coloured resin composites and glass ionomer cements are the main materials now being used for fillings. Resin composites are stronger and have the ability to last longer. On the other hand, glass ionomer cements present desirable properties for fillings, among which are biocompatibility, release of fluoride and the ability to bond to the dental tissues. Due to their limited strength, however, these cements are contra-indicated for use in high stress bearing areas [2]. If the mechanical properties of glass ionomer cements can be enhanced, their range of applicability can be extended.

The mechanical properties of these water-based dental cements are to a significant extent dependent on the presence of surface flaws, the total porosity and the powder-to-liquid ratio. The composition and particle size distribution of the glass powder, the molar mass and concentration of the polyacid solution, and the mixing technique also affect durability. Our aim was to investigate the extent to which the strength of these materials (**figure 1**) can be influenced by the pore structure and the time-dependent hydration.

Figure 1

Biaxial flexural strength (BFS) of the investigated cements as a function of ageing. We fabricated six cylindrical specimens (diameter 10 mm, height 1 mm) from each material and for each storage period (1, 7 and 32 days). The specimens were stored in water at 37 °C to simulate the oral environment. During the test, the specimens were supported on a ring and a load was applied with a ball-shaped indenter in a universal testing machine. The load at fracture was recorded and the strength was calculated, for further details see [3]. The mean strength of Aqua is lower and remains almost constant across the 32-day period.

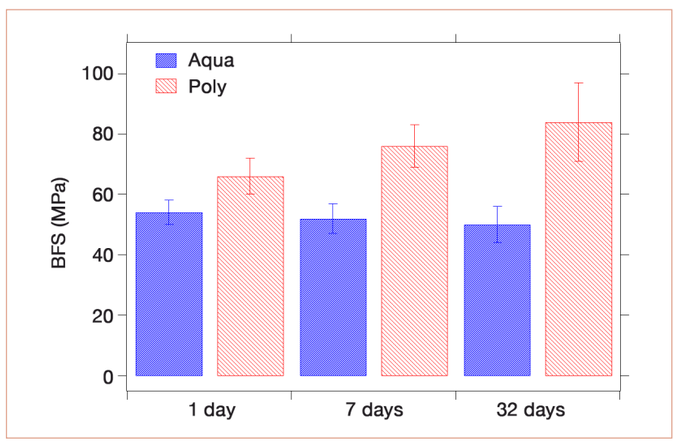

Figure 2

Monitoring the elastic signal as a function of temperature allows us to determine the onset of proton mobility by noting points of inflexion in the elastic scattering response. These were detected at 205 K (-68 °C) for the Aqua **(a)** and at 200 K (-75 °C) for the Poly **(b)** and on the nanosecond time scale. Additionally, the drop in intensity at the lowest value of Q suggests differences in the diffusivity of the liquid in both materials for the 5-day-old Poly and Aqua samples. No changes in the temperature at which motions were activated was noticed for the Poly **(d)** after 23 days of ageing, while a significant reduction in the amount of mobile protons was detected for the Aqua **(c)**. This implies that important structural changes occurred in the structure of the latter.

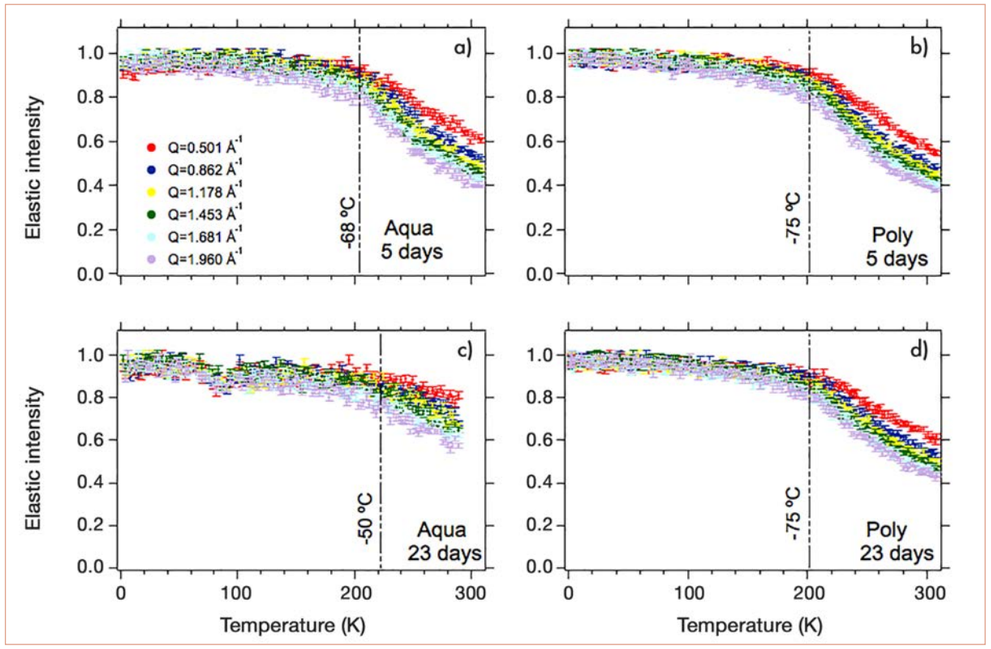

We used both neutron and X-ray imaging to investigate the highly complex pore structure within these cements, and neutron spectroscopy to assess hydrogen mobility [3]. We compared two commercial glass ionomer cements, both based on fluoroaluminosilicate glass powders, but set using different liquids. In the cement denoted "Poly" the liquid is composed of an aqueous polyacid solution. In contrast, in the cement denoted "Aqua" the liquid used was water, since the powder already contains the freeze-dried polyacid.

Using the ILL's backscattering instrument IN10 we evaluated the evolution of the energy distribution of neutrons scattered by each sample, the IN10 instrument providing information about proton mobility on the nano-second time scale. In particular our experiment was interested in monitoring the intensity of only those neutrons scattered elastically (i.e. without a change of energy), to obtain information about the number of immobile protons. Such analysis, performed as either a function of time or temperature, is known as the elastic fixed window (EFW) method [4]. When using the EFW approach as a function of setting time, more immobile protons were observed in the Aqua on the nanosecond time scale [3]. When using the EFW approach as a function of temperature, we observed the onset of proton mobility by noting the inflection points in the elastic scattering response of both cements upon ageing (**figure 2**). While no differences in proton mobility were observed for Poly (**figure 2b** and **2d**), ageing reduces proton mobility for Aqua (**figures 2a** and **2c**). At the same time, the increase in the activation temperature for the Aqua with ageing means that less energy is necessary to produce proton mobility in this material. The latter suggests that perhaps the motions under investigation are faster than the time window of IN10 or that a different proton population is being probed.

Our results indicate that the development of the pore structure plays an important role in the strength of the cements investigated. Findings from the neutron scattering experiments further suggest that the lower mechanical strength of Aqua (**figure 1**) results not only from its increased pore volume, but also, apparently, from the influence of hydrogen mobility within the material. These results open up new opportunities for research in dental cements, with neutron scattering providing a unique tool with which to better understand how to improve restorative dental material.

MATERIALS SCIENCE

Lattice dynamics modified by excess oxygen in Nd_2NiO_{4+d}: triggering low-temperature oxygen diffusion

Time-of-flight spectrometer IN6 and C-Lab

AUTHORS

A. Perrichon, M. Ceretti and **W. Paulus** (Institut Charles Gerhardt de Montpellier, France)
A. Piovano, M. Böhm and **M. Johnson** (ILL)

REFERENCES

[1] W. Paulus *et al.*, J. Am. Chem. Soc. 130 (2008) 16080
[2] M. Ceretti *et al.*, J. Mater. Chem. A 3 (2015) 21140
[3] A. Perrichon *et al.*, J. Phys. Chem. C 119 (2015) 1557

Oxygen ionic conductors are materials of fundamental interest for the development of ambient temperature working devices for energy conversion, such as solid oxide fuel cells (SOFC). In this regard the Nd_2NiO_{4+d} system proved to be a good candidate, showing oxygen ion mobility down to room temperature. Coupled molecular dynamics simulations and inelastic neutron scattering experiments on IN6 on phases with d = 0, 0.10 and 0.25 provided a unique way to follow the evolution of lattice dynamics upon increase of excess oxygen content. In this way we unveiled the microscopic mechanism of diffusion, and in particular we pointed out that excess oxygen strongly impacts specific low-energy modes of the lattice dynamics, favouring diffusion events.

Previous works on related ionic conductors of the Re_2MO_{4+d} family (Re = La, Pr; M = Ni, Cu, Co) and Brownmillerite-type $Sr(Fe,Co)O_{2.5}$ have suggested that specific phonon modes may be at the origin of the unexpectedly high oxygen mobility at moderate temperature [1]. Furthermore, a pronounced delocalisation of apical oxygen atoms in MO_6 octahedra has been evidenced in Re_2MO_{4+d} systems by single-crystal neutron diffraction [2]. The Nd_2NiO_{4+d} compositions also have the advantage of including up to d = 0.25 of excess oxygen. Interestingly they show at the same time three single-phases at d = 0, 0.10 and 0.25, making them systems of choice to investigate lattice dynamics and apical oxygen delocalisation as a function of excess oxygen content.

We have performed the inelastic neutron scattering experiment on IN6 and compared our results with molecular dynamics simulations done at the C-Lab, on the $Nd_2NiO_{4.0}$, $Nd_2NiO_{4.10}$ and $Nd_2NiO_{4.25}$ single-phases. The trends in the spectral weights of the generalised density of states (DOS) as a function of stoichiometry, highlighted by red arrows in **figure 1**, have been reproduced by the simulated vibrational DOS [3].

We observed three main variations of the DOS with excess oxygen content, marked A, B, and C in **figure 1**, associated with displacements of neodymium and apical oxygen atoms in the [100] direction (A), in the [110] direction (B), and octahedra modes (C), respectively.

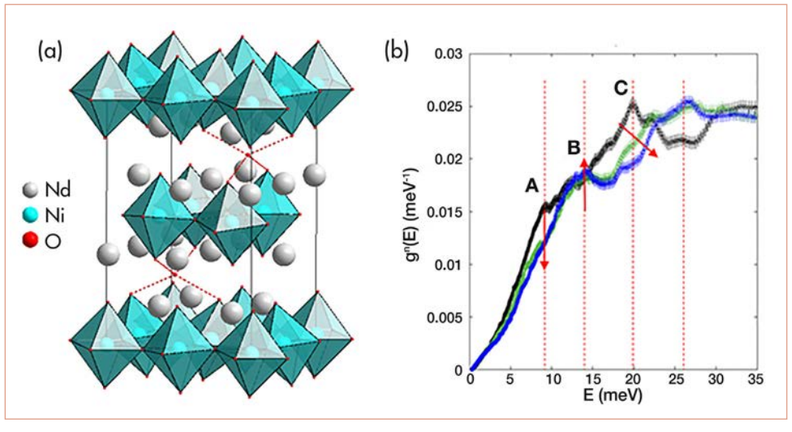

Figure 1

a) Schematic of the Nd_2NiO_{4+d} system which evidenced the interstitial sites that can be present with inclusion of extra oxygen. **b)** Generalised phonon density of states collected on the IN6 spectrometer of $Nd_2NiO_{4.0}$ (black), $Nd_2NiO_{4.10}$ (green), and $Nd_2NiO_{4.25}$ (blue) at T = 310K.

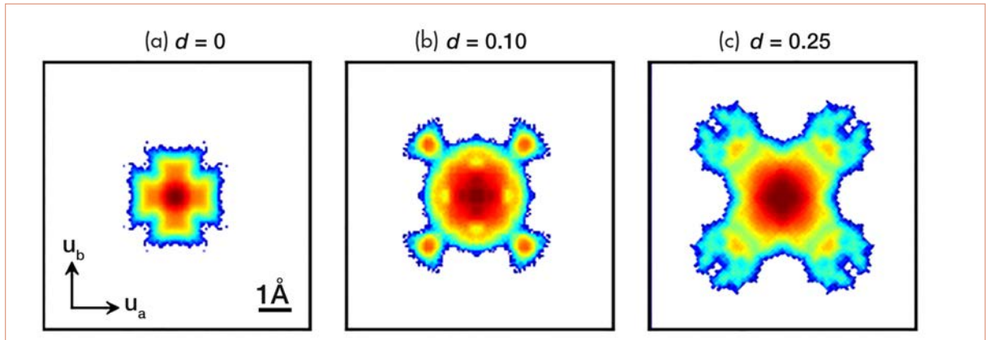

To go one step further in the analysis of molecular dynamics trajectories, we developed a code to generate positional recurrence maps (PRM), in order to isolate the dynamical contribution of selected non-equivalent atom displacements [3]. **Figure 2** shows PRM maps from 40 ps-long molecular dynamics simulations of the three single-phases with an optimised structure. We observed a pronounced shift of the dynamical delocalisation of apical oxygen atoms from the [100] direction (the tilting direction of NiO_6 octahedra in d = 0), to the [110] direction (the diffusion pathway direction).

Figure 2

Positional recurrence maps: displacement vectors of apical oxygen atoms in the Nd_2O_2 rock-salt layer from centre-of-mass positions projected on unitary vectors (u_a,u_b), with respect to the conventional F-cell. PRMs are calculated from *ab initio* molecular dynamics at T = 310K, of (a) $Nd_2NiO_{4.0}$, (b) $Nd_2NiO_{4.10}$ and (c) $Nd_2NiO_{4.25}$. The colour scale is logarithmic. Each PRM is cut in space to the conventional F-cell (black border).

Considering results from both densities of states and positional recurrence maps, we have evidenced that the mobility of oxygen atoms at room temperature in Nd_2NiO_{4+d} is directly correlated to variations of lattice dynamics with oxygen excess, with a shift of displacements from the [100] direction to the diffusion pathway direction toward [110]. The diffusion pathway itself, as shown in **figure 3**, is similar to the interstitials mechanism calculated at high temperature for related Re_2MO_{4+d}.

We can conclude that, if in the high-temperature regime, the densities of states are independent of the excess oxygen content, as excess oxygen does not contribute to lattice dynamics and behaves as single-particle defects, the coupling of lattice dynamics with oxygen mobility is specific to the moderate-temperature regime.

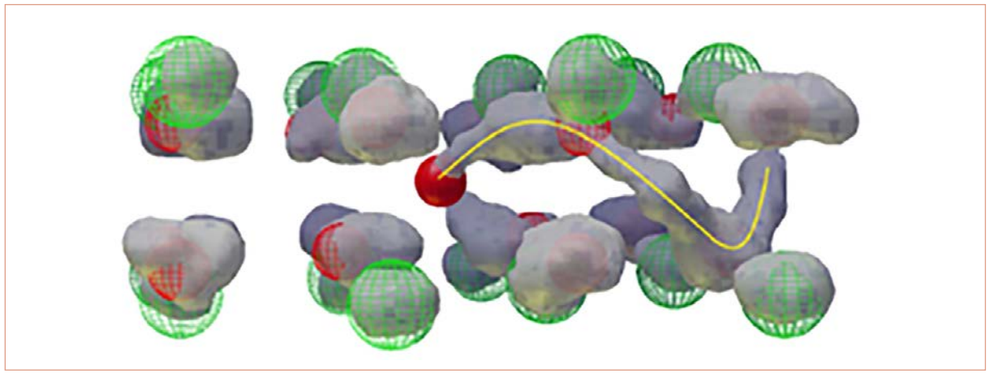

Figure 3

Diffusion pathway calculated from molecular dynamics simulations: zoom on a rock-salt layer containing the interstitial sites. Wired and plain red spheres represent respectively the initial position of apical oxygen atoms and excess oxygen in interstitial site. Grey clouds connecting interstitial sites to apical sites mean the oxygen atoms are mobile on this two-sites pathway, highlighted in yellow.

MATERIALS SCIENCE

Improved casting of high strength aluminium alloys for aeronautics applications

Stress analyser for engineering applications SALSA

AUTHORS

J.-M. Drezet (École Polytechnique Fédérale de Lausanne, Switzerland)
P. Celle and **O. Ribaud** (Constellium Technology Center, Voreppe, France)
T. Pirling (ILL)

REFERENCES

[1] J.-M. Drezet and T. Pirling, Influence of a wiper on residual stresses in AA7050 rolling plate ingots, Journal of Materials Processing Technology, 214 (2014) 1372

[2] J.-M. Drezet, A. Evans and T. Pirling, 14th International ESAFORM Conference on Material Forming, AIP Conf. Proc. 1353 (2011) 1131

The performance, lifetime and safety of any technical object depends strongly on the properties of the material. This is particularly true in the very demanding domain of aerospace technologies, which is always looking for materials that combine light weight with best performance. One such material is aluminium alloy 7050. Its strength is comparable to many steels: it has good fatigue strength, high resistance to stress corrosion cracking and high toughness. At the same time it guarantees good machinability. It is the number one material for fuselage frames, bulk head sections and wing skins.

This alloy is cast using the vertical direct chill casting process. The ingots are then cut before rolling. They can also be machined out. Direct chill casting is a semi-continuous process where the liquid metal is cooled rapidly through contact first with an open mould and second with cooling water running on its surface. This process allows casting of very large sections up to one metre thick.

As the ingot surface solidifies before and more rapidly than the centre, high thermal stresses appear in the bulk material. Although permanent plastic deformation partially relaxes stresses, tensile stresses appear during solidification at the centre of the ingot and can lead to the formation of solidification cracks, also called hot tearing. During further cooling these cracks might propagate in regions under tension. In any case, this flaw is detrimental and leads to the rejection of the casting. Furthermore, high thermally induced stresses can cause personnel injury and severe safety issues during downstream processing such as sawing, the step before rolling. Saw pinching or crack propagation ahead of the saw can cause violent ejection of material. These problems are more crucial in large-sized ingots (**figure 1**). Therefore huge efforts have been undertaken during the past decades to develop models for calculating thermally induced stresses and for better controlling their level.

The validity of mathematical models depends on the correctness of physical parameters describing the materials' properties and the determination of proper boundary conditions. Of course such models must be validated against experimental data. Up to now most have been assessed only against measured surface distortions. Particularly difficult is the validation of computed residual stresses, since most methods – such as hole-drilling, cut compliance or layer removal techniques – are limited to near surface regions or provide only two stress tensor components.

Figure 1
Aluminium ingot taken out after casting (**left**); cold cracking of ingot (**right**).

Figure 2
One of the ingots wrapped in a security net and mounted on SALSA for stress determination (**left**); measuring locations of line scans (**right**). The sketch shows a quarter section of the sample.

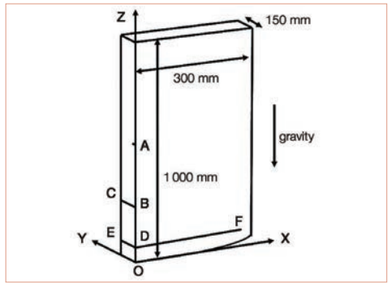

The way forward is neutron stress imaging. Due to the high penetration power of neutrons in metals, especially in aluminium, it is possible to non-destructively determine stress distribution within the material. Neutrons provide the full stress tensor in industrial-size engineering parts with a lateral resolution in the millimetre range. For the first time we applied this technique on large cast aluminium billets at PSI and the ILL [2]. Industrially cast round billets can be 8 m long. This is too big even for SALSA, the stress analyser for engineering applications at the ILL. But we calculated that within a length of 1 m, stresses in the region of interest are not affected by sawing. For rectangular ingots, the dimensions of the samples chosen for stress determination were 0.3 x 0.6 x 1 m^3 and had a weight of about 500 kg. In order to be protected against unexpected ejection of material, the ingots were wrapped in security nets (**figure 2**). The samples were cast at a speed of 90 mm/min at the experimental cast house at Constellium CRV in Voreppe, near Grenoble.

The purpose of our measurements was not only to verify our numerical casting model but also to prove whether it is possible to reduce the above-described casting stresses. As already described, direct chilled casting uses flowing water to rapidly cool the metal. As aluminium solidifies very rapidly, the idea is to eject the running water from the ingot surface at a certain distance below the mould using a rubber wiper. Reducing the water cooling efficiency keeps the alloy warmer during casting and thus increases its ability to relax stresses by plastic deformation. The amount of reduction of as-cast residual stresses was determined at SALSA on two ingots: one cast using a wiper and one cast without a wiper (**figure 3**).

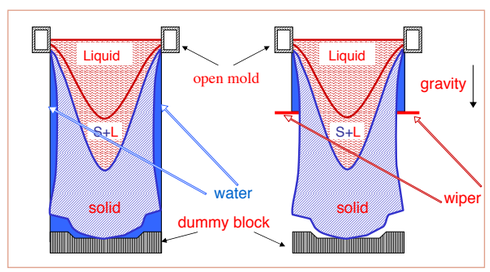

Figure 3
DC-casting (**left**); DC-casting with a wiper (**right**) that takes cooling water away after a short distance.

The measuring locations for neutron stress determination were chosen as shown in **figure 2**. Scans were performed along lines OA, DE, BC and DF with a lateral resolution of 2 x 2 x 4 mm^3 in the three principal directions of the stress tensor. This was possible due to the unique set-up of SALSA using radial focusing collimators for beam definition, since they allow for precise definition of the gauge volume and leaving space for sample manipulation.

As predicted by the thermomechanical model of casting, the region where the alloy remains at a temperature higher than 250 °C is extended when using a wiper. As a result stresses can relax (**figure 4a**). We measured an overall reduction of tensile residual stresses by one third, when using a wiper (**figure 4b**).

Figure 4
a) Computed and measured stress profiles in the principal axes' directions along OA for the ingot cast without a wiper. ND stands for neutron diffraction and FEM for finite element modelling.
b) Von Mises stresses along the symmetry axis of the ingot. Stresses are reduced by about 35 % when using a wiper.

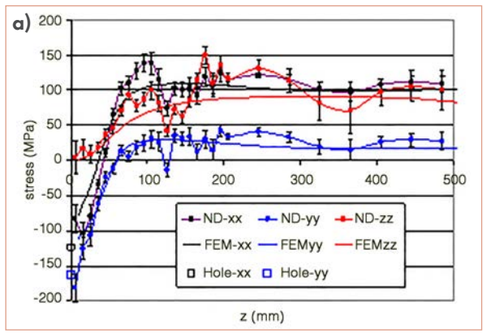

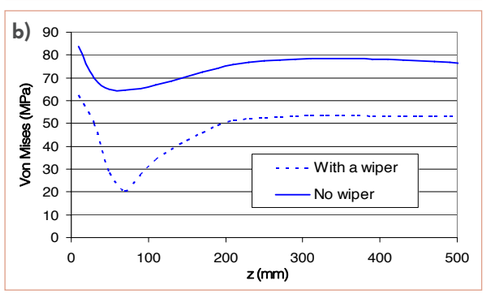

MATERIALS SCIENCE

Ice XVI – how emptying clathrate hydrates helps to keep pipelines in flow and unlock a potent energy source of the future

High intensity diffractometer D20

Empty clathrates belong to a family of tetrahedrally co-ordinated structures in which H-bonded water molecules are organised in the form of cages. Such topologies possess densities lower than that of ordinary Ice I and require substantial negative pressures (the equivalent of tension) to be thermodynamically stable. Lacking experimental means to probe such environments, these solids were studied in the past exclusively via computational methods. The present discovery of one of these empty structures, Ice XVI, brings them into real life, adding a new jewel to the fascinating treasure chest of water ices.

AUTHORS

A. Falenty and **W.F. Kuhs** (Göttingen University, Germany)
T.C. Hansen (ILL)

REFERENCES

[1] A. Falenty, T.C. Hansen and W.F. Kuhs, Nature 516 (2014) 231

[2] A.N. Salamatin, A. Falenty, T.C. Hansen, and W.F. Kuhs, Energy & Fuels 29 (2015) 5681

Empty clathrates are by far not merely scientific curiosities. In their filled form they were known for many decades as gas hydrates, in which water cages are stabilised under elevated pressures and/or low temperatures by various guests, usually small apolar and hydrophobic molecules or atoms. Not by accident is one of these empty hydrate structures the best answer to Lord Kelvin's question of how to fill space with minimum partitional area. This unique marriage of convenience between substances usually considered alien, like water and methane, received growing attention from the scientific community and industry due to its numerous old and novel applications.

Gas hydrates are known from their natural occurrences within marine sediments where they lock away huge quantities of hydrocarbons. In recent years marine gas hydrates have also become a target of CCS (carbon capture and storage) studies where carbon dioxide injected in existing methane hydrate deposits would spontaneously replace CH_4 in cages and leave a stable CO_2 hydrate behind. The technical challenges of such CH_4 recovery are certainly large but still worth exploring. The University of Göttingen is a member of the SUGAR project funded by the German government, whose aim is to explore the scientific, technical and economic possibilities of such an undertaking. Similar activities are currently underway in Japan, China, India and elsewhere. An area where clathrate research is of more immediate benefit is in the flow-assurance of pipelines where hydrocarbons are transported at high pressures. Under these conditions the formation of gas hydrates is possible, causing substantial blockages the prevention of which costs industry half a billion euros per year worldwide. The use and control of gas hydrates largely depends on the ability to accurately predict thermodynamic stability boundaries of gas hydrates; these still remain questionable for mixed systems with two or more guest species. One of the ways to improve this situation is to get reliable data on the chemical potential of the empty water frame, which plays a central role in the statistical thermodynamic theory of these compounds. As values for this quantity were at best educated guesses, their experimental verification was considered as reaching the "holy grail" of gas hydrate research.

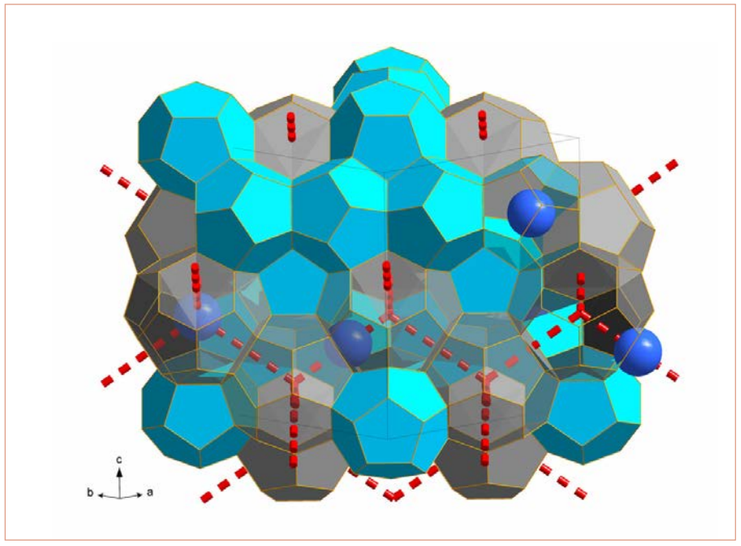

Figure 1

The Ice XVI structure is obtained by leaching of Ne atoms shown in blue; they can easily travel between large cages (in grey) passing through six-membered rings of water molecules (red dashed lines). Removal of Ne atoms from the small cages (in blue) requires the presence of a water vacancy in one of the five-membered rings [2].

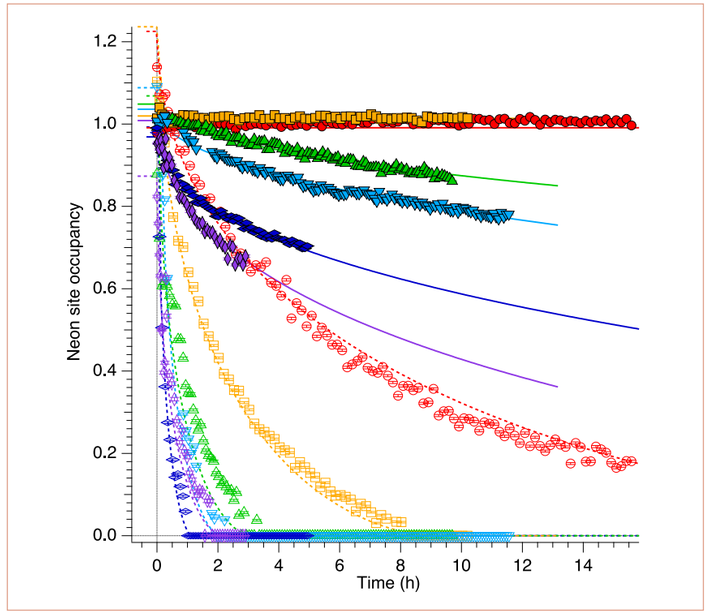

Figure 2

Cage filling as a function of time for different temperatures. A shrinking core model of the Ne leaching process fits values from sequential Rietveld refinements. Solid markers – and solid line for the fits – present the small cage (Ne1), empty markers – and dashed lines – the large ones (Ne2). Red circles and lines represent 110 K, orange squares and lines 120 K, green triangles and lines 130 K, light blue triangles and lines 135 K, dark blue flat rhombi and lines 140 K, magenta upright rhombi and lines 145 K.

Recently we have established an experimental path leading to the first *empty* clathrate hydrate [1] shown in **figure 1**. We started by synthesising a clathrate filled with neon atoms locked into a structure of "type II" – one of three observed clathrate types in nature. This neon hydrate was then exposed to vacuum at temperatures up to about 140 K for hours up to several days, while neutron diffraction data was taken by the ILL's high flux diffractometer D20. The *in situ* data obtained and shown in **figure 2** provided a direct view on the emptying process. The larger of the two different cavities was emptied first, most likely *via* a three-dimensional network of shared hexagonal faces. Emptying the smaller cages, exclusively made up of pentagonal faces, takes distinctly longer; eventually neon escapes through a pentagonal face into an adjacent large cage, from which it can migrate further by the aforementioned route. While hexagonal faces are probably wide enough for neon to pass through, jumping through pentagonal faces most likely needs the presence of water vacancies. Such a mechanism was recently established by our *in situ* experimental studies on the CO_2-hydrate system, also performed on D20 [2].

As a stable solid, composed entirely of molecules of water, the empty clathrate also represents a new phase of ice: Ice XVI. In contrast to all gas hydrates, but in agreement with normal hexagonal ice, it exhibits negative thermal expansion at low temperatures. Moreover, its water framework shows an expansion of cages upon emptying, a fact which had been ignored in any form of statistical thermodynamic theory so far. Thus, Ice XVI not only provides a unique benchmark for any model that pretends to describe the interaction of water molecules but also permits the accurate determination of some fundamental structural and thermodynamic properties of gas hydrates. This in itself is an important step forward. It is *via* this better understanding that one can hope to advance on various possible routes to securing the world's energy resources.

MATERIALS SCIENCE

Understanding the structures of the new hybrid lead iodide photovoltaics

High intensity diffractometer D20

Materials that can be used in printable solar cells offer cheap, renewable energy combined with ease of device construction. Powder neutron diffraction studies on D20 allowed us to gain unprecedented insight into the structures of the new hybrid lead perovskite photovoltaic materials as a function of temperature [1]. These results, particularly on the phase stable at room temperature, have in turn generated a deeper understanding of how these materials function within practical solar cells.

AUTHORS

M.T. Weller and **O.J. Weber** (University of Bath, UK)
P.F. Henry (ESS, Lund, Sweden)
A.M. Di Pumpo and **T. Hansen** (ILL)

REFERENCES

[1] M.T. Weller, O.J. Weber, P.F. Henry, A.M. Di Pumpo and T.C. Hansen, Chem. Comm., 51 (2015) 4180
[2] M.M. Lee, J. Teuscher, T. Miyasaka, T.N. Murakami and H.J. Snaith, Science 338 (2012) 643
[3] W.S. Yang, J.H. Noh, N.J. Jeon, Y.C. Kim, S. Ryu, J. Seo and S.I. Seok, Science 348 (2015) 1234
[4] J.M. Frost, K.T. Butler and A. Walsh, APL Materials 2 (2014) 081506

The hybrid perovskite phases methylammonium lead iodide ($[CH_3NH_3]PbI_3$, MAPI) and formamidinium lead iodide $(HC(NH_2)_2PbI_3$, FAPI) are attracting intense scientific attention as highly efficient and low cost photovoltaic materials [2]. Device efficiencies have rapidly risen to over 20 % in 2015 (see **figure 1** [3]).

We have investigated the full structure of MAPI using neutron powder diffraction on a fully hydrogenous sample. The results provided key information on light atom positions in this heavy metal compound and distinguished carbon and nitrogen, due to their contrasting neutron scattering lengths. Investigation of a hydrogenous sample also had the advantage of avoiding isotope effects, while also providing a strong contrast between carbon, nitrogen and hydrogen, due to the latter's negative scattering length. The ability to extract good structural information from hydrogenous materials requires the use of a high flux, medium resolution neutron diffraction instrument, such as D20.

Between 100 K and 340 K, MAPI undergoes two phase transitions as can be readily seen in **figure 2**. Above 327 K the structure is a metrically cubic perovskite with regular PbI_6 octahedra; between 327 and 165 K, i.e. including room temperature, the material is tetragonal; while below 165 K an orthorhombic unit cell is adopted. These phase transitions have been found in this work to be associated with the orientational ordering of the methylammonium cation on its site at the centre of the perovskite unit cell and the formation of weak NH…I hydrogen bonds.

Full analysis of the data used a rapid parametric approach to extract the complete structure at 5 K intervals in each of the orthorhombic, tetragonal and cubic unit cell regions. At all temperatures the methylammonium cation (MA) in MAPI is oriented towards an open face of the (distorted) cube formed by the linked PbI_6 octahedra. At low temperatures the orientation of the MA cation is fixed as a result of hydrogen bonding between the $–NH_3$ terminal groups and the framework iodide atoms. Above 165 K, after the transition to tetragonal phase, the MA cations become rotationally disordered in the crystallographic *ab* plane over four orientations, similar to those found for the orthorhombic phase and directed towards the distorted cube faces (**figure 3**). The MA cation is displaced slightly off centre of the unit cell with very weak hydrogen-bonding interactions between N-H and framework iodide. Analysis of atomic displacement parameters infers that the $–NH_3$ and CH_3 groups undergo almost unhindered rotation around the C–N bond. Heating to room temperature results in increasingly free motion of the MA cation and a slow migration towards a central position within the perovskite A-site cavity. This is accompanied by a decrease in the reduced *c/a* ratio towards unity and straightening of the inorganic framework Pb-I-Pb bonds before the transition to the cubic phase at 327 K.

In the cubic phase the MA^+ cation appears to remain directed towards the cube faces, orientationally disordered over six positions – though a high level of positional and thermal disorder exists in this phase.

The observed high level of orientational motion of the MA^+ cation in the tetragonal phase at room temperature is likely to be related to the excellent photovoltaic performance of this material but also the anomalous hysteresis effect that has been reported from experiment. Reference [4] proposed that the internal electrical fields associated with microscopic polarisation domains contribute to hysteretic anomalies due to variations in electron-hole recombination process. The formation of these domains is likely to be related, in turn, to the local orientation patterns of the MA cations, and further computational modelling work is ongoing using the full structural models discovered and reported in this work.

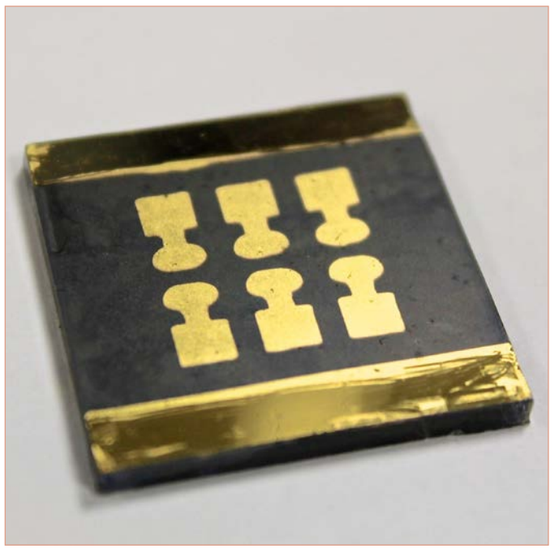

Figure 1
A solar cell constructed of the new hybrid perovskite materials (courtesy of R. Niemann and P. Cameron, University of Bath).

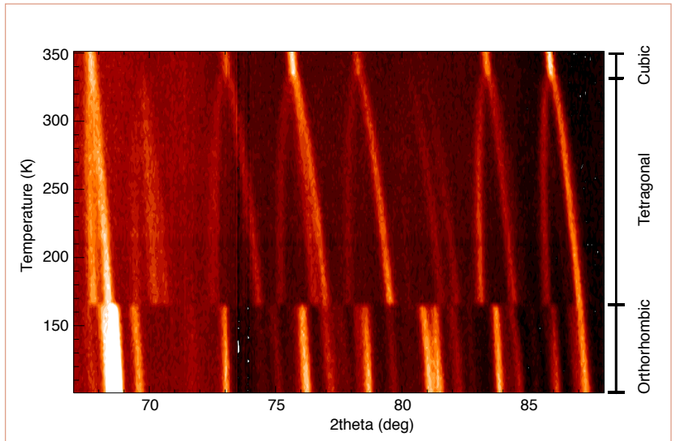

Figure 2
Stacked plot, viewed vertically, of part of the neutron powder diffraction data (67-88°) collected on D20 from MAPI over the temperature range 100 - 352 K. Peaks are shown as white and pale orange on a black background. The phase changes at 165 and 327 K are clearly observed, as is the overall unit cell expansion.

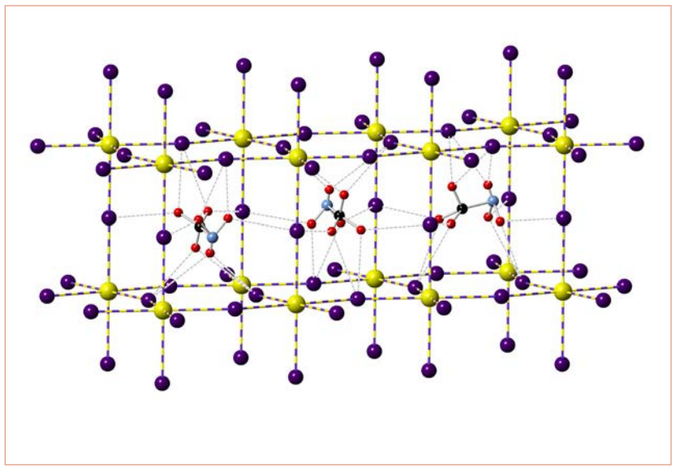

Figure 3
Representation of the structures of MAPI in the room temperature tetragonal phase showing three adjacent cells. Pb = yellow, I = purple, N = blue, C = black and H = red. The orientation of the methylammonium cation in neighbouring unit cells is shown in three of the four possible orientations.

MAGNETISM

Intra-unit-cell magnetic correlations near optimal doping in $YBa_2Cu_3O_{6.85}$

Diffuse scattering spectrometer D7
Three-axis spectrometer 4F1 at LLB

The cuprate high-temperature superconductors were discovered 30 years ago. However, the mechanism at the origin of high-temperature superconductivity remains an unsolved problem. The most surprising fact about the cuprates is that they are derived from insulators and, when they are not superconductors, they act as bad or strange metals (see the phase diagram in *figure 1*). In particular, a phase called the "pseudo-gap" appears before superconductivity appears. This phase is regarded as the "Rosetta Stone" for discovering the physical principles that underlie the cuprates' behaviour.

AUTHORS

L. Mangin-Thro, Y. Sidis and **P. Bourges** (LLB, CEA Saclay, France)
A. Wildes (ILL)

REFERENCES

[1] P. Bourges and Y. Sidis, C.R. Physique 12 (2011) 461
[2] C.M. Varma, Nature 468 (2010) 184
[3] L. Mangin-Thro, Y. Sidis, A. Wildes and P. Bourges, Nature Comm. 6 (2015) 7705

Polarised neutron scattering experiments on four cuprate families, including $YBa_2Cu_3O_{6+x}$, reported the existence of an intra-unit-cell (antiferro)magnetic order which develops below the pseudo-gap transition temperature T_{mag} (= T*) [1]. This order indicates that translation invariance is preserved but time-reversal symmetry is broken, demonstrating that the pseudo-gap is a broken symmetry state. This magnetic order could be the result of loop currents, flowing within the unit cell, producing staggered orbital magnetism [2]. In this scenario, the order is likely to vanish around a quantum critical point (QCP) close to the hole doping p = 0.19. Experimentally, the existence of the intra-unit-cell magnetic order is well-documented over a wide, hole-doping range. The order is long-ranged at low doping and vanishes at high doping (around p = 0.19). However, its evolution around optimal doping (where the superconducting dome shows its maximum) had not yet been addressed.

Our study [3] on a $YBa_2Cu_3O_{6.85}$ (p = 0.15) single crystal, performed on 4F1 (LLB), proves the persistence of the intra-unit-cell magnetic order at relatively high temperature near optimal doping. However, the magnetic intensity is strongly reduced compared with lower doped samples, which could be triggered by a redistribution of the magnetic scattering in momentum space. Thanks to polarised neutron diffraction measurements performed on the ILL instrument D7, we did indeed observe finite magnetic correlation lengths [3]. The intra-unit-cell magnetic order is short-ranged around optimal doping.

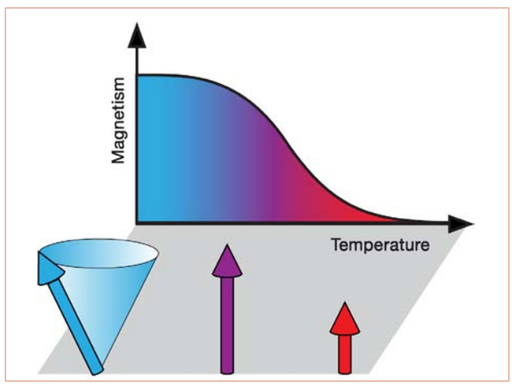

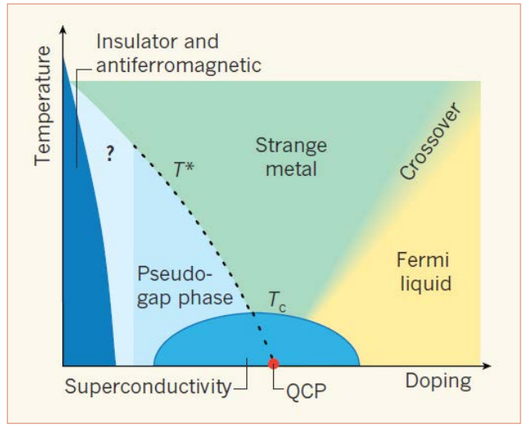

Figure 1
Generic temperature vs. hole doping (p) phase diagram for the cuprates [2].

In addition, we were able to extract the temperature dependencies of the components of the magnetic moment M (see **figure 2**). At low temperature, both out-of-plane (M_c) and in-plane (M_{ab}) components are present, yielding a tilt of the magnetic moment in agreement with previous reports [1]. Surprisingly, the in-plane component vanishes at high temperature (above T_{mag}). The moment thus points perpendicular to the plane, as originally expected in the loop current model [2]. While at first glance a tilt of the magnetic moment upon cooling is rather counterintuitive in the framework of loop currents, the evolution of the scattering magnetic intensity could actually highlight the stabilisation of a ground state made of a quantum superposition of different loop current patterns. In this scenario, thermal fluctuations would overcome quantum effects at high temperature, restoring classical magnetic correlations involving purely out-of-plane magnetic moments. The discovery of these two temperature regimes puts stringent constraints on any model that tries to describe the pseudo-gap physics.

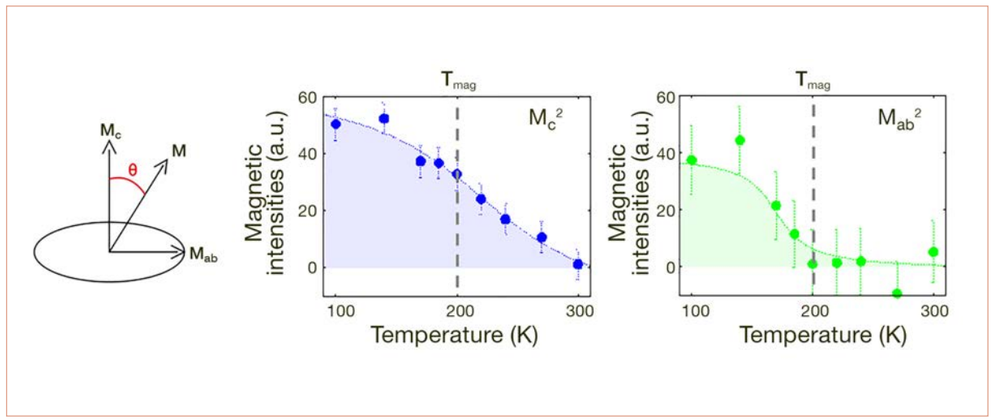

Figure 2
Temperature dependencies of both out-of-plane (M_c) and in-plane (M_{ab}) magnetic moment components, from polarised neutron measurements performed on the ILL instrument D7.

SCIENTIFIC HIGHLIGHTS

MAGNETISM

Spin-stripe phase in a frustrated zigzag spin-1/2 chain

Spin-polarised diffractometer D3
TriCS single-crystal diffractometer at PSI

In strongly correlated electron systems, periodic modulations on the nanoscale have typically been associated with competition between short- and long-range interactions, for example, exchange and dipole–dipole interactions in the case of ferromagnetic thin films. Here we highlight that spin-stripe textures may also develop in antiferromagnets where long-range dipole–dipole magnetic interactions are absent. We have discovered a magnetic stripe structure that appears at the transition between the spiral and collinear magnetic orders in the β-$TeVO_4$ compound [1].

AUTHORS

M. Pregelj and **A. Zorko** (Jožef Stefan Institute, Ljubljana, Slovenia)
O. Zaharko (Paul Scherrer Institut (PSI), Villigen, Switzerland)
H. Nojiri (Tohoku University, Sendai, Japan)
H. Berger (École Polytechnique Fédérale de Lausanne, Switzerland)
L.C. Chapon (ILL)
D. Arčon (Jožef Stefan Institute, Ljubljana and University of Ljubljana, Slovenia)

REFERENCES

[1] M. Pregelj, A. Zorko, O. Zaharko, H. Nojiri, H. Berger, L.C. Chapon and D. Arčon, Nature Commun. 6 (2015) 7255
[2] Yu. Savina, O. Bludov, V. Pashchenko, S.L. Gnatchenko, P. Lemmens and H. Berger, Phys. Rev. B 84 (2011) 104447
[3] J. Sudan, A. Lüscher and A. Läuchli, Phys. Rev. B 80 (2009) 140402(R)

Initial interest in the β-$TeVO_4$ system occurred due to a chain arrangement of the magnetic V^{4+} (S = ½) ions (**figure 1b**). Previously this system was interpreted as a simple spin-1/2 chain with only nearest-neighbour antiferromagnetic interaction [2]. By a combination of magnetic susceptibility, magnetisation, specific heat, neutron diffraction and spherical neutron polarimetry measurements we reveal that competing ferromagnetic nearest-neighbour (J_1) and antiferromagnetic next-nearest-neighbour (J_2) interactions are comparable in magnitude. The experimentally derived magnetic phase diagram (**figure 1d**) corroborates the main features of the theoretical one (**figure 1a**) developed for the frustrated ferromagnetic spin-1/2 chain model [3], establishing β-$TeVO_4$ as a nearly ideal realisation of this model. At very low temperatures, weak but sizeable inter-chain couplings assist long-range magnetic orders to develop. The competition of the frustrated magnetic interactions leads to several magnetic states appearing at T_{N1} = 4.65 K, T_{N2} = 3.28 K and T_{N3} = 2.28 K. A combination of neutron diffraction integrated intensity datasets collected on the TriCS single crystal diffractometer at SINQ (PSI), Switzerland and neutron spherical polarimetry matrices from the D3 diffractometer at the ILL allows us to establish the higher temperature magnetic phase as an amplitude modulated state with the wave vector k = (-0.195 0 0.413), while the lowest temperature phase acquires the spiral character with k = (-0.208 0 0.423). In between, in a narrow temperature range between T_{N2} and T_{N3}, peculiar 'super-satellites' to the main incommensurate magnetic reflections appear (**figure 2**). The map in the inset of **figure 2a** shows that the shift is only Δk = (-0.030 0 0.021) at 2.5 K and that the 'super-satellites' are resolution limited. Thus the magnetic order experiences additional nanometer-scale stripe modulation with the well-defined period of 12.7 nm. This state can be named 'domain wall crystal', as it is reminiscent of domain patterns observed in two-component systems but at the same time corresponds to a coherent and uniform magnetic state.

In future we shall focus on the magnetic field behaviour of this extremely rich system. The theory of frustrated ferromagnetic zigzag chains predicts that the vector-chiral (VC) ground state is at elevated magnetic fields succeeded by collinear spin-density-wave (SDW) phases, with two- (p = 2) or three-magnon (p = 3) bound states (**figure 1a**). Moreover, when magnetisation M approaches saturation (M/M_{sat} = 1), intriguing multipolar orders should develop. For β-$TeVO_4$ such quadrupolar/spin-nematic phases could occur already at 18.7 T, and we plan to investigate this regime with high-field neutron diffraction.

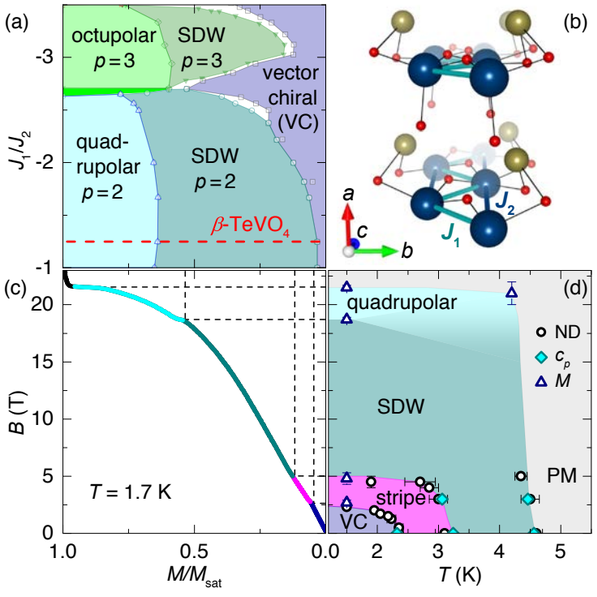

Figure 1

a) Theoretical phase diagram of the frustrated ferromagnetic spin-1/2 chain model as a function of J_1/J_2 and M/M_{sat} [2]). VC and SDW denote vector-chiral and spin-density-wave phases respectively, and *p* is the order of the bound magnon state;
b) The fragment of the crystal structure of β-$TeVO_4$ with zigzag-chain interactions. Small, medium and large spheres denote O, Te and V atoms respectively;
c) Magnetisation normalised to the saturation value (M/M_{sat}) B//a-axis;
d) The experimental magnetic phase diagram of β-$TeVO_4$. PM stands for the paramagnetic state; ND, c_p and M denote data points from neutron diffraction, specific heat and magnetisation measurements, respectively.

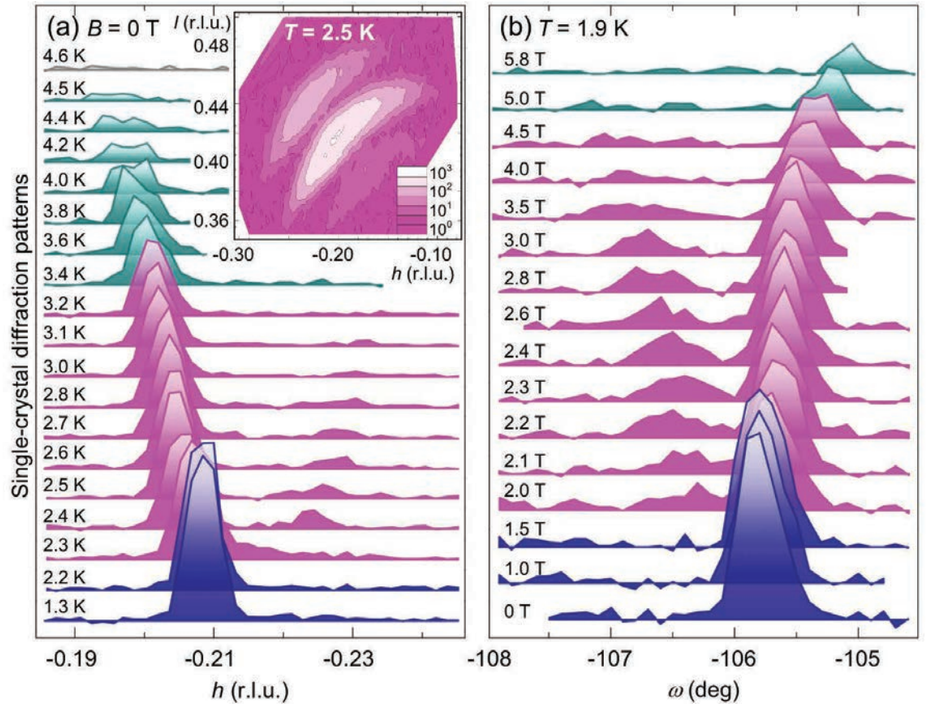

Figure 2

a) The temperature evolution of the main (-0.208 0 0.423) magnetic reflection **inset)** the corresponding k-map measured at 2.5 K.

b) The magnetic-field dependence (B||a) of the (0.208 2 0.577) reflection at 1.9 K. The colour coding denotes the spiral, VC (purple), stripe (magenta) and amplitude modulated, SDW (dark cyan) ordered phases.

MAGNETISM

Finite size effects in chains of antiferromagnetically coupled spins

Spin-polarised diffractometer D3 and single-crystal diffractometer D19 5C1 diffractometer at LLB

The current race for miniaturisation of magnetic devices for information storage and processing is reaching the ultimate limit of a few atoms per magnetic unit, a promising new route being offered by the exploitation of the spins of atoms organised in short chains. Functionalising such spin segments requires a thorough characterisation of their spin structure. For that purpose, we used single-crystal diffraction with polarised neutrons on D3 at the ILL and on 5C1 at LLB, and unpolarised neutrons on D19 to accurately measure the spin distribution along a chain of eight antiferromagnetically coupled magnetic ions [1]. Our results show that the parity and topology of the chain govern the spin distribution under an applied magnetic field.

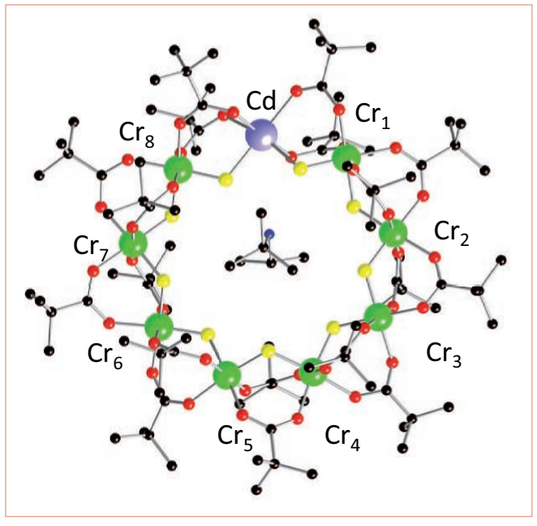

AUTHORS

T. Guidi (ISIS, UK) and **B. Gillon** (Laboratoire Léon Brillouin (LLB), France)
S.A. Mason and **A. Stunault** (ILL)
E. Garlatti, S. Carretta and **P. Santini** (University of Parma, Italy)
R. Caciuffo (Joint Research Centre (JRC), Karlsruhe, Germany)
J. van Slageren (University of Stuttgart, Germany)
G.A. Timco and **R.E.P. Winpenny** (University of Manchester, UK)

REFERENCES

[1] T. Guidi, B. Gillon, S.A. Mason, E. Garlatti, S. Carretta, P. Santini, A. Stunault, R. Caciuffo, J. van Slageren, B. Klemke, A. Cousson, G.A. Timco and R.E.P. Winpenny, Nat. Commun. 6 (2015) 7061 [doi: 10.1038/ncomms8061]
[2] M. Affronte, S. Carretta, G. A. Timco and R.E.P. Winpenny, Chem. Commun. 18 (2007) 1789
[3] S. Carretta *et al.*, Phys. Rev. B 67 (2003) 094405
[4] A. Bianchi *et al.*, Phys. Rev. B 79 (2009) 144422

Finite spin chains made of a few magnetic ions are the ultimate-size structures that can be engineered to perform spin manipulations for quantum information devices. Their spin structure is expected to show finite size effects, and this is of great importance both for fundamental physics and applications. The experimental realisation of finite spin chains has traditionally involved a top-down approach, where an ideal infinite chain is 'cut' into segments by introducing diamagnetic impurities. This procedure leads to an ensemble of chains with different lengths, containing a number of atoms with varying parity. Therefore the study of their magnetic behaviour and the effect on their magnetic properties associated with the parity of the chain is averaged out in the experimental measurements.

A more flexible and controlled bottom-up approach is offered by the chemistry of antiferromagnetic molecular rings. These are magnetic molecules with a ring-shaped cyclic structure and a dominant antiferromagnetic (AF) coupling between nearest-neighbour ions [2].

We have investigated the local moment distribution of two prototypical members of this family of molecules: the homonuclear Cr_8 "closed" ring, and the heteronuclear Cr_8Cd "open" ring. Homonuclear AF rings, like Cr_8, are characterised by a singlet ground state and periodic boundary conditions. The introduction of a non-magnetic atom (Cd) in the ring breaks the cyclic symmetry with an open-boundary condition resulting in an effective model system for an "open" finite chain (**figure 1**). The advantage of open rings with respect to doped chains is that all the rings have the same length. Thus no distribution of chain length has to be considered, allowing the possibility of unique interpretation of experimental data.

For both molecules, the AF coupling between first-nearest-neighbour Cr^{3+} ions carrying a spin $s = 3/2$ leads to a singlet spin ground state $S = 0$ and to excited states with integer-spin values $S = 1,2,...$ The energy-level diagram of the molecules has been investigated using multiple techniques, namely inelastic neutron scattering [3, 4], high-field magnetisation and muon spin relaxation.

Figure 1

Structure of the Cr_8Cd molecular ring. Cr atoms are represented in green, Cd in purple, O in red, F in yellow and C in black. Hydrogen atoms are omitted for simplicity.

Figure 2

Top) Spin density map for Cr_8Cd (in muBA–2 units) obtained by the refinement of the D3 experimental data for applied field 9 Tesla at $T = 1.8$ K (projection along the crystallographic *b* axis).
Bottom) Classical spin ground state configuration for an even-open chain and an even-closed chain under an external magnetic field.

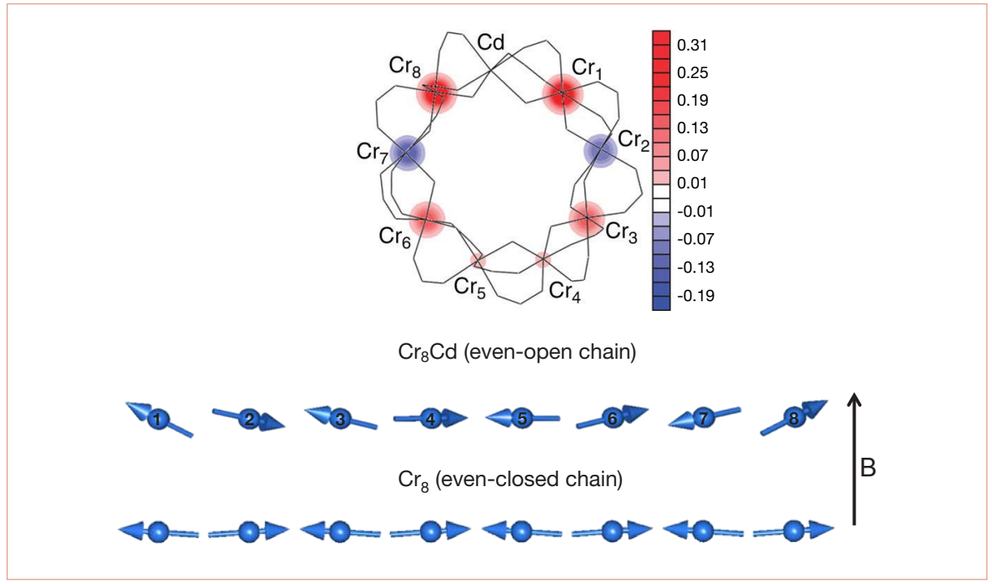

Despite the very similar exchange coupling constant *J* for both molecules, the energy-level diagrams are significantly different. In particular the energy of the first excited spin state $S = 1$ is lowered from 0.7 meV in Cr_8 to 0.2 meV in Cr_8Cd. This can be qualitatively understood if we consider that it requires less energy to rotate the two spins at the end of an open chain as they only have one nearest-neighbour exchange interaction, as compared with the two neighbours in a closed chain.

We used polarised neutron diffraction (PND) for determining the experimental spin distribution in Cr_8Cd in non-zero spin ground states induced by applying a magnetic field at low temperature. For a spin density PND study it is first necessary to determine the nuclear structure factors at low temperature, and therefore a neutron structural study of a single crystal of Cr_8Cd was performed at 15 K using the D19 diffractometer.

We used D3 equipped with a 9 T cryomagnet to measure the spin density distribution for two excited spin states stabilised by an external magnetic field. At 4.6 Tesla and $T = 1.8$ K, the spin ground state is $|S = 1, M_S = 1>$, whereas at 9 Tesla the lowest energy spin state becomes $|S = 2, M_S = 2>$. The spin densities derived from the D3 experiment at 9 T are shown in **figure 2** (top). From the data refinement it is found that most of the spin density is located at the Cr positions. Moreover, there is an accumulation of spin density at the edges of the open ring and negligible spin density at the Cr positions further away from the Cd. The sign of the spin moments alternates from positive to negative along the ring, which indicates a staggering of the magnetisation. The distribution of local magnetisation is consistent with a non-collinear spin arrangement, as predicted by theory for an even, AF finite open chain.

Similar PND studies were performed on a single crystal of the closed ring Cr_8 complex. The experiments were performed using the 5C1 diffractometer at Laboratoire Léon Brillouin and a small, uniform, local moment was found on each Cr in the ring. This is consistent with a spin-flop state where the components along **B** of the spin moments are small and uniform due to the cyclic symmetry of the cluster (see **figure 2** bottom, showing the classical spin configuration in a magnetic field for an open and closed chain of eight atoms).

In summary, the neutron diffraction experiments have allowed us to demonstrate that there is a substantial difference between the behaviour of an 'open' and a 'closed' even-numbered chain under an applied magnetic field. In particular, even-open antiferromagnetic chains have a non-collinear arrangement of the spin moments whilst a spin-flop state is observed for even-closed chains. These results demonstrate that the investigated systems and the technique used in the present study give unprecedented and accurate information on the effect of topology on the spin structure of finite spin chains.

MAGNETISM

Hidden order in spin-liquid $Gd_3Ga_5O_{12}$

Four-circle diffractometer D9

The famous ability of neutron scattering experiments to reveal the microscopic ordering in materials usually relies on analysis of the observed Bragg peaks. "Hidden" orders do not produce Bragg peaks in scattering experiments and are therefore more difficult to observe experimentally. We used single-crystal neutron diffraction experiments to show that the diffuse (non-Bragg) component of the magnetic scattering provides indirect evidence for a type of hidden order in a frustrated magnet, $Gd_3Ga_5O_{12}$ (GGG). This order is multipolar and is driven by an interplay of antiferromagnetic spin correlations and local spin anisotropy.

AUTHORS

J.A.M. Paddison (University of Oxford and ISIS, UK and Georgia Institute of Technology, Atlanta, USA)
H. Jacobsen and **P.P. Deen** (Niels Bohr Institute, University of Copenhagen, Denmark and ESS, Lund, Sweden)
O.A. Petrenko (Department of Physics, University of Warwick, UK)
A.L. Goodwin (University of Oxford, UK)
M.T. Fernández-Díaz (ILL)

REFERENCES

[1] R. Moessner and A.P. Ramirez, Phys. Today 59 (2006) 24
[2] O.A. Petrenko, C. Ritter, M. Yethiraj and D. McK. Paul, Phys. Rev. Lett. 80 (1998) 4570
[3] J.A.M. Paddison and A.L. Goodwin, Phys. Rev. Lett. 108 (2012) 017204
[4] P. Schiffer *et al.*, Phys. Rev. Lett. 74 (1995) 2379
[5] Work published in Science 350 (2015) 179

In frustrated magnetic materials the lattice geometry prevents all magnetic interactions from being satisfied simultaneously, suppressing the formation of conventional spin-dipolar order [1]. This makes frustrated magnets ideal systems to look for unconventional forms of order. The material we studied, $Gd_3Ga_5O_{12}$ (GGG), has long been investigated as a spin-dipole liquid ([2] and refs therein). Magnetic Gd^{3+} ions are coupled by antiferromagnetic interactions and occupy two interpenetrating, three-dimensional networks of corner-sharing triangles (**figure 1a**). The key topological feature is that each Gd^{3+} ion is surrounded by a loop of ten Gd^{3+} ions, as shown in **figure 1b**. While GGG undergoes a transition to an unconventional spin-glass state at $T_g \sim 0.14$ K, here we focus on the spin-liquid state that exists just above this temperature.

While Gd-containing magnets can provide exemplary models of frustrated magnetism, studying them using neutron scattering is notoriously difficult since the neutron-absorption cross-sections of the isotopes ^{155}Gd and ^{157}Gd are extremely large. The four-circle diffractometer D9 at the ILL has the ideal combination of characteristics to ameliorate this problem: high neutron flux, low background and, most importantly, a high-energy neutron beam with which the neutron absorption cross-section is reduced. These factors allowed us to measure scattering from a GGG single crystal, despite the fact that our sample was not enriched with a non-absorbing isotope. We obtained the magnetic contribution to the diffuse scattering at T = 0.175 K by subtracting a T = 10 K background measurement. Our experimental data are shown in **figure 1c**.

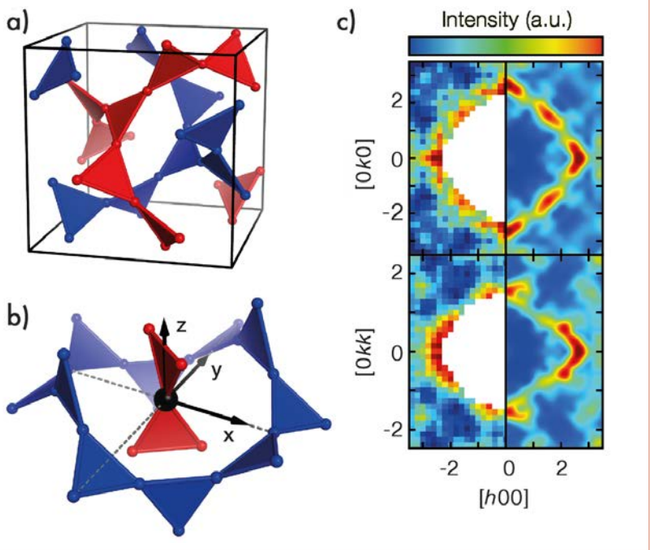

Figure 1
a) Crystal structure of GGG showing only magnetic Gd^{3+} ions. The two interpenetrating networks of corner-sharing triangles are coloured red and blue.
b) Local environment of Gd^{3+} ions. The local axes *x*, *y*, and *z* are defined by the three twofold axes of point symmetry of the Gd^{3+} site.
c) Magnetic diffuse scattering data measured on the D9 diffractometer (left) and calculation from reverse Monte Carlo refinement (right).

Figure 2
a) Relationship between representative spin orientations and loop director for a ten-ion loop. Spins are coloured alternating green and orange as the loop is traversed. The multipole formed by the ten spins is shown at the centre of the loop and the loop director is shown as a red double-headed arrow.
b) Stereographic projection showing that the distribution of loop directors is strongly peaked along the local z axis.
c) Crystal structure showing the unit cell of the magnetic multipole crystal.

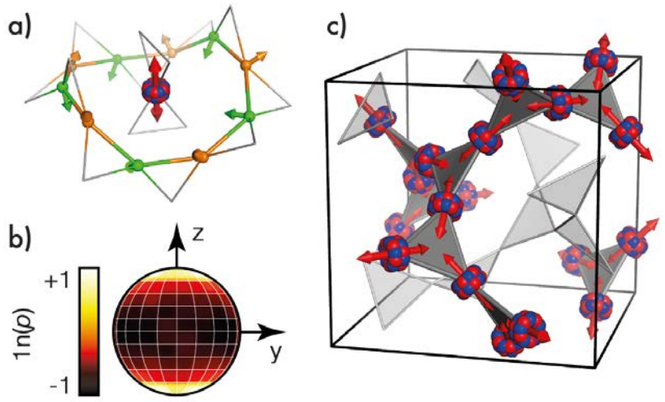

To analyse our data, we used reverse Monte Carlo (RMC) refinement, a computational method in which the orientations of spin vectors in large configurations are adjusted to match experimental data [3]. This approach considers only spin orientations and so does not depend on pre-conceived exchange parameters. We used previously published powder-diffraction data [2] to drive our refinement, which were collected using the D1B diffractometer at the ILL. Because the RMC method produces a three-dimensional model of the spin structure, we could calculate the single-crystal magnetic diffuse scattering from our model and compare it with the D9 data. Our results show good agreement between calculation and experiment (**figure 1c**).

Analysis of the RMC spin configurations revealed two important features. First, the distribution of spin orientations is anisotropic – spins preferentially lie within the local-*xy* planes defined by the axes shown in **figure 1b**. Second, local antiferromagnetic alignment persists not just between nearest neighbours but throughout the ten-ion loops, as illustrated in **figure 2a**. We calculated the average spin-alignment director, **L**, of each loop by summing the ten spins in a loop, flipping every second spin to take into account the antiferromagnetic correlation. The two-fold rotational point symmetry of the loop dictates that **L** and –**L** are equivalent, so the loop director **L** describes an axis without direction. A multipole expansion of the magnetic field due to such a loop of ten antiferromagnetic spins contains a large contribution from the spherical harmonic of order six, which contains five nodal planes perpendicular to the plane of the loop and one nodal plane parallel to it. The loop director thus describes the multipole orientation associated with a given ten-ion loop.

Our main result is that loop directors are preferentially aligned along the local *z* direction (**figure 2b**). This shows that the loop directors do not possess the rotational degree of freedom of planar spins and that their corresponding multipole orientations are ordered. The unit cell of the magnetic multipole crystal is shown in **figure 2c**. Because this order is multipolar, neutron scattering data are not directly sensitive to it. However, neutron scattering is directly sensitive to both spin-dipolar correlations and local spin anisotropy. We were able to show that it is precisely this combination of antiferromagnetic spin correlations and *xy* anisotropy that leads to the hidden-order state.

The observation of hidden order in GGG helps to explain thermodynamic anomalies observed in the specific heat and non-linear susceptibility, which show broad peaks over the temperature range over which hidden order develops [3]. The broadening of these peaks may arise because the hidden order does not break the crystal symmetry. More generally, our results show that the diffuse contribution to the diffraction pattern can actually help to identify hidden, long-range order through the coupling of long-range, non-dipolar order to the local spin structure. This work could only be achieved due to the unique short-wavelength capability and high neutron flux of D9 at the ILL.

MAGNETISM

Magnetically-induced ferroelectricity in the $(ND_4)_2[FeCl_5(D_2O)]$ molecular compound

High-resolution powder diffractometer D2B and single-crystal, four-circle diffractometer D9

Multiferroics – materials simultaneously presenting at least two ferroic orders – have attracted special interest in the last decade, in particular magneto-electric multiferroics which offer a control of electrical polarisation *via* a magnetic field or conversely. The so-called type-II multiferroics, where ferroelectricity is induced by magnetic long-range order, have been studied extensively for their fundamental properties as well as their potential applications in memories, sensors, transducers, etc. [1].

AUTHORS

J.A. Rodríguez-Velamazán (ICMA-CSIC, University of Zaragoza, Spain and ILL)
Ó. Fabelo and **L. Chapon** (ILL)
Á. Millán and **J. Campo** (ICMA-CSIC, University of Zaragoza, Spain)
R.D. Johnson (University of Oxford, UK)

REFERENCES

[1] M. Fiebig, J. Phys. D 38 (2005) R123
[2] M. Ackermann, D. Brüning, T. Lorenz, P. Becker and L. Bohatý, New J. Phys. 15 (2013) 123001
[3] J.A. Rodríguez-Velamazán, Ó. Fabelo, Á. Millán, J. Campo, R.D. Johnson and L. Chapon, Scientific Reports 5 (2015) 14475
[4] a) I. Dzyaloshinskii, J. Phys. Chem. Solids 4 (1958) 241; b) T. Moriya, Phys. Rev. 120 (1960) 91; c) A. Sergienko and E. Dagotto, Phys. Rev. B 73 (2006) 094434

So far multiferroicity has been found in a large variety of transition metal oxides, but such an effect remains rare in molecular-based magnets despite the vast playground offered by chemistry when bridging magnetic ions with a large diversity of organic ligands. The recent discovery of magneto-electricity in ammonium pentachloroaquaferrate(III) [2], a relatively simple molecular compound, is of high interest to the community. Specifically, one needs to understand which microscopic mechanism is at play and determine whether polar molecules in the system play a role in coupling magnetism and ferroelectricity, unlike most multiferroic oxides that do not contain acentric units.

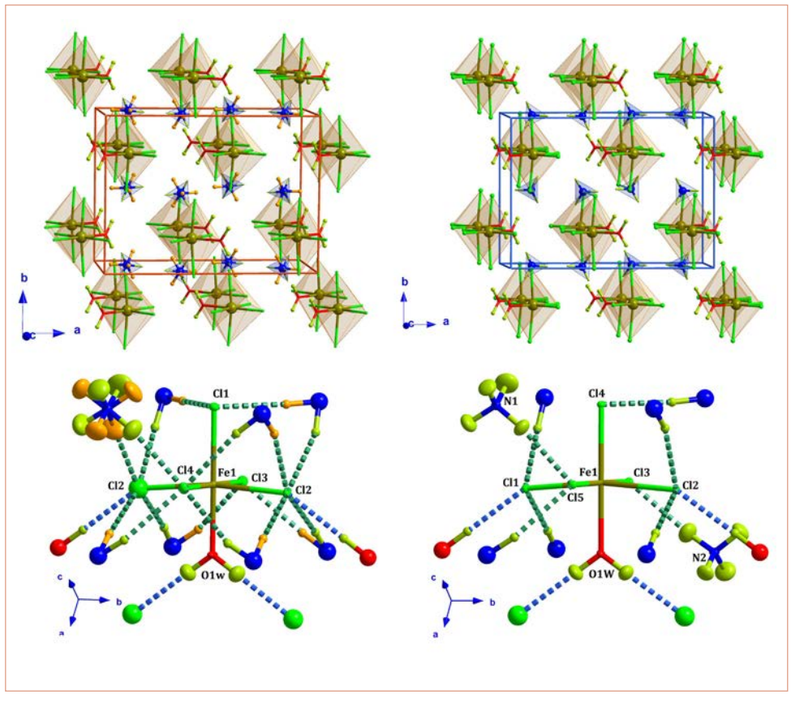

Figure 1
View of the crystal packing of the $(ND_4)_2[FeCl_5(D_2O)]$ compound at 100 (**top left**) and 2 K (**top right**). Detail of the hydrogen-bond interactions between the $[FeCl_5(D_2O)]$ unit and the adjacent molecules obtained from the neutron diffraction at 100 K (**bottom left**) and 2 K (**bottom right**). The O-D···Cl and the N-D···Cl hydrogen bonds have been represented as blue and green dashed lines, respectively.

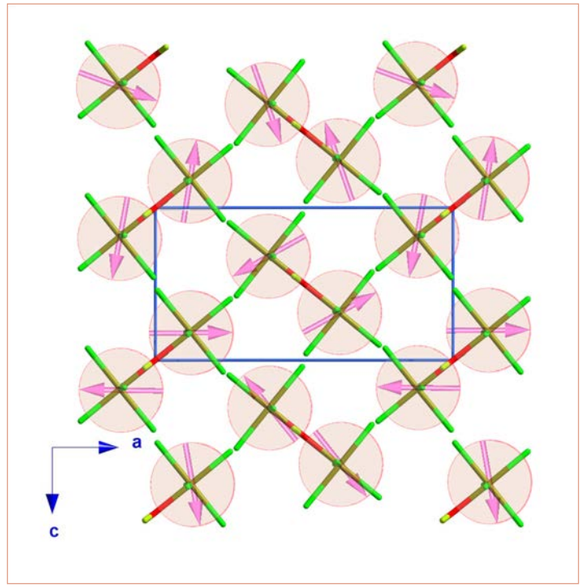

Figure 2
View along the *b*-axis of the superposition of the nuclear and magnetic structures for the combination of the two single irreducible representations. For the sake of clarity the ND_4 counterions have been omitted.

The heat capacity of deuterated samples of formula $(ND_4)_2[FeCl_5(D_2O)]$ presents a sharp peak at *ca.* 7.9 K, which was attributed to a possible structural phase transition. However, previous attempts to determine the crystal structure below this transition using X-ray diffraction did not show any significant crystallographic changes. At lower temperature the heat capacity shows two closely spaced peaks at *ca.* 6.9 and 7.2 K, of magnetic origin due to the corresponding accidents in the magnetisation. Pyroelectric measurements indicate the onset of a spontaneous electric polarisation at $T_{FE} \sim 6.9$ K in zero magnetic field.

The combination of single-crystal (D9) and powder neutron diffraction (D2B) provides a clear insight into the nature of the high-temperature phase transition at 7.9 K [3]. Above the transition (100 K), the crystal structure reveals ammonium counterions for which the D nuclear density is split into 8 positions with 50 % occupation, i.e. a disordered configuration with two equi-probable ammonium positions, each with almost perfect tetrahedral environments (see **figure 1**). Below the transition, our neutron work reveals that the structure becomes monoclinic and corresponds to an ordering of the ND_4 molecules (**figure 1**). This order-disorder transition, not seen by X-ray, does not however induce a polar phase, as the low-temperature, monoclinic space group of symmetry $P2_1/c$, is centrosymmetric.

The magnetic structure was studied at 2 K on single crystals. A survey of reciprocal space was carried out with a series of *Q*-scans in the first Brillouin zone showing the occurrence of magnetic reflections indexed by the incommensurate propagation vector $\mathbf{k} = (0, 0, 0.2288)$.

A symmetry analysis indicates that none of the solutions spanned by single irreducible representations of the wave-vector group is able to properly fit the experimental data. The only acceptable solution is found by combining two magnetic modes belonging to two irreducible representations, corresponding to a cycloidal modulation of the Fe^{3+} spins (**figure 2**). This explains the presence of two peaks in the specific heat, as two magnetic order parameters of different symmetries are broken successively on cooling. Since the cycloids centred on different Fe sites of the unit-cell are rotating in the same direction, it appears that the coupling mechanism between magnetisation and ferroelectricity is easily explained by the so-called *inverse* Dzyaloshinskii-Moriya effect or spin-current mechanism, [4] predicting that the electric polarisation, $\mathbf{P}$, is directed along a direction $\mathbf{r}_{ij} \times (\mathbf{S}_i \times \mathbf{S}_j)$, where $\mathbf{r}_{ij}$ is the vector connecting the nearest spins, $\mathbf{S}_i$, and $\mathbf{S}_j$, and $(\mathbf{S}_i \times \mathbf{S}_j)$ is the so-called spin-chirality vector. The refined magnetic structure with magnetic moments contained mostly in the *ac*-plane with a small tilt along the *b*-axis (*ca.* 4°) and propagating along the *c*-axis, does indeed induce through this coupling scheme an electric polarisation in the directions observed by the authors in [2].

Whilst this system shows a sequence of magnetic transitions very similar to that found in $TbMnO_3$, the archetype of cycloidal multiferroics, it appears that the change of electric polarisation under an applied magnetic field is not consistent with what has been observed so far in this kind of system. Further neutron work should shed light into the polarisation flop in field. It also remains to be seen whether one can find a way to accommodate polar molecules in such networks, which could enhance the magnitude of the electric response generated by magnetic ordering.

MAGNETISM

Discovery of Néel-type magnetic skyrmions with polar dressing

Small-angle scattering diffractometer D33

Skyrmions are nanometric spin vortexes that emerge in certain materials. Originally just an abstract theoretical concept, skyrmions raised great interest when it was discovered that chiral crystals can host magnetic skyrmions. The great potential of these tiny magnetic objects in novel spintronic and magnetic data storage devices has triggered a boom in this recently emerging field of materials science and nanotechnology.

AUTHORS

I. Kézsmárki and **S. Bordács** (Budapest University of Technology and Economics and MTA-BME Lendület Magneto-optical Spectroscopy Research Group, Budapest, Hungary)
J.S. White (Paul Scherrer Institute (PSI), Villigen, Switzerland)
C.D. Dewhurst (ILL)

REFERENCES

[1] S. Mühlbauer *et al.*, Science 323 (2009) 915919
[2] X.Z. Yu *et al.*, Nature 465 (2010) 901904
[3] N. Romming *et al.*, Science 341 (2013) 636639
[4] A. Fert *et al.*, Nature Nanotech. 8 (2013) 152156
[5] A.N. Bogdanov *et al.*, Zh. Eksp. Teor. Fiz. 95 (1989)178182
[6] I. Kézsmárki *et al.*, Nat. Mater. 14 (2015) 116
[7] Z. Wang *et al.*, Phys. Rev. Lett. 115 (2015) 207601
[8] E. Ruff *et al.*, Sci. Advances 1 (2015) e1500916

Up to now magnetic skyrmions have only been observed in a very limited class of materials with chiral crystal structures [1, 2]. Chiral crystals can exist in left- and right-handed forms that are the mirror images of each other. This structural chirality is transferred to the electron spins, making a topological twist in their magnetic pattern. Correspondingly, the spin texture of such skyrmions – the so-called Bloch-type skyrmions – is reminiscent of a small tornado in which the spins whirl around the centre. The three important properties of magnetic skyrmions are i) nanometric size, ii) topological protection, due to which individual skyrmions created in chiral ferromagnets persist on long time scales and iii) weak pinning to the underlying crystal lattice, facilitating their easy manipulation with very low current densities. These key factors make them promising candidates for the development of novel spintronic and magnetic data storage devices [3, 4].

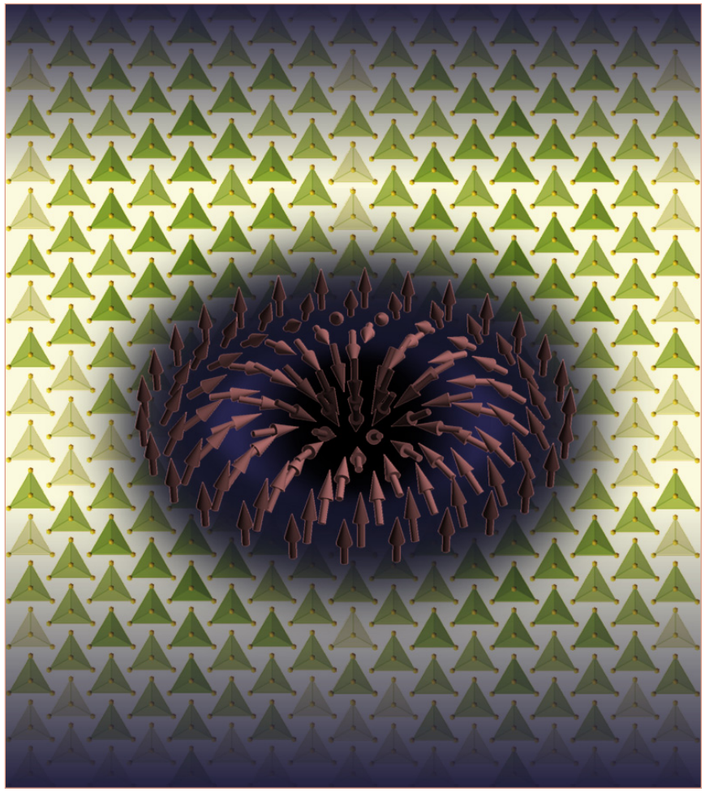

Figure 1
Schematic representation of the spin texture of a Néel-type skyrmion overlayed on the lattice of the host crystal. The individual spins, represented by arrows, rotate radially when approaching the centre of the skyrmion from its periphery.

Figure 2
Hexagonal pattern of the magnetic modulation vectors—[1-10], [-101] and [01-1]—as detected by small-angle neutron scattering in the Néel-type skyrmion lattice state of GaV_4S_8 when the magnetic field (B) is applied parallel to the [111] crystallographic axis being the easy axis of the magnetisation.

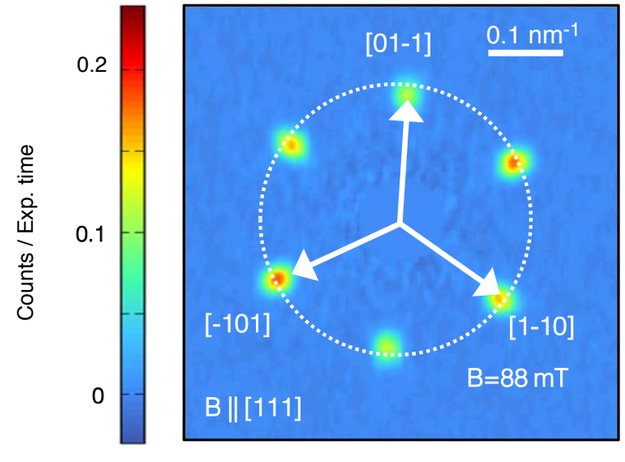

Strangely enough, skyrmions have never been found in the material class where they were first theoretically predicted by Bogdanov and co-workers [5], in magnetic crystals with not chiral but polar structures. In polar crystals the ions are arranged in a fashion that gives rise to a uniform electric polarisation also called ferroelectricity. Gallium-vanadium sulphide (GaV_4S_8), a magnetic semiconductor with such a polar crystal structure, belongs to the class of materials originally predicted to host skyrmions. Exploiting a powerful technique called small-angle neutron scattering (SANS) and taking advantage of the high neutron flux of the ILL, we could discover a new class of skyrmions—the so-called Néel-type skyrmions—in the low-temperature phase of GaV_4S_8 [6].

In contrast to the Bloch-type skyrmions, the Néel-type ones are not spin whirlpools. Instead they are hedgehog-like magnetic textures where the spins rotate in the radial planes when approaching the centre of the skyrmion from its periphery. This skyrmion lattice is more robust than the Bloch-type skyrmion lattices found in chiral magnets: it is stable over a wide temperature range, whereas the Bloch-type skyrmion lattice has only been observed in bulk crystals as fluctuation-stabilised tiny phase pockets near the paramagnetic-ferromagnetic phase boundaries.

Due to the polar nature of the host crystal [7], besides their magnetic texture Néel-type skyrmions can also wear a ferroelectric dressing. As a consequence of the coupling between the charge and spin degrees of freedom, the Néel-type skyrmions in GaV_4S_8 exhibit strong magneto-electric effects that can be exploited to the electric control of their magnetic state [8].

Magnetic skyrmions could be used as data bits in future devices. In such systems, the state of the bit (e.g. the 1 or 0 level) is encoded by the presence or absence of a magnetic skyrmion. Since polar materials like GaV_4S_8 can be controlled by electric fields, a nearly dissipation-less writing and deleting of Néel-type skyrmions may be realised in such compounds.

SCIENTIFIC HIGHLIGHTS

MAGNETISM

Spectrum of a bond-disordered spin liquid: on the route to criticality

Time-of-flight spectrometer IN5

There is a fundamental interest in studying the properties of bosons in a disordered potential, especially close to the point separating the "insulating" and "superfluid" phases of the system. As the spin Heisenberg Hamiltonian can be exactly mapped onto an ensemble of bosons, chemically disordered quantum magnets offer a convenient option for investigating "dirty boson" physics [1]. In the present experiment we uncover the full excitation spectrum in a material with a non-magnetic ground state (bosonic "insulator"), undergoing spin-gap softening due to disorder in magnetic interactions. This implies that this magnet is on the randomness-induced route to long-range ordering ("superfluidity" in bosonic language) – a highly unconventional situation.

AUTHORS

K.Yu. Povarov, E. Wulf, A. Zheludev (ETH Zürich, Switzerland)
D. Hüvonen (National Institute of Chemical Physics and Biophysics, Tallinn, Estonia)
J. Ollivier (ILL)
A. Paduan-Filho (University of São Paulo, Brazil)

REFERENCES

[1] A. Zheludev and T. Roscilde, C. R. Physique 14 (2013) 740
[2] V.S. Zapf *et al.*, Phys. Rev. Lett. 96 (2006) 077204
[3] R. Yu *et al.*, Nature 489 (2012) 379
[4] E. Wulf *et al.*, Phys. Rev. B 88 (2013) 174418
[5] M. Vojta, Phys. Rev. Lett. 111 (2013) 097202
[6] K.Yu. Povarov *et al.*, Phys. Rev. B 92 (2015) 024429

It has long been recognised that $NiCl_2$-4SC$(NH_2)_2$ (often called DTN) provides a perfect model system for studying quantum magnetism [2]. Nickel ions here host a spin S = 1, confined within a plane by strong crystal field effects. This XY anisotropy, dominating the Heisenberg exchange, results in a ground state with on-site S = 0, separated by an energy gap of 0.3 meV from the bosonic excitations with S = ±1. The excitations carrying the magnetic moment can, in consequence, only be activated thermally and the ground state has no magnetic susceptibility. There is recent evidence from bulk measurements [3, 4] that the slight substitution of bromine on the chlorine site leads to substantial softening of the gap.

This is an exciting situation, implying that, with some degree of disorder, the gap should close completely and the system end up in a different ground state [5]. However, the microscopic details of the magnetic excitation spectrum in the presence of disorder were missing.

In the present experiment we used the ILL's high-resolution time-of-flight instrument IN5 to investigate the spectrum of DTN with 6 % bromine content at the low temperature of 60 mK. By combining neutron beams of different wavelength we were able to obtain a complete and extremely detailed picture of magnetic excitations, as shown in **figure 1**.

The gap is indeed softened, from 0.3 to 0.2 meV, and the spectrum has undergone a certain renormalisation. The S = 1 quasiparticles have also acquired some damping, due to the disorder, which is most pronounced near the bottom of the band. A peculiar finding is the localised state above the excitation band, shown in **figure 2**. Such non-dispersive states are endemic to random systems [5].

By comparing the spectrum measured with the reference magnetic interactions in the extensively studied parent system, we identified the control parameter in the Hamiltonian which is primarily responsible for the gap magnitude and hence for the ground state selection. This parameter is the ratio of the single-ion anisotropy to the strength of a single superexchange constant (mediated by the halogen ions).

Figure 1

Spectrum of DTN with 6 % bromine substitution: map of the scattering intensity as a function of momentum and energy transfer. The trajectory through the first Brillouin zone is drawn on the figure. The light white line shows the reference dispersion of non-disordered DTN. The hatched region is the domain of parasitic quasi-elastic scattering.

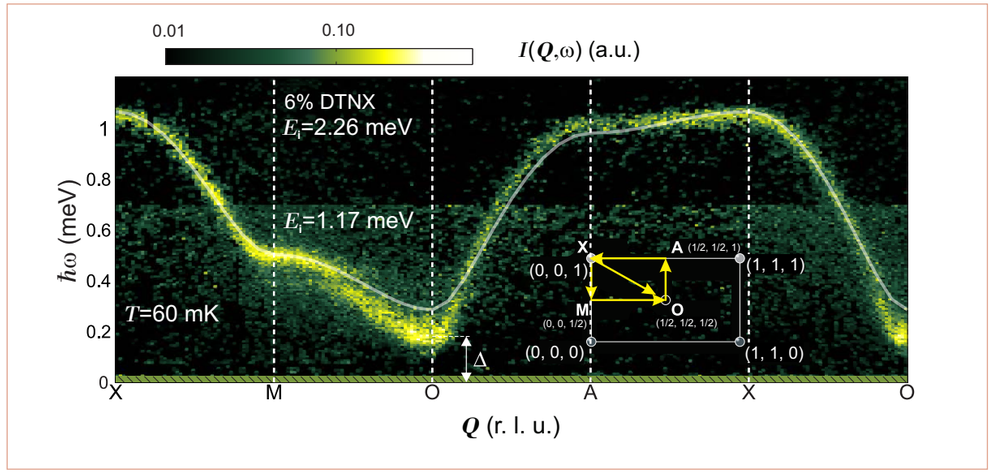

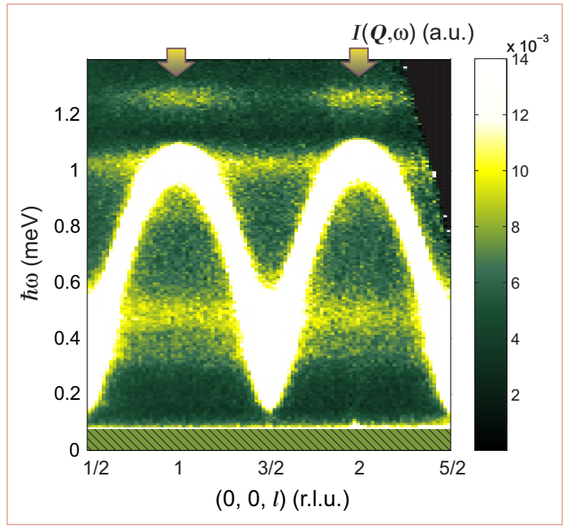

Figure 2

High-contrast plot of the spectrum of DTN with 6 % bromine substitution, integrated along the weaker dispersion direction. Note the presence of localised states above 1.2 meV, as denoted by arrows.

The analysis of more subtle spectrum features, such as the excitation lifetimes and the presence of weak non-dispersive states, as well as a comparison between these findings and the numerical results of reference [5], allow us to draw some conclusions about the distributions of disorder in various interaction parameters [6].

In conclusion, the rather modest 6 % bond randomness in DTN leads to significant changes in the spectrum and the emergence of novel features. This is the result of disorder-induced tuning of the interactions, making the system approach the quantum critical state.

SCIENTIFIC HIGHLIGHTS

MAGNETISM

Unusual continuous excitations in a quantum square-lattice antiferromagnet

Three-axis spectrometer IN20

Precise, inelastic, polarised neutron scattering on the quantum square-lattice antiferromagnet CFTD (deuterated copper formate tetrahydrate, $Cu(DCOO)_2 \cdot 4D_2O$) challenges the magnon paradigm for a simple, collinear antiferromagnetic structure: isotropically polarised magnetic excitations with a broad extension in energy evidence the proximity of a singlet quantum ground state with unbroken spin-rotation symmetry.

AUTHORS

M. Enderle (ILL)
M. Mourigal (Georgia Institute of Technology, Atlanta, USA)

REFERENCES

[1] B. Dalla Piazza, M. Mourigal, N.B. Christensen, G.J. Nilsen, P. Tregenna-Piggott, T.G. Perring, M. Enderle, D.F. McMorrow, D.A. Ivanov and H.M. Rønnow, Nature Phys. 11 (2015) 62
[2] M. Powalski, G.S. Uhrig and K.P. Schmidt, Phys. Rev. Lett. 115 (2015) 207202

Amongst all two-dimensional networks, the square lattice is the simplest: a Mott insulator with spin *S* and antiferromagnetic interaction along the edges of the square orders into a collinear magnetic structure. By adopting a common direction, spins break the rotation symmetry of the exchange interaction. Thus, elementary excitations are expected to be magnons (spin waves) with a sharp dispersion relation and magnetic amplitudes (or polarisation) perpendicular to the spin direction. Within this paradigm zero-point fluctuations weaken, but do not fully suppress, the magnetic order and allow magnon–magnon interaction. Weak continuous features live behind the scenes of an otherwise sharp spectrum and are attributed to two-, three- (and more) magnon excitations, with importance decreasing in powers of $1/S$. Two-magnon excitations carry a polarisation along (i.e. parallel to) the ordered moment, while three-magnon excitations have purely transverse (i.e. perpendicular) polarisation.

In the square-lattice antiferromagnet CFTD [1] the spin per site is $S = 1/2$. The ordered moment reaches only 62 % of the full spin value, and in $1/S$ expansions the contribution of multi-magnons explodes. This suggests the close proximity of a singlet quantum ground state that conserves the full spin-rotation symmetry and hosts a different type of elementary excitations. Much like in particle physics, the examination of magnetic excitations at high energy – corresponding here to wave vectors at the magnetic zone-boundary – has the potential to reveal physics beyond the standard magnon paradigm.

Inelastic, polarised neutron scattering experiments on single crystals of CFTD performed on IN20 clearly evidence the remnants of a nearby singlet ground state in the excitation spectrum: in addition to the ordinary one-magnon (a sharp mode with transverse polarisation, **figure 1d**), the scattering at the zone boundary wave vectors $q = (\pi, 0)$ and $(\pi/2, \pi/2)$ displays broad and continuous features in energy (**figure 1a, b**). At $q = (\pi/2, \pi/2)$ the continuous spectrum begins at higher energy than the sharp one-magnon (**figure 1a**), is clearly peaked (**figure 1c**) and is polarised longitudinally, i.e. purely parallel to the ordered moment (**figure 1a, c**). This is indicative of a bound state [2], a massive Higgs-boson that, if massless, would restore the spin-rotation symmetry together with the transverse one-magnon branch.

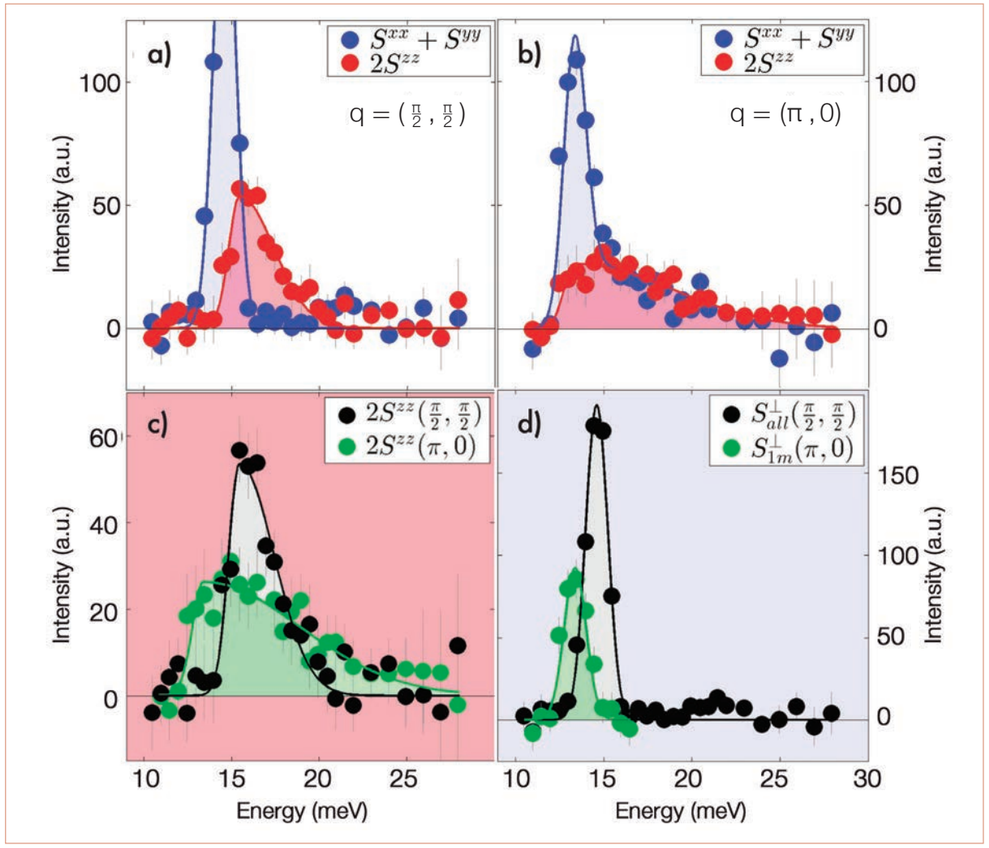

Figure 1

Transverse (blue) and longitudinal (red) magnetic excitations at the zone-boundary wave vector
a) $q = (\pi/2, \pi/2)$,
b) $(\pi, 0)$,
obtained background-free via differences of polarised cross-sections.
c) Longitudinal spectra at $q = (\pi/2, \pi/2)$ (black) and $(\pi, 0)$ (green),
d) The entire transverse spectrum at $q = (\pi/2, \pi/2)$ (black), compared with the remaining (green) transverse spectrum at $(\pi, 0)$ after subtraction of the continuous part (blue minus red shown in **(b)**).

At $q = (\pi, 0)$, the one-magnon is reduced in intensity (**figure 1d**) and is inseparable from a broad continuum which begins at the same energy and is isotropic in polarisation (**figure 1b, c**). The restored spin-rotation symmetry of this continuum evidences even stronger the proximity of an isotropic quantum ground state. An isotropic continuum is difficult to reconcile with the magnon paradigm, since two-magnons are purely longitudinal, three-magnons purely transverse, and their line shapes in general very different.

It is very tempting to interpret the spectrum starting from a singlet ground state of nearby energy that preserves full spin-rotation symmetry. One such starting point is the resonating valence-bond liquid, with isotropic triplet excitations made of nearly free fermion pairs [1]. When the spin-rotation symmetry is broken, bound states of two fermions form and acquire a transverse and gapless character, mimicking one-magnon excitations [1]. Wave vectors exist, however, where the fermions remain nearly free and where the spectrum appears continuous and isotropic. A variational approach of a resonating valence-bond liquid does indeed lead to free fermions at $q = (\pi, 0)$ and bound pairs at $q = (\pi/2, \pi/2)$ [1]. Within the magnon paradigm [2], the close proximity of an isotropic singlet ground state enhances the attractive interaction between magnons, such that a short-lived, longitudinal bound state can form at slightly higher energy (or "mass"), resembling a Higgs-boson [2].

Irrespective of the base language preferred, the polarised IN20 data challenge the conventional magnon picture for the quantum square-lattice antiferromagnet, indicate the proximity of an isotropic ground state and provide precise characteristics of the excitation spectrum to be met with a future, fully comprehensive, theory.

MAGNETISM

Nanophase separation responsible for hour-glass spectra in cobaltates

Three-axis spectrometers IN8, IN12 and IN22

The so-called hour-glass magnetic excitation spectrum has fascinated physicists for many years. This phenomenon has been found in copper oxide-based, high-temperature superconductors and it is widely believed that fluctuating charge-stripes are involved in the physics of these excitation spectra. Here, we studied an isostructural but insulating cobaltate that also exhibits an hour-glass magnetic spectrum. We can exclude not only Fermi surface effects but also any substantial role of charge stripes for the hour-glass spectrum in this cobalt oxide material. Instead, we observe electronic and magnetic nanophase separation within the cobalt oxygen planes and unravel a microscopically split origin of hour-glass spectra on the nanoscale.

AUTHORS

A.C. Komarek, Y. Drees, Z.W. Li, H. Guo and **L.H. Tjeng**
(Max-Planck-Institute for Chemical Physics of Solids, Germany)
A. Piovano and **W. Schmidt** (ILL)

REFERENCES

[1] A.T. Boothroyd, P. Babkevich, D. Prabhakaran and P.G. Freeman, Nature 471 (2011) 341
[2] Y. Drees, D. Lamago, A. Piovano and A.C. Komarek, Nature Commun. 4 (2013) 2449
[3] Y. Drees, Z.W. Li, A. Ricci, M. Rotter, W. Schmidt, D. Lamago, O. Sobolev, U. Rütt, O. Gutowski, M. Sprung, A. Piovano, J.P. Castellan and A.C. Komarek, Nature Commun. 5 (2014) 5731
[4] H. Guo, W. Schmidt, L.H. Tjeng and A.C. Komarek, Phys. Status Solidi RRL 9 (2015) 580
[5] Z.W. Li *et al.*, J Supercond. Nov. Magn. (2015), DOI 10.1007/s10948-015-3302-4

The appearance of a magnetic excitation spectrum with an hour-glass shape in energy-momentum space is a universal characteristic property of high-temperature superconducting cuprates. Despite numerous studies, the origin of this peculiar excitation spectrum is not well understood. Therefore, the recent observation of hour-glass shaped magnetic excitation spectra in isostructural cobaltate materials gives rise to the study of hour-glass spectra within insulating reference systems where Fermi surface effects play no role [1, 2]. The initially studied cobaltate $La_{5/3}Sr_{1/3}CoO_4$ exhibits broad magnetic peaks roughly around one-third-integer positions in reciprocal space. At about the same positions in reciprocal space magnetic reflections appear in the isostructural nickelate $La_{5/3}Sr_{1/3}NiO_4$, which exhibits robust, diagonal charge-stripe ordering. Thus also in the cobaltates, the presence of disordered diagonal charge-stripe phases had been assumed and, hence, the importance of charge-stripe phases for the emergence of hour-glass spectra.

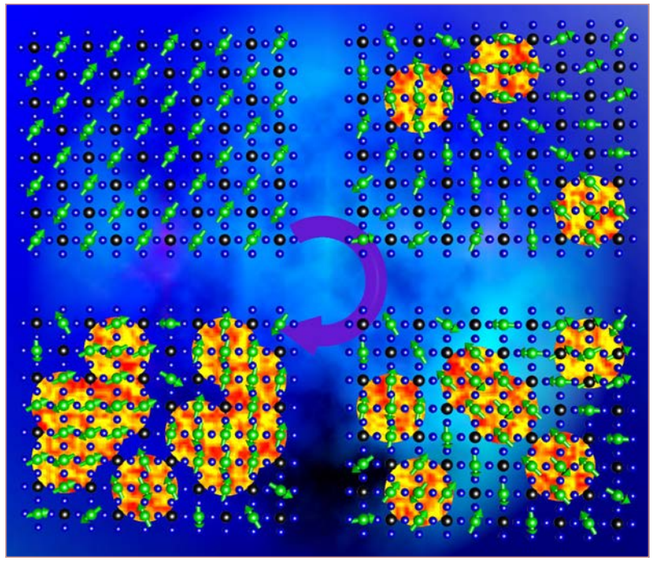

Figure 1
A graphical presentation of the process of electron-doping into a checkerboard charge-ordered matrix. The non-magnetic Co^{3+} ions and magnetic Co^{2+} ions are represented by black and green spheres respectively. The green arrows symbolise the magnetic moments of the Co^{2+}-ions [4].

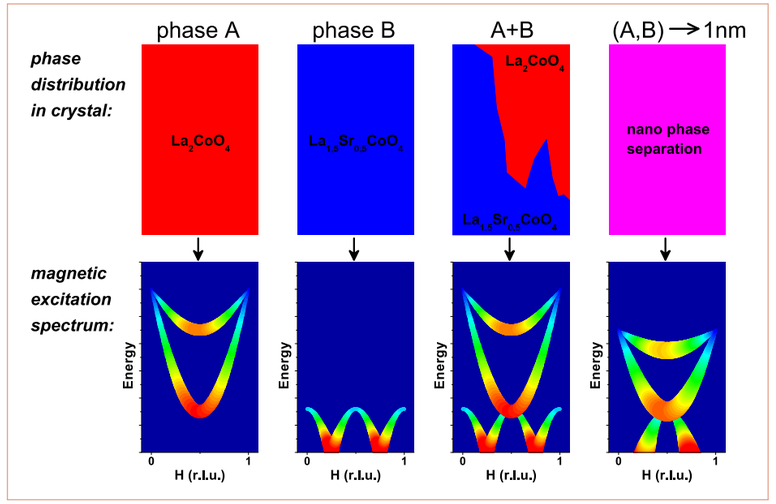

Figure 2
In the first two columns a schematic presentation of magnetic excitations in undoped (red) and half-doped (blue) cobaltate phases A and B is shown. In the third column the case of conventional phase separation is shown where the former two phases A and B coexist. Finally, the last column shows what happens once the A and B domain sizes get close to the dimensions of a few unit cells, i.e. roughly nanometer-sized – nanophase separation appears.

In neutron and X-ray diffraction experiments we were not able to detect any signatures of charge-stripe phases, either in $La_{5/3}Sr_{1/3}CoO_4$ or in $La_{1.6}Sr_{0.4}CoO_4$ [2, 3]. Instead, we observe broad peaks at half-integer positions in reciprocal space [2-5] very similar as in reference measurements on the ideal, half-doped checkerboard charge-ordered compound $La_{1.5}Sr_{0.5}CoO_4$ with a high charge-ordering temperature of the order 800 K. Thus, in the layered cobaltates rather robust checkerboard charge-ordering correlations still persist distinctly below half-doping down to ⅓ hole-doping [4]. In compounds with less than 50 % hole-doping the additional electrons have to be distributed in some way into the cobalt oxygen planes. Since no signatures of charge stripes could be observed within these strongly localised insulators, the occurrence of undoped islands like those of the undoped parent insulator La_2CoO_4 appears to be an unavoidable consequence, see **figure 1**.

Therefore we proposed a novel nanophase separation scenario, where checkerboard charge-ordered regions are interspersed with undoped islands on the nanometer scale. Our complementary microdiffraction measurements corroborate this scenario [3]. Another interesting discovery that we made was the observation of a hitherto unknown, additional high-energy magnetic mode above the entire hour-glass shaped magnetic spectrum with polarised neutrons at the ILL [3]. Thus, the part of the spectrum above the crossing of the hour-glass somehow resembles the magnetic excitation spectrum of La_2CoO_4. Hence the question arises as to whether the magnetic excitations in the upper part of the spectrum are basically hosted within the nanometer-sized undoped islands of La_2CoO_4-type. Comparing $La_{5/3}Sr_{1/3}CoO_4$ and $La_{1.6}Sr_{0.4}CoO_4$ the additional high-energy magnetic mode seems to be distinctly weaker in $La_{1.6}Sr_{0.4}CoO_4$. Since the fraction of undoped islands should be much smaller in $La_{1.6}Sr_{0.4}CoO_4$ than in $La_{5/3}Sr_{1/3}CoO_4$ this is, indeed, evidence for our nanophase separation scenario [3]. The study of the temperature dependence of the magnetic excitations in $La_{5/3}Sr_{1/3}CoO_4$ also corroborates our novel nanophase separation scenario: e.g. the usually expected temperature-induced broadening of the low-energy magnetic excitations is not visible when temperature rises. Within our model this would naturally follow from the limiting factor of the static domain size of the checkerboard charge-ordered regions, which is temperature-independent [3]. Finally, we made spin-wave calculations for our nanophase separation model which are able to describe the observations within our neutron scattering experiments.

These simulations clearly show that at higher energies basically the undoped islands can be excited [3]. Hence, we observed not only nanophase separation in the charge sector (nanometer-sized, checkerboard charge-ordered regions and undoped islands) but also a kind of magnetic nanophase separation due to a strong decoupling of spins within checkerboard charge-ordered regions with very small exchange interactions J' and spins within undoped islands with large exchange interactions J >> J'. This novel electric and magnetic nanophase separation effect is very different from conventional phase separation because these Co-oxide materials are macroscopically homogenous. Also, the total magnetic excitation spectrum is not simply a superposition of the excitation spectra of La_2CoO_4 and $La_{1.5}Sr_{0.5}CoO_4$ that could be expected for conventional phase separation; see the schematic presentation in **figure 2**.

MAGNETISM

Ising incommensurate spin resonance of $CeCoIn_5$: a dynamical precursor of the Q-phase

Three-axis spectrometer IN12

Unconventional superconductivity often occurs on the verge of magnetic ordering. This begs the question of the relationship between these phases and whether they are competitive or collaborative states. A new generation of inelastic neutron scattering experiments performed on the unconventional superconductor $CeCoIn_5$ reveals a strong link between the spin dynamics associated with superconductivity and the magnetic-field-induced magnetic ordering, the former being the soft mode associated with the latter.

AUTHORS

S. Raymond and **G. Lapertot** (University Grenoble Alpes and CEA-Grenoble, France)

REFERENCES

[1] C. Stock *et al.*, Phys. Rev. Lett. 100 (2008) 087001
[2] C. Stock *et al.*, Phys Rev. Lett. 109 (2012)167207
[3] S. Raymond *et al.*, Phys. Rev. Lett. 109 (2012) 237210
[4] M. Kenzelmann *et al.*, Science 321 (2008) 1652
[5] S. Raymond and G. Lapertot, Phys. Rev. Lett. 115 (2015) 037001

Unconventional superconductivity modifies the magnetic excitation spectrum of a metal through a feedback effect corresponding to the apparition of a new collective mode in the superconducting phase: the spin resonance. This dynamical mode has an energy scale and a wave-vector dependence directly related to the magnitude and topology of the superconducting gap. Beside these aspects of the spin dynamics, it is often found that long-range antiferromagnetic ordering can be induced by a magnetic field starting from the superconducting state. These phenomena are shared by many unconventional superconductors: cuprates, iron-based materials and heavy fermion systems. The heavy fermion materials display an intrinsic low-energy scale and therefore respond strongly to the magnetic field magnitudes available in a laboratory. This provides fertile ground for the discovery of new states of matter.

$CeCoIn_5$ is a model unconventional superconductor with a transition temperature T_c = 2.3 K and a superconducting gap following a d_{x2-y2} symmetry. Its spin resonance was first reported to be peaked at the antiferromagnetic wave-vector $\mathbf{Q}_{AF}$ = (0.5, 0.5, 0.5), corresponding to nodes of the d_{x2-y2} order parameter, and at an energy of 0.6 meV that scales approximately with $3k_BT_c$ [1]. The unique feature of the $CeCoIn_5$ spin resonance is its Zeeman splitting under magnetic fields [2, 3]. A parallel effect of the magnetic field is to induce long-range incommensurate magnetic ordering. The so-called Q-phase is a spin-density wave characterised by the propagation vector $\mathbf{Q}_{IC}$= (0.45, 0.45, 0.5) [4]. Surprisingly, this magnetic ordering disappears together with superconductivity above the upper critical field H_{c2}: the magnetic Q-phase needs superconductivity!

Up to now, the dynamical and static aspects of the magnetism of such unconventional superconductors seemed not to be correlated: the spin resonance of $CeCoIn_5$ was believed to be peaked at the antiferromagnetic wave-vector $\mathbf{Q}_{AF}$ while the magnetic-field-induced ordering occurs at $\mathbf{Q}_{IC}$.

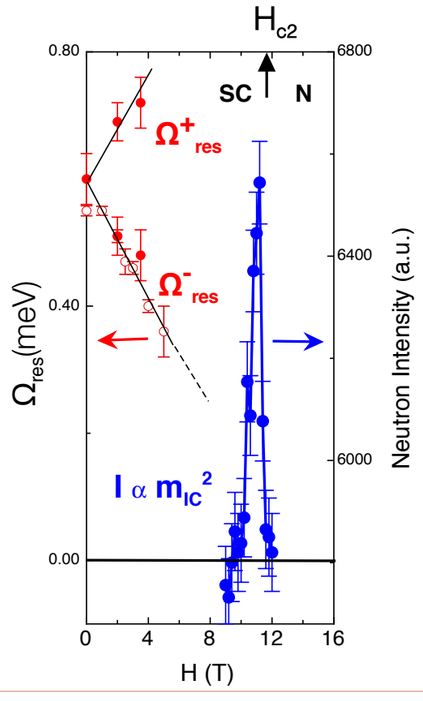

Figure 1

The spin resonance energy (red points) splits under the magnetic field. A field-induced incommensurate magnetic ordering, the Q-phase, induced at 10.5 T in the superconducting (SC) phase, disappears at H_{c2} in the normal (N) phase. The corresponding elastic neutron intensity is shown as blue points.

Figure 2

a) Colour-coded intensity plot of the inelastic neutron scattering spectra, as a function of Q_H and E for Q = (Q_H, Q_H, 0.5) at 1.45 K: two incommensurate peaks are clearly resolved on both sides of the antiferromagnetic position Q_H = 0.5.
b) Polarised INS spectra taken at Q_{AF} in the spin-flip channel for the three canonical polarisation directions: the fluctuations are polarised solely along the *c*-axis of the tetragonal structure.

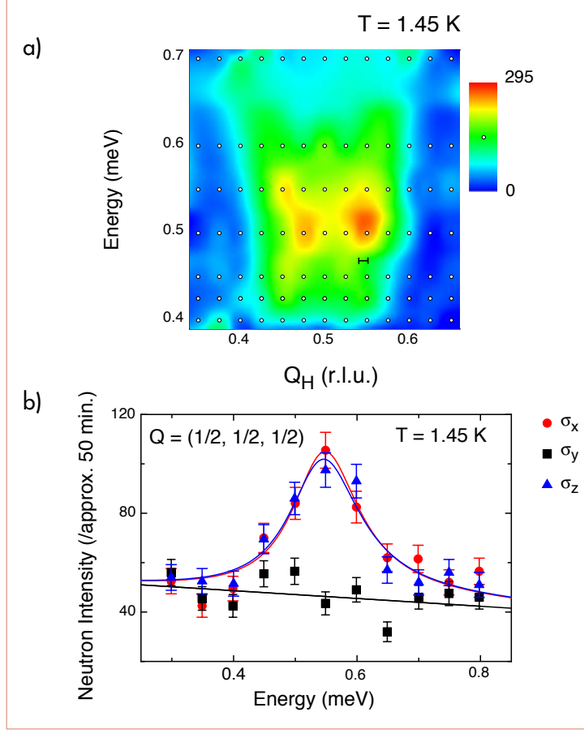

The upgrade of the IN12 spectrometer allows not only a net gain in the neutron flux but also greater versatility. Taking advantage of this, a detailed investigation of the spin resonance was performed using high wave-vector resolution. **Figure 1** shows a colour-coded intensity plot of the inelastic neutron scattering spectra, collected as a function of wave-vector and energy at 1.45 K. Two incommensurate peaks are clearly resolved on both sides of the antiferromagnetic position and their positions correspond to $\mathbf{Q}_{IC}$=(0.45, 0.45, 0.5), which is also the propagation vector of the Q-phase. In a second step, the direction of magnetic fluctuation was investigated using longitudinal polarimetry. **Figure 2b** shows energy spectra measured in the spin-flip scattering channel for the three canonical polarisation directions at 1.45 K. From the absence of scattering for polarisation along *y*, and from the same intensity measured in the *x* and *z* channels, the selection rules associated with polarised neutron scattering lead to the conclusion that the resonance spin fluctuations are polarised in a single direction (perpendicular to *x* and to *z*). In the sample frame, this corresponds to the *c*-axis of the tetragonal structure and this direction corresponds to one of the magnetically ordered moments of the Q-phase.

This detailed investigation of the spin resonance of $CeCoIn_5$ has established that the excitation is incommensurate and located at $\mathbf{Q}_{IC}$, and that the corresponding fluctuations are Ising and polarised along the *c*-axis [5]. These two characteristic features are shared with the Q-phase: it is an incommensurate sine-wave modulated magnetic structure of propagation vector $\mathbf{Q}_{IC}$ and the magnetic moments are ordered along the *c*-axis. The fact that the dynamical mode and the field-induced static order share the same symmetry underlines the fact that the resonance is a dynamical precursor of the Q-phase. This, together with the known softening of the lowest energy mode of the Zeeman split resonance, strongly supports the theoretical scenario in which magnetic ordering is obtained by a field-induced condensation of the resonance.

To date this behaviour is only evidenced in $CeCoIn_5$, and these magneto-superconducting phenomena challenge our understanding of matter. It is the intrinsic low-energy scale associated with the small transition temperature of $CeCoIn_5$ that has enabled us to reveal new physics in modest magnetic fields of about 10 T. Whether this is common to other superconductors is an important issue, and the rapid progress being made in high magnetic field experiments at neutron scattering facilities may lead to similar effects being observed in systems with higher transition temperatures (e.g. cuprates or Fe-based superconductors).

SCIENTIFIC HIGHLIGHTS

LIQUIDS, GLASSES AND SOFT MATTER

Collective dynamics of liquid zinc: the complex behaviour of a simple system

Brillouin spectrometer BRISP

Starting from early work by Copley and Rowe [1], who demonstrated the existence of a long-living collective mode in liquid rubidium, the collective THz dynamics of a large number of liquid metals were investigated using inelastic neutron scattering (INS) and inelastic X-ray scattering (IXS) [2]. This class of materials appears generally to be characterised by simple behaviour, with a longitudinal acoustic mode exhibiting a single, almost sinusoidal dispersion over a wide range of momentum transfers Q. Conversely, non-metallic or molecular liquids, like water, show a more complex pattern of excitations, characterised by the existence of at least two different modes, possibly related to anisotropic interactions.

AUTHORS

M. Zanatta, A. Paciaroni and **L. Sani** (University of Perugia, Italy)
A. Orecchini, C. Petrillo and **F. Sacchetti** (University of Perugia and IOM-CNR, Perugia, Italy)

REFERENCES

[1] J.R.D. Copley and J.M. Rowe, Phys. Rev. Lett. 32 (1974) 49
[2] L. Sani, C. Petrillo and F. Sacchetti, Phys. Rev. B 90 (2014) 024207
[3] S. Klotz, M. Braden, and J.M. Besson, Phys. Rev. Lett. 81 (1998) 1239
[4] R.E. DeWames, T. Wolfram, and G.W. Lehman, Phys. Rev. 138 (1965) A717
[5] V.M. Giordano and G. Monaco, Proc. Natl. Acad. Sci. U.S.A. 107 (2010) 21985

Interestingly, recent studies point out that even monoatomic liquid metals can show unexpectedly complex dynamics at the atomic scale. This is the case with zinc. In the periodic table, this element lies at the end of the transition metal series, where the full *d*-like band still contributes to the screening of the electron-ion potential. The crystalline phase of zinc is well-known for the presence of anisotropic interactions that stabilise its *hcp* structure and also seem related to an anomalous electronic-topological transition observed at high pressure [3]. From the experimental point of view, Zn is a perfect sample for INS measurements: it is an almost coherent neutron scatterer, with a relatively accessible melting temperature of 693 K and a longitudinal sound velocity well within the range of the time-of-flight neutron Brillouin spectrometer BRISP. This instrument is specifically designed to perform INS experiments at small Q and can effectively tackle the study of THz collective dynamics in liquid systems.

A typical example of the measured scattering intensity of Zn is shown in **figure 1**. The plotted data have been thoroughly corrected for all unwanted contributions, including multiple scattering. The spectra are characterised by a resolution-limited quasi-elastic peak, with inelastic

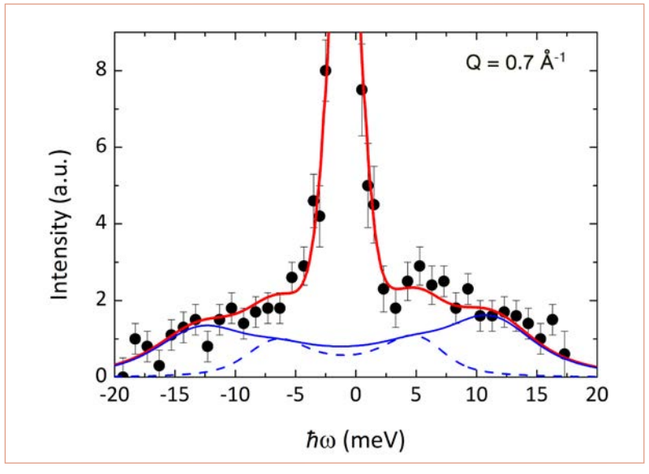

Figure 1

Experimental data at Q = 0.7 Å^{-1}. The red line represents the best fit to the data. Blue lines are the fit components: the longitudinal mode (solid blue line) and the low energy mode (dashed blue line).

Figure 2

a) Dispersion curves for liquid zinc as obtained by the fit (dots). The dashed black lines are guides to the eye, marking the behaviour of the two excitations. The colour map represents the overall intensity of the inelastic excitations as obtained by the fit. The solid black line indicates the limit of BRISP's kinematic range; **b)** Projected components of the vibrational density of states of crystalline *hcp* zinc obtained, as described in the text. Colours are as in the legend.

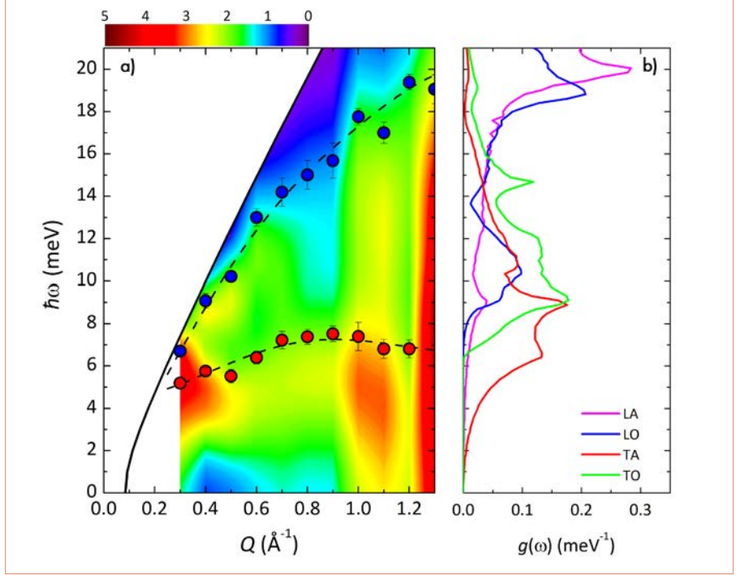

side structures related to the collective modes. These features cannot be coherently described with just one inelastic excitation; this suggests the presence of an additional mode with a Q-dependent intensity. To account for this complex behaviour, we consider a model composed of a sharp Lorentzian function plus the dynamic structure factor of two interacting oscillators. This interaction is necessary because scattering experiments only detect longitudinal density fluctuations, and modes characterised by the same symmetry are known to interact with each other. The model provides an accurate description of the spectrum. A typical resulting best-fit curve is shown in **figure 1** (red lines), together with the individual inelastic components (blue lines).

Figure 2a shows the dispersion relation of the energies of the two bare modes, as obtained from the fitting procedure. As expected, the high-energy mode (blue dots) displays a sinusoidal shape, and can be identified as a longitudinal acoustic mode. Conversely, the low-lying mode (red dots) is almost Q-independent and its identification is not straightforward. As a matter of fact, precise knowledge of both vibrational eigenvalues and eigenvectors is only possible for single crystals, as it is prevented in liquids by the isotropy.

To provide new insights into the nature of the modes in liquid Zn, we can thus compare their behaviour with the phonon dynamics of the crystalline phase, where phonon eigenvalues and eigenvectors can be obtained within a model using the force constants deduced by previous neutron experiments [4]. **Figure 2b** shows the vibrational density of states $g(\omega)$ of an ideal high-temperature crystalline phase. This corresponds to the spherical average of the phonon dynamics over all Q values, and hence to the vibrational density of states of an ideal polycrystal heated to the temperature of the liquid measured. Contributions of the acoustic (A) and optic (O) modes, in either the longitudinal (L) or transverse (T) directions, are shown separately. By comparison with **figure 2a**, the measured dispersion curves of the liquid phase appear related to the main features of the acoustic components $g_{LA}(\omega)$ and $g_{TA}(\omega)$ in the crystal. In particular, the low-lying mode can be related to transverse acoustic phonons, whose peak in $g_{TA}(\omega)$ is very close to the high-Q limit of the dispersion curve.

The existence of a complex pattern of excitations has also been observed in other liquid metals such as liquid sodium [5]. Such complex behaviour breaks the paradigm of monoatomic liquid metals as the prototype of simple liquids. The atomic origin of this dynamical complexity might be ascribed to the presence of anisotropic contributions in the atomic interaction potential giving rise to local structural units, such as dimers, even in the liquid phase.

SCIENTIFIC HIGHLIGHTS

LIQUIDS, GLASSES AND SOFT MATTER

Neutron diffraction of hydrogenous materials: measuring incoherent and coherent intensities separately

Spin-polarised diffractometer D3

The determination of the structure of disordered materials containing substantial amounts of proton (^{1}H) nuclei is problematic when using neutron diffraction, due to the large spin-incoherent cross-section of ^{1}H (80.26 barns, in comparison with the structure-related coherent scattering cross-section of 1.76 barns). Polarised neutrons can be useful to overcome this issue: diffraction techniques with polarisation analysis can help us determine the coherent and spin-incoherent scattering contributions from the sample separately.

AUTHORS

L. Temleitner and **L. Pusztai** (Hungarian Academy of Sciences, Budapest, Hungary)
A. Stunault and **G.J. Cuello** (ILL)

REFERENCES

[1] G.L. Squires, Introduction to the Theory of Thermal Neutron Scattering, Dover Publications (1996)
[2] Th. Brückel and W. Schweika eds., Polarized Neutron Scattering, Forschungszentrum Jülich (2002)
[3] J.G. Powles, J.C. Dore and D.I. Page, Mol. Phys. 24 (1972) 1025

For liquids, diffraction experiments provide information about positional correlations between pairs of atoms. The wider the available momentum transfer range during the measurement, the better the resolution in real space. It is for this reason that we chose to work with the D3 spin-polarised, hot neutron beam instrument of the ILL. D3 provides a unique wide-momentum transfer range for polarised neutron diffraction (0.8 - 21 Å^{-1}). Using advanced techniques, such as the He^3 analyser filter, which is the most efficient polarisation filter at the applied wavelength (0.52 Å), we were able to separate the coherent and spin-incoherent scattering contributions from five mixtures of light and heavy water (0 %, 20 %, 40 %, 64 % and 100 % H_2O).

Under ideal circumstances, the structure-related coherent scattering comes only from scattering events in which the spin state of the neutron does not change (non-spin-flip). On the other hand, incoherent scattering is the result of both non-spin-flip and spin-flip (when the spin state of the neutron changes) events. The combination rules are simple: if we measure the scattered intensities of both spin-flip and non-spin processes from the sample, we can reconstruct the incoherent (1.5 x spin-flip intensities) and the coherent (by subtracting 0.5 x spin-flip intensities from the non-spin-flip intensities) scattering parts [1, 2].

Figure 1 summarises our experimental results for the H/D isotopically substituted water samples. Clearly, as the ^{1}H content increases, so does the intensity of incoherent scattering. In the case of the fully deuterated sample, coherent scattering dominates the pattern that would be measured by standard neutron scattering (without polarisation analysis), although incoherent contributions are non-negligible. At another extreme of the composition range, the conventional pattern for the fully protonated sample is dominated by incoherent scattering contributions: the coherent scattering intensity is marginal. This is the main reason why the use of non-deuterated samples in conventional neutron diffraction experiments is problematic: the approximations developed over the past four decades (see for example [3]) are still not perfect for removing the large (and, from the structural point of view, useless) incoherent contributions. This figure therefore demonstrates why the separate experimental determination of coherent and incoherent contributions is vital.

Figure 1
Total and separated coherent and spin-incoherent scattering contributions of water for various H_2O/D_2O mixtures.

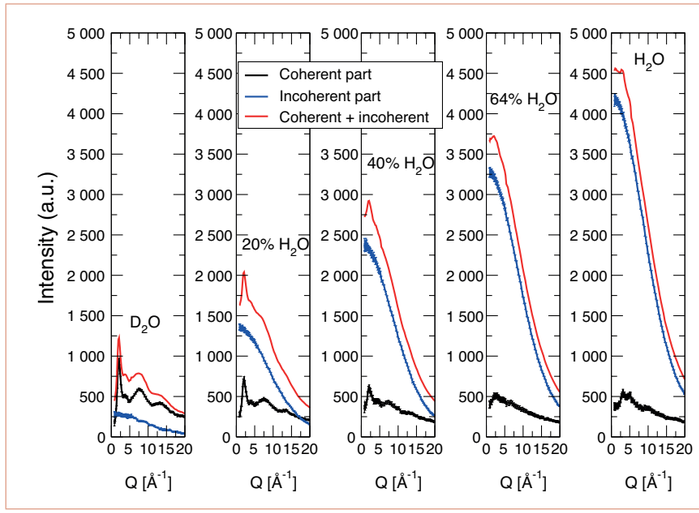

The isotopic substitution of hydrogen by deuterium provides a remarkable contrast: the coherent scattering lengths of the two isotopes are b_c^H = -3.7406 fm and b_c^D = 6.671 fm. In order to make good use of this contrast for structural investigations, the incoherent scattering part had to be approximated until now by empirical functions [3] so that the coherent scattering intensity from non-polarised neutron diffraction data could be deduced. As we have now measured this contribution separately, we can examine its functional form.

We show (**figure 2**) that a suitable form for describing the spin-incoherent scattering contribution follows a Q = 0 centred Gaussian function (plus a constant term). We also found a common full-width at half maximum for each composition, without any significant alteration of the residuals.

We believe that this study could have far-reaching consequences:

- We have demonstrated that (polarised) neutron diffraction can handle hydrogenous samples without deuteration, which means that it is possible to deal with the microscopic structure of 'soft matter' systems of any complexity.
- H/D isotopic substitution may now gain an enhanced reputation, since the large contrast between the coherent scattering lengths of H^1 and H^2 may be fully exploited.
- We foresee an inevitable boost in the development of polarised neutron instrumentation capable of performing experiments of the type described here.
- As we have provided the functional form of the incoherent background (**figure 2**), this result could be applied to correct data recorded on neutron diffractometers without polarisation analysis.

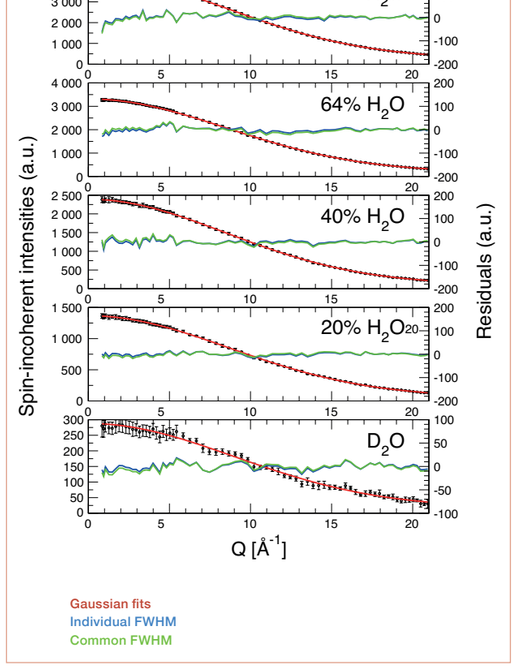

Figure 2
Gaussian fits to the experimentally-determined, spin-incoherent scattering contribution of water for different H_2O/D_2O mixtures. Residuals of the fits with individual and common FWHM values are also shown.

SCIENTIFIC HIGHLIGHTS

LIQUIDS, GLASSES AND SOFT MATTER

Self-assembly of magnetic nanoparticles at silicon surfaces

Reflectometer D17

Ferrofluids (FF) are textbook examples of a fluid tailored on a nanometer scale. They are colloidal suspensions of magnetic particles with a diameter of a few nanometers. The particles are smaller than the minimum size of a magnetic domain and therefore they are expected to be in a mono-domain state "superspin"[1, 2]. Due to thermal motion the magnetic moments of the particles are randomly oriented in the absence of an external magnetic field and the liquid as a whole exhibits a paramagnetic behaviour. Typically the particles are suspended in a carrier fluid such as oil, water, or other and are coated by long-chain ligands. This geometry leads to a competition between magnetic and steric interactions, resulting in strong correlations between magnetic and translational degrees of freedom. By applying an external magnetic field the individual particles orient their magnetic moments along the field lines [3], while dipolar interaction simultaneously leads to an ordering of their positions in space. This property results in field-induced viscosity anisotropy, which allows applications as seals or as heat dissipators in modern hard disc drives, high-power loud speakers and other mechanical devices [4]. More recent applications are discussed, like drug delivery or hyperthermia of cancer cells by using magnetic nanoparticles [5].

AUTHORS

K. Theis-Bröhl (University of Applied Sciences Bremerhaven, Germany)
P. Gutfreund (ILL)
A. Vorobiev (ILL and Uppsala University, Sweden)
M. Wolff (Uppsala University, Sweden)
B.P. Toperverg (ILL and Petersburg Nuclear Physics Institute, Gatchina, Russia)
J.A. Dura and **J.A. Borchers** (NIST, Gaithersburg, USA)

REFERENCES

[1] R.E. Rosensweig, Ferrohydrodynamics, Cambridge University Press, Cambridge, England, (1985)
[2] E. Blums, A. Cebers and M.M. Maiorov, Magnetic Fluids, W. de Gruyter, Berlin (1997)
[3] R. Schmidt, J. Benkoski, K. Cavicchia and A. Karim, Soft Matter 7 (2011) 5756
[4] H. Shahnazian, D. Gräf, D. Yu. Borin and S. Odenbach, J. Phys. D: Appl. Phys. 42 (2009) 205004
[5] I. Torres-Diaz and C. Rinaldi, Soft Matter 10 (2014) 8584
[6] K. Theis-Bröhl *et al.*, Soft Matter 11 (2015) 4695

In the present study [6] we investigated the interactions of ferrofluids with a solid interface under the influence of both magnetic field and shear by using a shear cell in a vertical geometry. Measurements using a commercial water-based FF with 10 nm-sized magnetite particles with an oleic acid-based ligand dispersant are presented in this article. The type chosen represents the most common type of ferrofluids and is close to what is used in industry, in particular concerning polydispersity, as can be seen in the transmission electron microscopy (TEM) image in **figure 1**.

Neutron reflectivity was employed on the ILL reflectometer D17 in order to gain insight into the out-of-plane structural ordering of the magnetic nanoparticles on a Si/SiO_2 surface, as well as insight into the characteristics of the organic layers between the nanoparticle cores.

From the scattering length density depth profiles (see **figure 2**) the following behaviour could be concluded: the silicon surface is covered by a dry layer of excess carboxylic acid, followed by a densely packed layer of nanoparticles. In the case of shear this wetting layer is slightly spread out in thickness, which can be explained by the assumption that this layer is very stable and only immobile particles stick to the silicon surface. Between the moving ferrofluid and the static wetting layer, a depletion layer occurs as a result. In the case of an applied magnetic field, the prolate particles experience a torque and align with their long axes along the silicon surface, which leads to a higher particle density at the surface.

In summary we have demonstrated that the interactions between a ferrofluid and a solid interface lead to the formation of self-assembled, multilayer structures. The hybrid organic layer that forms on the substrate surface appears to stabilise the complex wetting layer even in the presence of shear. The composition and thickness of the individual layers are sensitive to nanoparticle size and shape distributions as a result of the competing energetic interactions in the system. These results thus provide a path forward for controlling and tuning these self-assembled structures for device applications.

Our measurements set the stage for a wide range of studies into fundamental magnetic interactions on the nanoscale. From a basic science perspective this may serve as a tool to test interactions of magnetic domains of various sizes, strengths and separations. This will be of particular value in validating nanomagnetic modelling. From an applied perspective, understanding the rheology and surface interactions of ferrofluids will help extend the range of ferrofluid application. Furthermore, no measurements to date have determined the surface interactions of ferrofluids in the presence of flow and magnetic field with angstrom-level precision as was performed in the present study.

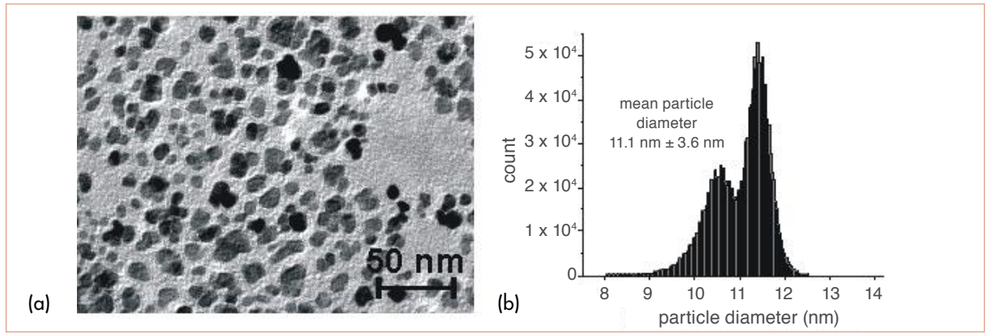

Figure 1

TEM image taken from the magnetite nanoparticles **(a)** and size distribution of the particles displayed as histogram **(b)**.

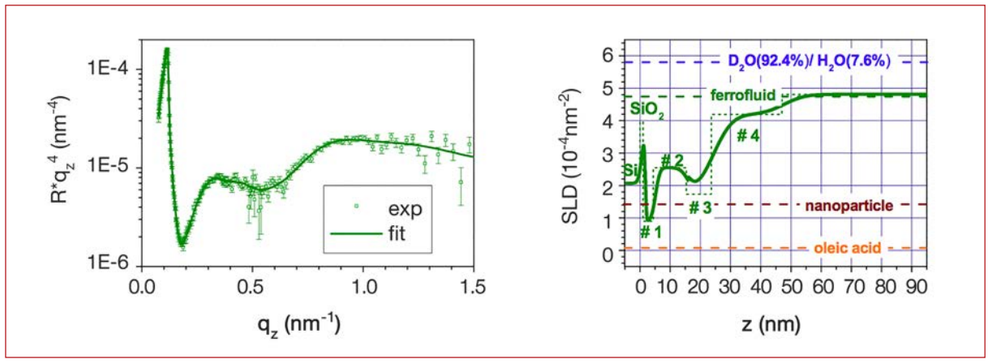

Figure 2

NR data taken in static conditions without magnetic field. Plot of Rq_z^4 as function of q_z. The solid lines represent fits to the data (**left**). Profile of nuclear scattering length density plotted as function of distance from the Si surface (**right**).

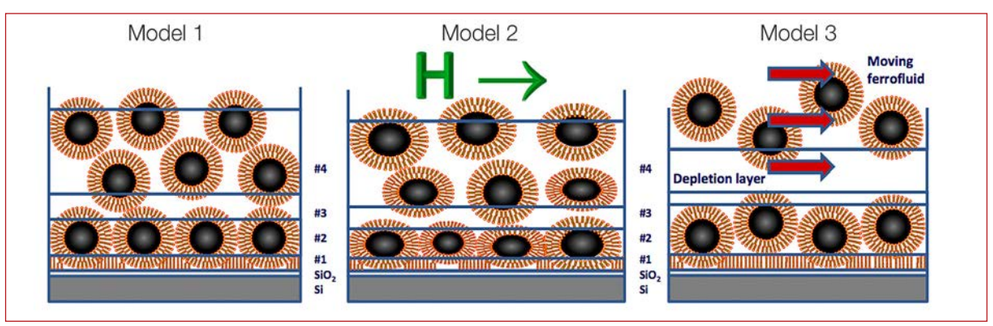

Figure 3

Models for the layering of the nanoparticles close to the silicon surface for the following conditions: static and no field (**Model 1**); static and applied magnetic field (**Model 2**); and, under shear (**Model 3**).

SCIENTIFIC HIGHLIGHTS

LIQUIDS, GLASSES AND SOFT MATTER

Dynamic phase diagram of soft nanocolloids – a recipe book

Small-angle diffractometer D11

We introduced new block polymer micelles which enable us to investigate a broad range of micellar aggregation numbers $10 \leq N_{agg} \leq 1000$ and concentrations $0.1 \leq \psi/\psi^* \leq 10$ of soft colloids using the same well-defined model system. We interpret rheological and dynamic light scattering (DLS) data in terms of recently developed experimental and theoretical approaches that quantitatively describe microscopic structure as observed by complementary small-angle neutron scattering (SANS) experiments. This finally enabled us to derive the dynamic phase diagram of soft colloids showing convincing agreement between experiment and theory without any adjustable parameter.

AUTHORS

S. Gupta (JCNS-SNS, Oak Ridge National Laboratory, USA)
M. Camargo (Universidad Antonio Nariño, Santiago de Cali, Colombia)
J. Stellbrink, J. Allgaier and **D. Richter** (JCNS-1 and ICS-1, Forschungszentrum Jülich, Germany)
A. Radulescu (JCNS-FRM II, Forschungszentrum Garching, Germany)
P. Lindner (ILL)
E. Zaccarelli (CNR-ISC and Universitá di Roma La Sapienza, Italy)
C.N. Likos (University of Vienna, Austria)

REFERENCES

[1] D. Vlassopoulos and M. Cloitre, Soft Matter 8 (2012) 4010
[2] S. Gupta, M. Camargo, J. Stellbrink, J. Allgaier, A. Radulescu, P. Lindner, E. Zaccarelli, C.N. Likos and D. Richter, Nanoscale 7 (2015) 13924
[3] S. Gupta, J. Stellbrink, E. Zaccarelli, C.N. Likos, M. Camargo, P. Holmqvist, J. Allgaier, L. Willner, and D. Richter, Phys. Rev. Lett. 115 (2015) 128302

Recent studies of soft matter include a large variety of complex fluids like synthetic polymers, biological macromolecules, colloids, amphiphilic systems, membranes as well as liquid crystals. A currently active field of research is focused on the special class of soft colloids, i.e. elastic and deformable colloidal particles, which display a dual character between polymers and hard spheres [1]. Examples of such soft colloids are vesicles, dendrimers, microgels, polymer-grafted nanoparticles, block copolymer micelles and star polymers. Due to their hybrid nature, soft colloids macroscopically show interesting structural and dynamic properties resulting from their unique microscopic structure.

We present a comprehensive experimental and theoretical study covering micro-, meso- and macroscopic length and time scales, which enables us to establish a generalised view in terms of the structure-property relationship and equilibrium dynamics of soft colloids. We introduce a new, tunable block copolymer model system that allows us to vary the aggregation number,

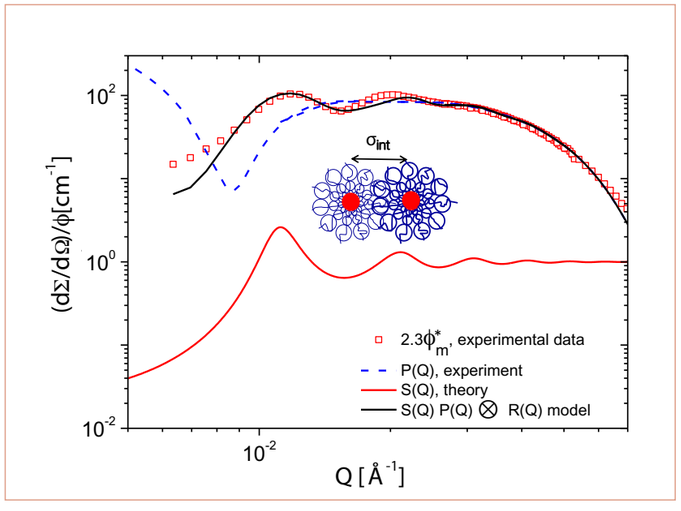

Figure 1

Normalised intensity $(d\Sigma/d\Omega)/\varphi$ for N_{agg} = 176, φ/φ^* = 2.3 and m:n = 1:37, compared to theoretical results, together with contributions from form factor, P(Q), and structure factor S(Q). **Inset)** schematic illustration of overlapping micelles and their interaction length.

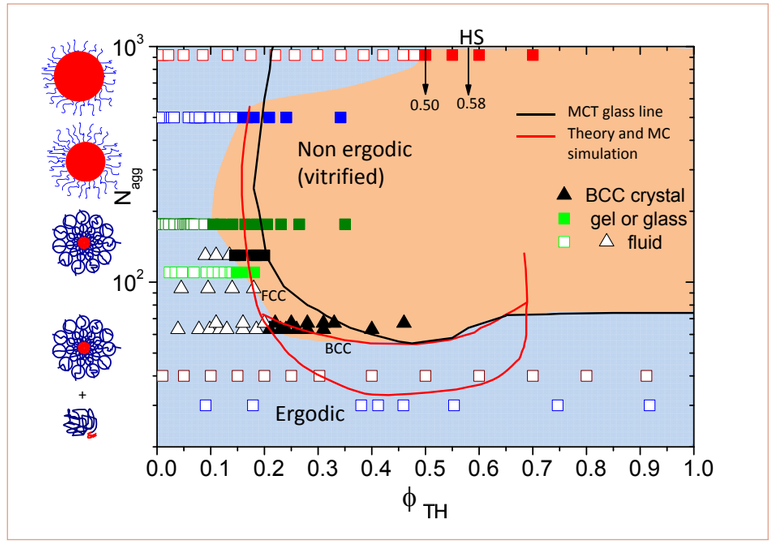

Figure 2

Dynamic phase diagram for soft colloids as a function of N_{agg} and the φ. Open symbols: fluid or ergodic phase; solid squares and stars: gel/glass phase (non-ergodic); solid triangles: BCC; solid lines: theoretical equilibrium phase diagram, and the MCT ideal glass line; stars: star-polymers from Vlassopoulos *et al.* Side sketches: schematic representation of micelles and unimers with change in N_{agg}.

and consequently its softness, by changing the solvophobic-to-solvophilic block ratio (m:n) over two orders of magnitude. Based on a simple and general coarse-grained model of the colloidal interaction potential, we verify the significance of interaction length σ_{int} governing both structural and dynamic properties. We put forward a quantitative comparison between theory and experiment without adjustable parameters, covering a broad range of experimental polymer volume fractions and regimes from ultra-soft, star-like to hard, sphere-like particles, which finally results in the dynamic phase diagram of soft colloids. In particular, we find throughout the concentration domain a strong correlation between mesoscopic diffusion and macroscopic viscosity, irrespective of softness, manifested in data collapse on master curves using the interaction length σ_{int} as the only relevant parameter. A clear re-entrance in the glass transition at high aggregation numbers is found, recovering the predicted hard-sphere (HS) value in the hard-sphere-like limit.

Small-angle neutron scattering (SANS) reveals experimental structure factors S(Q) which, in combination with liquid state theory and simulations, lay the basis for understanding soft colloids. As a representative example in **figure 1**, the partial core contrast SANS I(Q) for m:n = 1:37 and φ/φ^* = 2.3 is illustrated in the open symbols for the forward scattering. The curves for S(Q) calculated for N_{agg} = 176 and the corresponding φ_{TH} = 0.162, form factor P(Q) from SANS and P(Q)S(Q) ⊗ R(Q) (resolution) are also displayed.

All information related to both statics and dynamics has been brought together in an experimental dynamic phase diagram which was compared with the theoretical one, as shown in **figure 2**. Again, packing fraction φ based on σ_{int} as the only relevant length scale, was shown to be the appropriate reduction parameter, allowing a generic description of the macroscopic viscosity $\eta_0(\varphi)$, the mesoscopic diffusivity dynamics D(φ) and microscopic structure S(Q), and comparison of these properties for particles with varying softness.

The excellent agreement between our new experimental systems with different but already established model systems shows both the relevance of block copolymer micelles as a clever realisation of soft colloids, and the general validity of the coarse-graining approximation for describing structural, dynamical and phase features of dense, soft colloid suspensions. This understanding could provide guidance in the rational design of materials for targeted applications. Finally, this recipe book for soft colloids enabled us to prove the validity of the Stokes-Einstein relation in soft colloids up to the glass transition [3].

SCIENTIFIC HIGHLIGHTS

LIQUIDS, GLASSES AND SOFT MATTER

Contrast matching gone wrong? A study of polymer conformation in nanocomposites

Small-angle scattering diffractometer D11 ID02 beamline at the ESRF

Neutron scattering with isotopic substitution is a powerful tool for the structural characterisation of complex multi-component systems. Elucidating the chain structure of polymer nanocomposites by small-angle neutron scattering has triggered 15 years of effort and led to unexpected failure. We have recently proposed experiments and a statistical model explaining why in particular the smallest nanoparticles cause failure [1], thereby opening the road to strategies circumventing this problem.

AUTHORS

A. Banc, A.-C. Genix, C. Dupas, and **J. Oberdisse** (CNRS-Université de Montpellier, France)
M. Sztucki (ESRF, Grenoble, France)
R. Schweins (ILL)
M.-S. Appavou (Forschungszentrum Jülich, Outstation at MLZ, Garching, Germany)

REFERENCES

[1] A. Banc, A.-C. Genix, C. Dupas, M. Sztucki, R. Schweins, M.-S. Appavou and J. Oberdisse, Macromolecules 48 (2015) 6596
[2] J.-P. Cotton, Advances in Colloid and Interface Science, 69 (1996) 1
[3] A.-C. Genix and J. Oberdisse, Current Opinion in Colloid and Interface Science 20 (2015) 293
[4] M. Krutyeva, A. Wischnewski, M. Monkenbusch, L. Willner, J. Maiz, C. Mijangos, A. Arbe, J. Colmenero, A. Radulescu, O. Holderer, M. Ohl, and D. Richter, Phys. Rev. Lett. 110 (2013) 108303

Small-angle neutron scattering (SANS) is particularly suited for the structural characterisation of binary systems on the nanoscale, as then only one correlation term is needed to describe structure. Things become more difficult for multi-component systems. Neutron scattering may offer a unique view in such cases, if selective deuteration can be used to either highlight or match contributions to scattering of specific components. The filler structure of polymer nanocomposites, for example, can be investigated by small-angle X-ray scattering (SAXS) or SANS, and electron microscopy (**figure 1**), as the structure of nanoparticles in a polymer matrix corresponds to a single correlation function. The chain structure in a pure matrix is already chemically more involved as certain chains need to be labelled isotopically [2], but the scattering experiment is still based on a single correlation function. Investigating the chain structure in polymer nanocomposites, however, is more involved. In theory, the so-called zero average contrast (ZAC) method based on well-chosen mixtures of hydrogenated (H) and deuterated (D) polymer chains allows matching of the filler scattering and renders only the polymer chains visible to neutrons [2].

However, for some mysterious reason perfect silica matching in nanocomposites proves to be impossible in general, as reported in the literature over the past 15 years ([3], and references therein). We have recently undertaken a study of model nanocomposites with two different silica filler nanoparticle sizes [1]. The system under investigation here consists of polyethylmethacrylate polymer chains in latex beads and silica nanoparticles. As schematically illustrated below [3], latex beads "dissolve" by letting polymer chains escape into the material *via* a diffusion mechanism.

Mixing appropriate amounts of H- and D-latex beads allows one in principle to exactly match the silica nanoparticle drawn in the middle, once the chains are well mixed. Our results for two different nanoparticle sizes are shown in **figure 2**. Surprisingly, this comparison highlighted the effect of the smallest nanoparticles, i.e. the very ones that are most interesting, for applications systematically perturb matching. In the case of small silica nanoparticles a strong evolution

Figure 1
Example of transmission electron microscopy picture of a polymer nanocomposite.

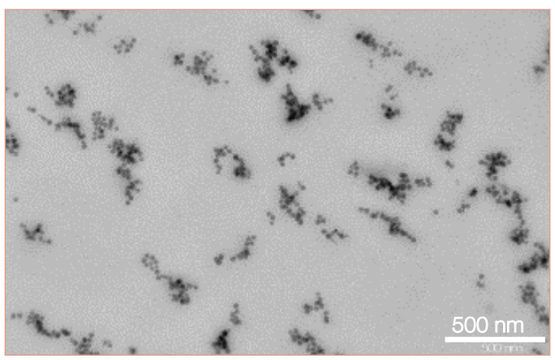

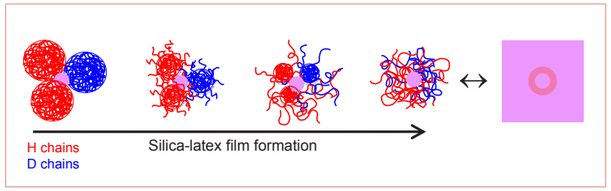

Figure 2
SANS intensities of polymer matrix and nanocomposites under zero-average contrast conditions for big (**left**: 15 nm radius) and small (**right**: 5 nm) nanoparticles. Filler volume fractions are given in the legend. The schemes below illustrate the contrast observed in annealed nanocomposites by SAXS (grey) and SANS (coloured).

with the filler volume fraction is seen on the right side of **figure 2**, proving that the silica is visible in spite of theoretically perfect matching. The chemically identical system on the left does not show such an evolution. Moreover, the SANS nanocomposite signal on the right is comparable to the SAXS signal, as superimposed for illustration.

We propose an explanation for this finding based on the statistical properties of the environment of the nanoparticles, where a size-dependent mismatch in the distribution of the protonated and deuterated chains in the vicinity of the silica is predicted and calculated theoretically, as schematically shown below. Indeed, the number of neighbours surrounding a given silica particle is typically very small, at most ten or so, due to the small size of the nanoparticles. It can thus be conjectured that the local concentrations of H- and D-latex around a silica particle may not necessarily match the global ones. Based on a simple calculation of the (binomial) probability distribution of concentrations in the shell of first neighbours surrounding a nanoparticle (see **scheme**), we are able to predict the moments of the scattering length density distributions. It is found that only the average obeys the ZAC-condition, whereas higher orders, and in particular

Scheme: Statistics of neighbouring

$$P(n_H) = \binom{N}{n_H} \Phi_H^{n_H} \Phi_D^{n_D}$$

the non-zero variance, express local mismatch. This leads to a situation where many shells of different composition highlight the encapsulated nanoparticles, even if the average over the composition of all shells matches them exactly. The resulting shells are drawn in the scheme of latex film formation, and lead to the many shells of different colour (illustrating the distribution of neutron contrasts – invisible to X-rays) at the bottom of **figure 2**.

The conjectured H/D mismatch induces a filler-dependent upturn of the Q intensity in the SANS spectra, which makes data interpretation difficult (see **figure 2**). We therefore developed a quantitative description of the low Q scattered intensity based on the existence of such mismatched layers, for the first time to the best of our knowledge [1]. By fitting the SAXS intensity describing the filler nanoparticles to the SANS intensity as shown for one concentration in **figure 2** on the right, we can extract a prefactor and relate it with our theory to the thickness of the mismatched layers.

Finally, one may note that the initial objective of measuring chain conformations in polymer nanocomposites is also reached (see the Debye-like scattering at intermediate angles leading to the determination of the radius of gyration (R_g) in **figure 2**). Such measurements may be of importance for a quantitative description of modern materials, like paints resisting frequent temperature changes *via* the elasticity provided by polymers, or car tyres, another important application of nanocomposites. The intrinsic difficulty of local concentration fluctuations in nanosystems as investigated here, however, should play a role in many different systems, as for instance in porous systems where the number of macromolecules filling a nanopore may very well be a small number subjected to large fluctuations [4].

SCIENTIFIC HIGHLIGHTS

LIQUIDS, GLASSES AND SOFT MATTER

Sensing the tube by ring topology

Spin-echo spectrometer IN15

Ring polymers are ideal probes granting direct access to molecular aspects of polymer motion. In blends of rings immersed in a linear polymer matrix the dynamics are controlled by the embedding matrix. As a consequence of the unique ring topology, in long chain matrices the entanglement spacing is directly revealed by neutron spin-echo spectroscopy, unaffected by local reptation of the host molecules beyond this distance. In addition, secondary relaxation processes could be quantified for shorter entangled matrices.

AUTHORS

S. Gooßen, M. Krutyeva, J. Allgaier, W. Pyckhout-Hintzen, A. Wischnewski and **D. Richter** (Jülich Centre for Neutron Science (JCNS-1) and Institute for Complex Systems (ICS-1), Jülich, Germany)
M. Sharp (ESS, Sweden and ILL)
A. Feoktystov (Jülich Centre for Neutron Science (JCNS) at Heinz Maier-Leibnitz Zentrum (MLZ), Garching, Germany)

REFERENCES

[1] J.D. Halverson, W.B. Lee, G.S. Grest, A.Y. Grosberg and K. Kremer, J. Chem. Phys. 134 (2011) 204905
[2] B.V.S. Iyer, A.K. Lele and S. Shanbhag, Macromolecules 40 (2007) 5995
[3] S. Gooßen, A.R. Brás, M. Krutyeva, M. Sharp, P. Falus, A. Feoktystov, U. Gasser, W. Pyckhout-Hintzen, A. Wischnewski and D. Richter, Phys. Rev. Lett. 113 (2014) 168302
[4] K. Niedzwiedz, A. Wischnewski, W. Pyckhout-Hintzen, J. Allgaier, D. Richter and A. Faraone, Macromolecules 41 (2008) 4866
[5] S. Gooßen, M. Krutyeva, M. Sharp, A. Feoktystov, J. Allgaier W. Pyckhout-Hintzen, A. Wischnewski and D. Richter, Phys. Rev. Lett. 115 (2015) 148302

Owing to their unique topology, macromolecular rings without chain ends are the subject of intense interdisciplinary research. In biology, for instance, plasmids, cyclic polysaccharides, peptides, RNA and DNA are investigated, where nature exploits the ring topology to facilitate super-coiling or catenation. Furthermore, in the fields of material science and engineering, blends of different polymer architectures including rings are employed to produce polymer materials with new properties. Recently, simulation science in particular led to new insights into ring dynamics on a coarse-grained level [1]. In chemistry, novel procedures have enabled the production of appreciable amounts of pure, well-defined rings that in turn permit detailed physical investigations of their structure and dynamics. One of the important and fundamental goals of this broad approach is the understanding of entangled polymer dynamics far beyond the state-of-the-art standpoint.

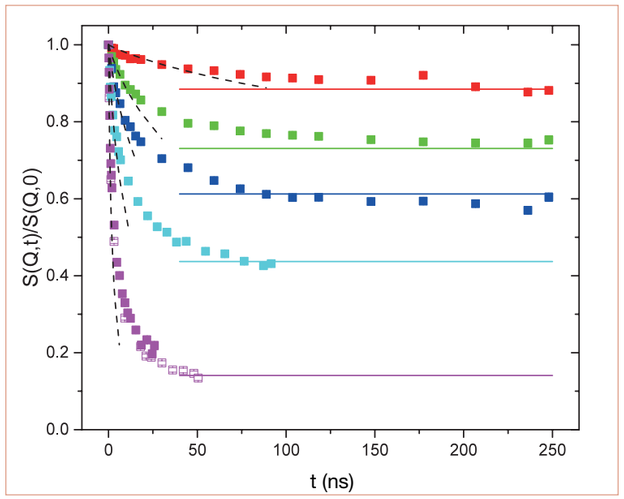

Figure 1

Neutron spin-echo spectra for the ring polymer ($\Phi = 0.1$) in a well-entangled, deuterated linear matrix for Q values (from the top down) 0.05, 0.08, 0.1, 0.13, and 0.2 Å^{-1} at $T = 413$ K. Full and empty symbols refer to two different wavelength setups. Dashed black lines: initial Rouse decay. Solid lines: plateaux with $d_e = 42$ Å.

Figure 2

Schematic illustration of a linear polymer and a ring polymer chain probing the tube formed by the surrounding linear matrix. The inner green tube represents the unrelaxed tube diameter explored by the ring polymer. On the other hand, a linear probe also accesses the outer light green tube by further relaxation of the linear chain along the tube and thereby overestimates the tube diameter.

Photo credit: APS/Alan Stonebraker (PHYSICS VIEWPOINT: Caught in the Tube; *Physics* 8,93).

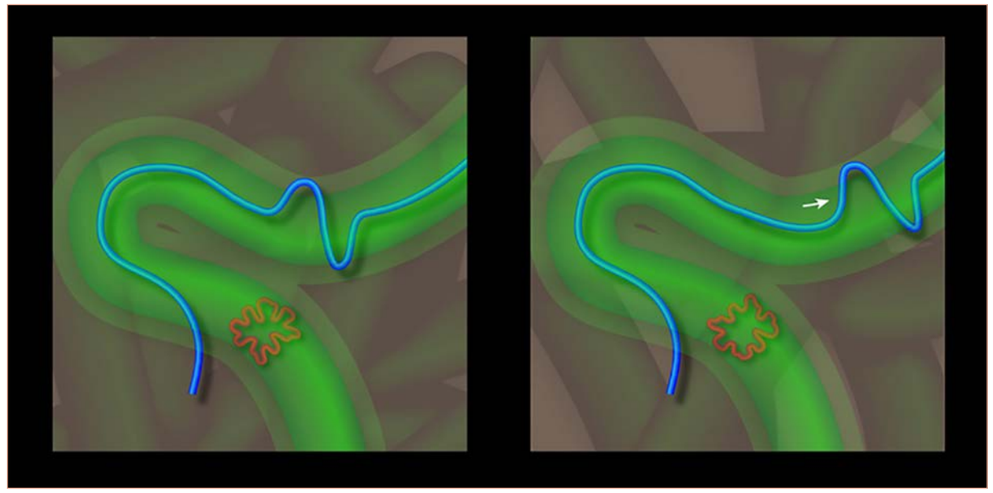

In this neutron spin-echo study at IN15, a dilute polyethylene oxide ring polymer was immersed in linear matrices of varying molecular weights – an unentangled matrix of 2 kg/mol, an intermediately long, entangled matrix of 20 kg/mol and a very long, well-entangled matrix of 80 kg/mol. Supplemental structural investigation was carried out by means of small-angle neutron scattering.

Unlike in pure ring polymer melts, rings in a blend do not exhibit a compact structure like a crumpled globule but rather fulfil the Gaussian prediction – both in agreement with recent simulation work [2]. Hence, considering the ring-closure the rings are a factor of √2 smaller than the corresponding linear chain. The ring topology has a severe influence on the dynamics of the ring in a blend. In general, the short-time behaviour can be described in terms of the Rouse model. However, for the pure ring polymer melt the compact structure yielded the generation of loops which resulted in an effective suppression of long wavelengths modes [3]. The Gaussian ring in a linear matrix, on the other hand, requires the full Rouse model for a description of the experimental data (see dashed black lines in **figure 1**). Thus, the loopy structure is not present in the blend, complementing the small-angle scattering results.

After the initial Rouse behaviour the dynamics are constrained by the linear matrix causing an effective slowing down of the dynamics. With increasing molecular weight these constraints get more and more influential, finally leading to plateaux in the intermediate scattering function for the longest matrix.

Describing these plateaux with a Gaussian distribution of obstacles, such as the tube constraints, we found $d_e = 42 \pm 1$ Å (see coloured lines in **figure 1**). However, for the chain dynamics of the pure linear matrix a tube diameter d of 52.5 Å was found experimentally [4]. How do these two quantities relate to each other?

The single chain pair correlation function $S(Q,t)$ for highly entangled linear chains contains the local reptation process, i.e. the relaxation of longitudinal Rouse modes along the tube. The description of the dynamic structure factor in terms of this local reptation model then provides an effectively relaxed tube diameter d, relating to those constraints that remain after the relaxation by the longitudinal Rouse modes has finished. With respect to rheology, d relates to the corresponding relaxed plateau modulus G_N. The ring segments, however, are not able to undergo longitudinal relaxation processes along the tube that is formed entirely by the confining linear chains. They remain confined by the lateral tube constraints and compare to the unrelaxed modulus G_e. Thus, the ring directly probes the tube devoid of any further relaxation processes. The ratio of the unrelaxed and relaxed constraints $(d_e/d)^2 \approx 2/3$ expresses this fact. In the case of the linear chains, one third of the modes, i.e. the longitudinal modes, are not affected by the tube confinement.

For the 20 kg/mol matrix the IN15 experiment allowed us to directly quantify contour length fluctuations. The rings probe the widening of the tube by the secondary relaxation caused by the ends of the linear chains of the matrix.

The presented approach is not limited to the investigation of linear polymers. We also anticipate that tube dilution effects in particular prominent in branched architectures can, for example, be quantitatively addressed by a small number of immersed rings.

SCIENTIFIC HIGHLIGHTS

BIOLOGY AND HEALTH

Unveiling the role of water translation in the onset of protein functional motions

Backscattering spectrometer IN16B and D-Lab

Water is often called the matrix of life because its presence is essential to all known living organisms. At the molecular level, proteins need to be covered by water in order to be biologically active. This so-called hydration water is generally acknowledged to enable the internal motions of proteins that are so fundamental for their capacity to fulfil a specific biological function. Yet, the molecular mechanism behind water's importance for functional protein dynamics has remained elusive. A combined approach using quasi-elastic neutron scattering experiments on perdeuterated proteins and molecular dynamics simulations recently provided new insights into the nature of water dynamics promoting functional protein motions. The same approach revelaed an effect of the pathological aggregation of a human brain protein on the mobility of its hydration water.

AUTHORS

G. Schirò, Y. Fichou and **M. Weik** (IBS, France)
M. Moulin, E. Mossou and **M. Härtlein** (ILL)

REFERENCES

[1] W. Doster, S. Cusack and W. Petry, Nature 337 (1989) 754
[2] G. Schirò, Y. Fichou, F-X. Gallat *et al.*, Nat. Commun. 6 (2015) 6490
[3] M. Tarek and D.J. Tobias, Phys. Rev. Lett. 88 (2002)138101
[4] Y. Fichou, G. Schirò, F-X. Gallat *et al.*, Proc. Natl. Acad. Sci U.S.A. 112 (2015) 6365

The complex ensemble of water-protein motions can be teased apart by extending experiments and simulations down to cryo-temperatures. A seminal experiment performed at the ILL about 25 years ago showed for the first time that hydrated proteins are characterised by an onset of structural flexibility as the temperature is increased above -30°C, revealed as a transition to large-amplitude anharmonic motions of hydrogen atoms on the picosecond timescale [1]. Since then the physical origin of this transition, known as the *protein dynamical transition*, has been controversially debated in the biophysical community and different scenarios proposed in the literature.

Now, an international team lead by researchers from the Institut de Biologie Structurale in Grenoble and the University of California, Irvine has shed light on the molecular mechanism behind the importance of water for functional protein dynamics [2]. The team has been able to characterise water motions on the protein surface at different temperatures, thereby highlighting the key dynamical features that correlate with protein activity. A combination of protein deuteration, quasi-elastic neutron scattering and molecular dynamics simulations was employed during the study. The use of perdeuterated recombinant proteins, expressed in high cell-density cultures of *Escherichia coli* at the D-Lab in the ILL's Life Sciences Group, allowed the researchers to focus solely on water motions on the protein surface in the neutron scattering experiments. The high quality of quasi-elastic neutron spectra and the introduction of a sophisticated multidimensional data analysis enabled an accurate description of the nature of water diffusive motions.

When "visualising" water movements on the protein surface (**figure 1**), the team discovered that the molecules rotate around their own axes at temperatures below -30° C; temperatures at which only very local protein motions are energetically accessible and proteins are biologically inactive. Above -30° C, however, whilst continuing to rotate the water molecules also undergo translational diffusion on the protein surface. This is the temperature at which proteins start to explore large-scale molecular fluctuations and to be biologically active. On the basis of their experimental pieces of evidence, the researchers suggested that the capability of water molecules to flow on the surface of proteins enables the dynamics they need to function. Unexpectedly, this connection between water and protein dynamics does not depend on the degree of order in the protein structure, as suggested by similar results obtained for a globular protein and for an intrinsically disordered protein. The role of water translational diffusion in the protein dynamical transition was previously postulated based on molecular dynamics simulations [3], but so far no experimental confirmation has been provided in the literature.

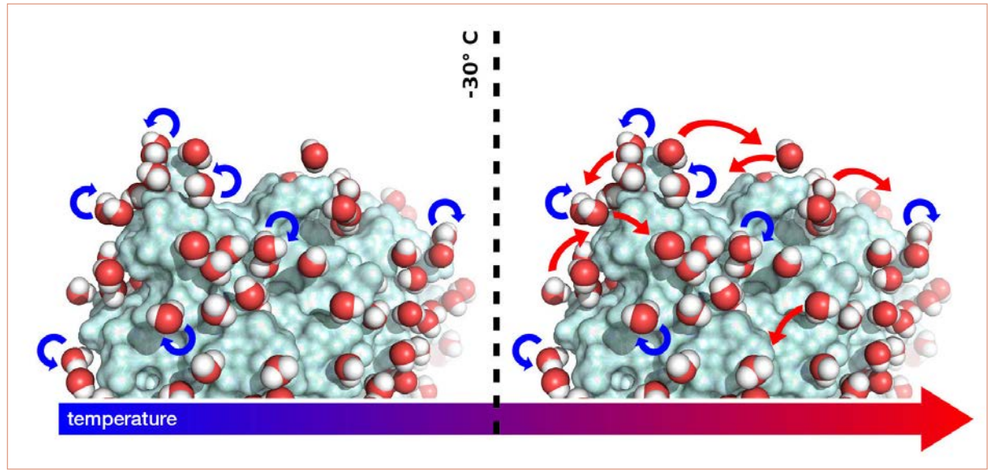

Figure 1
Water translational diffusion on the protein surface appears above -30 °C and enables protein large amplitude motions, which are essential for protein activity.

In order to further explore the importance of hydration water dynamics for protein function and malfunction, the experimental team also investigated water diffusion on the surface of paired helical filaments (PHF) formed by the intrinsically disordered human protein tau [4]. PHF are fibres of amyloid nature, known as one of the pathological hallmarks of Alzheimer's disease. The mechanisms of fibre formation, in particular the role that hydration water might play, remain poorly understood. Again by combining protein perdeuteration, neutron scattering and all-atom molecular dynamics simulations, the researchers found that in comparison with monomeric tau, hydration water on the surface of tau fibres is more mobile, as evidenced by an increased fraction of translationally diffusing water molecules, a higher diffusion coefficient and increased mean-squared displacements in neutron scattering experiments. The observed increase in hydration water dynamics is suggested to promote fibre formation through entropic effects.

The latter study [4] perfectly suggests that methodologies sensitive to the diffusion of water could be used to detect increased water mobility in Alzheimer-diseased brains. The ensemble results perfectly illustrate the benefits of using neutron scattering in combination with deuterium labelling in probing dynamics of biological samples.

BIOLOGY AND HEALTH

Neutrons look deep into the binding selectivity of protein kinases for cell-signalling molecules

Quasi-Laue diffractometer for biology LADI Advanced Light Source in Berkeley

A joint X-ray/neutron (XN) crystallographic study has been performed to locate H and D atoms and directly visualise hydrogen bonding in the cyclic nucleotide-binding domain of cyclic guanosine monophosphate (cGMP)-dependent protein kinase (PKG) in complex with the activator cGMP. Crystallographic evidence reveals crucial hydrogen-bond interactions between cGMP and the protein, shedding light on the atomic details of high cyclic nucleotide-binding domain selectivity towards cGMP relative to cyclic adenosine monophosphate (cAMP). These results will assist the structure-guided design of PKG activators in the treatment of hypertensive disease.

AUTHORS

C. Kim and **G.Y. Huang** (Baylor College of Medicine, Texas, USA)
A.Y. Kovalevsky, and **O.O. Gerlits** (Oak Ridge National Laboratory, Tennessee, USA)
M.P. Blakeley (ILL)
B. Sankaran (Lawrence Berkeley National Laboratory, California, USA)

REFERENCES

[1] J.A. Beavo, and L.L. Brunton, Nat. Rev. Mol. Cell Biol. 3 (2002) 710
[2] G.Y. Huang, J.J. Kim, A.S. Reger, R. Lorenz, E.W. Moon, C. Zhao, D.E. Casteel, D. Bertinetti, B. Vanschouwen, R. Selvaratnam, J.W. Pflugrath, B. Sankaran, G. Melacini, F.W. Herberg, and C. Kim, Structure 22 (2014) 116
[3] G.Y. Huang, O.O. Gerlits, M.P. Blakeley, B. Sankaran, A.Y. Kovalevsky, and C. Kim, Biochemistry 53 (2014) 6725

A protein kinase is an enzyme that modifies other proteins by chemically adding phosphate groups to serine, threonine or tyrosine amino acid residues, and is known to regulate the majority of cellular pathways, especially those involved in signal transduction. Cyclic guanosine monophosphate (cGMP)-dependent protein kinase or Protein Kinase G (PKG) is a serine/threonine-specific protein kinase that is activated by cGMP. It phosphorylates a number of biologically important targets and is implicated in the regulation of smooth muscle relaxation, platelet function, cell division and nucleic acid synthesis.

PKG is one of the major mediators of cyclic nucleotide signalling in mammalian cells [1]. Aberrant PKG signalling caused by genetic mutations is the leading cause of thoracic aortic aneurysms and dissections – a potentially life-threatening condition. PKG consists of two sub-units – catalytic (C) and regulatory (R) – that are fused into one polypeptide. The R sub-unit binds two cGMP molecules to its two cyclic nucleotide-binding domains (CNB-A/B) to undergo a large, conformational change that releases the C-domain and activates the kinase (**figure 1**). Interestingly, CNB-A binds cGMP and cAMP, another signalling molecule abundant in cells, with similar affinity. Conversely, CNB-B is 200-fold selective for cGMP over cAMP [2].

The molecular mechanism of reduced selectivity for cAMP has remained unknown. Because hydrogen bonding and water-mediated interactions are critical in ligand recognition by proteins, we have studied binding of cGMP to CNB-B using macromolecular neutron crystallography [3]. Hydrogen atoms are crucial players in ligand recognition by macromolecular targets, participating in directional hydrogen bonding and non-directional hydrophobic and electrostatic interactions. But hydrogen atoms are virtually invisible to X-rays due to their poor scattering power. Neutrons, however, being scattered by atomic nuclei, represent a superb probe to locate hydrogen atoms and obtain atomic details of intermolecular interactions in macromolecules. The visibility of hydrogen atoms is enhanced further when the light isotope H is exchanged with the heavy isotope D (deuterium).

Neutron crystallographic data to 2.2 Å resolution for the PKG CNB-B:cGMP complex (**figure 2**) were collected using the instrument LADI at the ILL. The neutron data were supplemented with low-temperature X-ray diffraction data on the complex CNB-B:cAMP. CNB-B:cGMP neutron structure is the first of its kind for a CNB domain of any protein kinase. Taken together, these structures provide new, atomic-level insights into the ability of CNB-B to filter out cAMP.

cGMP is captured in a shallow binding site in CNB-B by a group of residues called the phosphate binding cassette (PBC; **figure 2**). Several hydrogen bonds are formed by the phosphate and the D-ribose moieties of cGMP with PBC that would be very similar to the interactions made by cAMP. Thr317 accepts a deuterium atom in a hydrogen bond with guanine 2-ND_2 group of cGMP (**figure 3**). Thr317 is known to be a key residue responsible for high affinity for cGMP. Another key interaction of the guanine moiety is with the flexible side chain of Arg297. Importantly, low-temperature X-ray structure of CNB-B:cGMP complex showed tight contacts of the two groups, but in the room-temperature neutron structure interactions between guanine moiety of cGMP and Arg297 are more relaxed, indicating that the position of Arg297 side chain at low temperature may be "frozen out" and less physiologically relevant. The cGMP binding is further stabilised by Tyr351 located at the αC helix (**figures 2** and **3**) by π–π interactions and sandwiching the guanine moiety against aliphatic groups of Val283 and Leu296. Importantly, the neutron structure indicates no H/D exchange of the main chain amides of the residues in the cGMP binding pocket, suggesting significantly slowed dynamics that may be an important factor in CNB-B selectivity for cGMP.

When the neutron structure of CNB-B:cGMP complex is compared with the low-temperature X-ray structure of CNB-B-cAMP complex the major differences in the cyclic nucleotide binding are observed for the nucleic bases, guanine and adenine, respectively. In the cGMP complex the presence of 2-ND_2 group on guanine results in a hydrogen bond with Thr317 that ensures a single orientation of the nucleic base. On the other hand, adenine lacks this chemical group and binds in two different orientations related by a 180° flip of the adenine moiety, weakening interactions with Thr317. Moreover, Arg297 moves away from adenine to avoid collision and is positioned only to form van der Waals contacts with cAMP. Likewise, Tyr351 moves slightly away from cAMP. The reduced contacts directly demonstrate why cAMP binding to CNB-B is weakened.

In conclusion, in this study neutron and X-ray crystallographic results have been combined to demonstrate high selectivity of CNB-B of PKG toward cGMP compared with cAMP. The results reveal which atomic interactions are responsible for the high affinity to cGMP and the much lower affinity to cAMP of the cyclic nucleotide binding pocket. Our neutron structure provides an unprecedented view of the hydrogen bonding in an R sub-unit of PKG and can serve as a model for other CNB domains. Moreover, because PKG is an important drug target the directly visualised hydrogen bonds provide new information that can be used for structure-guided design of PKG activators.

Figure 1
Schematic representation of PKG activation through binding of cGMP molecules to the R sub-units.

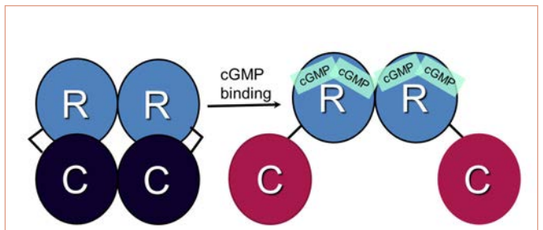

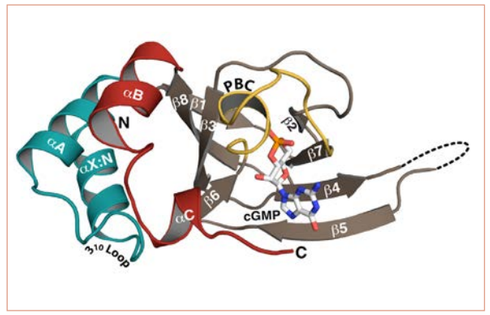

Figure 2
Overall structure of CNB-B of PKG in cartoon representation.

Figure 3
Intermolecular interactions made by cGMP with the binding pocket of PKG CNB-B. Inserts show neutron scattering length density maps contoured at 1 σ level indicating correct positions of deuterium atoms and visualising hydrogen-bonding interactions.

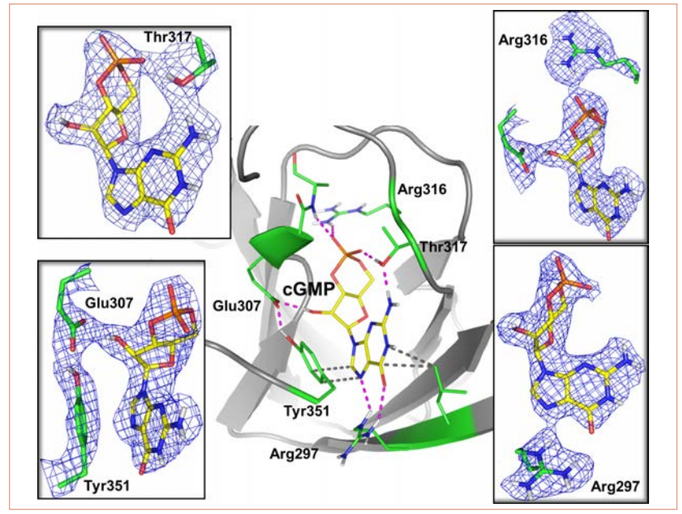

BIOLOGY AND HEALTH

Neutrons reveal the internal structure and assembly mode of a large, oligomeric peptide-degrading machine

Small-angle diffractometer D22 and D-Lab

Small-angle neutron scattering of a protein complex from a hyperthermophilic deep-sea organism living close to hydrothermal vents was measured at the D22 diffractometer at the ILL. The data provide new insights into the structural molecular details and control mechanisms of protein degradation pathways in living organisms, and suggest strategies to optimise the performance of macromolecular complexes for biotechnological applications.

AUTHORS

B. Franzetti and **A. Apollaire** (IBS) and **F. Gabel** (IBS, ILL)
M. Härtlein and **M. Moulin** (ILL)

REFERENCES

[1] A. Varshavsky, Trends Biochem. Sci. 30(6) (2005) 283
[2] C.A. Ross and M.A. Poirier, Nat. Med. 10 (2004) Suppl: S10-17
[3] A. Appolaire, M.A. Durá, M. Ferruit, J.P. Andrieu, A. Godfroy, S. Gribaldo and B. Franzetti, Mol. Microbiol. 94(4) (2014) 803
[4] A. Appolaire, E. Girard, M. Colombo, M.A. Durá, M. Moulin, M. Härtlein, B. Franzetti and F. Gabel, Acta Crystallogr. D Biol. Crystallogr. 70(Pt 11) (2014) 2983

All life at a cellular level requires that its proteome (i.e. the ensemble of different proteins present at a given moment in time) is accurately and tightly regulated. A part of this task is assumed by a multitude of molecular machines that identify, bind, unfold and digest proteins marked for destruction in complex metabolic pathways into their amino acid building blocks for recycling [1]. Dysregulation of these pathways can lead to severe diseases and death as a result of perturbations in the development and metabolism of organisms or as an accumulation of defective protein forms that have a tendency to build harmful aggregates [2].

Figure 1

Pyrococcus horikoshii cells (**inset**) were first extracted from deep-sea hydrothermal vents in more than 1 000 m depth.
© Ifremer and W. W. Norton & Co, Inc.

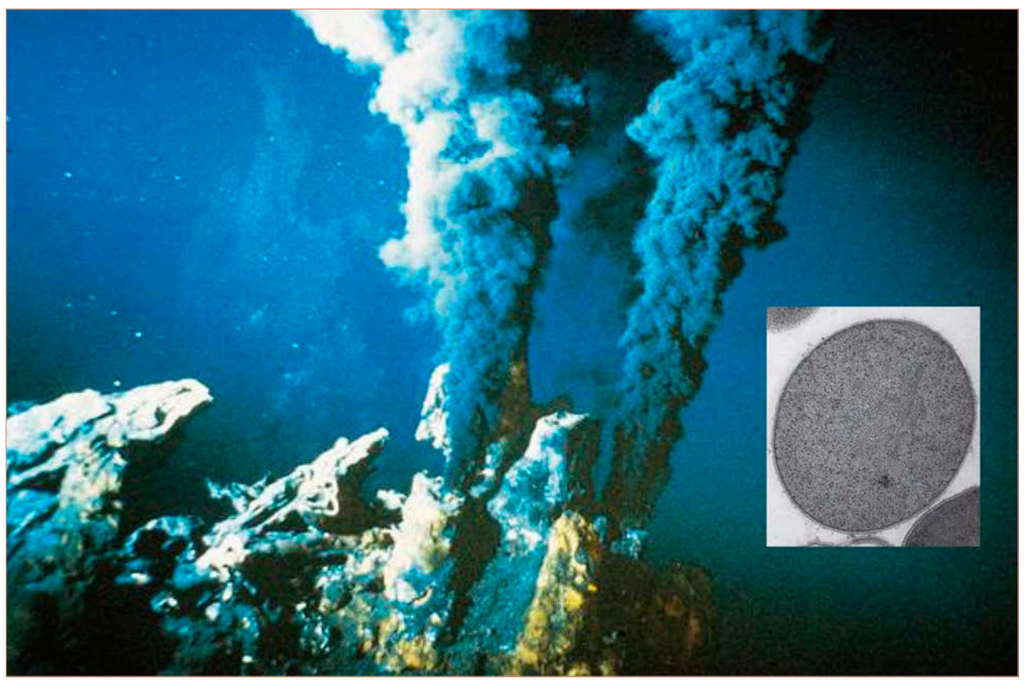

A key player at the downstream part of the protein degradation process in archaea (the third domain of life, alongside eukarya and bacteria) is the TET enzyme complex that digests short protein fragments (oligo-peptides) into amino acids [3]. It is a macromolecular machine of 470 kiloDalton, composed of twelve protein sub-units that are either identical (homo-dodecameric form) or different (hetero-dodecameric form). The hetero-oligomeric form contains two protein sub-units with complementary proteolytic properties that are specific to distinct classes of peptide bonds, and has been found to be more efficient than equimolar solutions of mixtures of homo-dodecameric forms of the enzyme. Even though structural studies were available on the homo-dodecameric complexes, the internal sub-unit organisation, assembly mode as well as substrate efficiency of the hetero-oligomeric complexes have long remained unclear.

In a collaboration between scientists of the Institut de Biologie Structurale (IBS), Grenoble, and the ILL, Grenoble, both the structure and the assembly pathway of the hetero-dodecameric TET complex from the hyperthermophilic archeon *Pyrococcus horikoshii* (**figure 1**) have been determined by combining data from crystallography, electron microscopy and small-angle X-ray and neutron scattering. Small-angle neutron data of hetero-dodecameric TET complexes, reconstituted *in vitro* from hydrogenated and deuterated sub-units (prepared at the ILL deuteration laboratory), were recorded at several contrast conditions (H_2O : D_2O ratio in solution) on the D22 diffractometer at ILL. The neutron data allowed us to visualise specific sub-units within the TET complex, yielding unique insight into the internal protein sub-unit arrangement as well as the assembly pathway [4].

Figure 2

Model for the hetero-dodecameric TET complex, composed of deuterated TET2 and hydrogenated TET3 sub-units and the small-angle neutron scattering data at various H_2O : D_2O ratios, measured at the ILL D22 diffractometer. Each apex of the assembled complex consists of one TET2 and two TET3 (or *vice versa*) sub-units with catalytic domains of complementary substrate specificity. The hetero-catalytic pockets thus formed optimise the overall proteolytic efficiency of the complex.

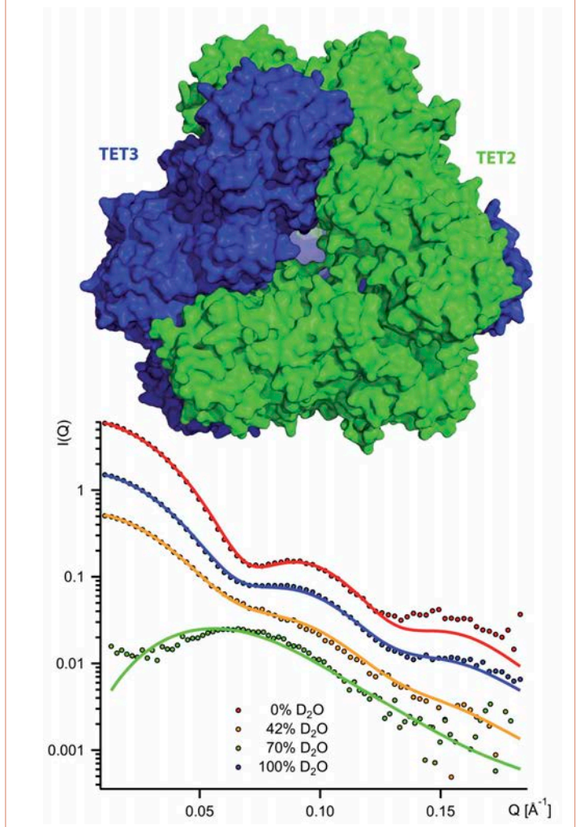

The specific structural arrangement of the two different protein sub-units TET2 and TET3, revealed by the neutron data, demonstrated that the enhanced proteolytic efficiency of the assembled hetero-dodecameric complex is due to an elegant arrangement of protein sub-units with complementary substrate specificities, exclusively into hetero-catalytic pockets at the apices of the assembled TET complex (**figure 2**). Furthermore, since the neutron data could exclude alternative internal sub-unit arrangements or stoichiometry, specific sub-unit assembly pathways could be proposed, in combination with small-angle X-ray and electron microscopy data.

Importantly, the protocol developed here for the interpretation of neutron contrast data from an archaeal system will be applicable to other challenging symmetric, macromolecular complexes that carry out crucial functions in eukaryotic organisms, including humans. Finally, the elegant internal topology, bringing together complementary catalytic sub-units to enhance substrate catalysis, indicates strategies to design and optimise the performance of other macromolecular complexes for biotechnological applications.

SCIENTIFIC HIGHLIGHTS

BIOLOGY AND HEALTH

Packing up your genes: condensation of chromatin

Small-angle scattering diffractometer D22 and D-Lab

AUTHORS
C. Edlich-Muth and **E.D. Laue** (University of Cambridge, UK)
T. Forsyth (ILL and Keele University, UK)

The genetic information of a eukaryotic cell is encoded in DNA and packaged into chromosomes. Each chromosome contains a single molecule of DNA which, if fully extended, would be of the order of centimetres in length. DNA in cells therefore has to be stored in a highly compacted form *in vivo*. This condensation occurs by wrapping the DNA around proteinaceous spindles that are further assembled into higher order structures, ultimately forming the distinctive and compact X-like chromosome structure. A crucial aspect of this highly efficient packaging is the fact that the genetic information is not readily accessible while the DNA is in this condensed state. Hence cells that are not dividing and need to carry out protein synthesis from genes adopt a more relaxed DNA conformation in which some part of the DNA is "unwound" and accessible while other parts are not. The proteins that form the DNA spindle (the nucleosome) are called histones, and proteins that are involved in their assembly, disassembly and chemical modification are called histone chaperones ("keeping young histones out of trouble"). Several proteins are known to be histone chaperones: the protein *nucleoplasmin* is perhaps the most prominent.

An international team led by scientists from the University of Cambridge and the ILL has discovered an unexpected connection between nucleoplasmin and several proteins that operate in relation to chromatin. The three-dimensional protein structure of nucleoplasmin was until now thought to be unique in the protein data bank, a rare occurrence in the post-genomic era. By combining three structural biology techniques – small-angle neutron scattering (SANS), small-angle X-ray scattering (SAXS) and nuclear magnetic resonance (NMR) – in combination with macromolecular deuteration, the team was able to determine three new structural models of nucleoplasmin-like domains, from plants, insects and fungi. The nucleoplasmin-like domain found in these proteins is a pentamer, having a molecular weight of 50 kDa. Key to solving the high-resolution NMR structure were a number of sophisticated isotopic labelling schemes including deuteration, ^{15}N and ^{13}C labelling, and residue-specific protonation in a deuterated background of aromatic and/or methyl side chains. All the isotopic labelling was carried out using the Deuteration Laboratory (D-Lab) in the ILL's Life Sciences Group.

The high-resolution NMR structure of the insect protein FKBP39 confirms the atomic architecture that is found in nucleoplasmin. The primary structures (the amino acid sequence) of nucleoplasmin and FKBP39 are quite unrelated, but key architectural elements – the beta sheets, the hydrophobic core and inter-sub-unit contacts – are conserved, leading to the same symmetric pentamer that has the appearance of a doughnut with a central hole. With the aid of the two structures and advanced sequence alignment techniques, it has now been possible for the first time to map the evolutionary relationship between all nucleoplasmin-like domain proteins and to interpret previous experimental data in light of these findings.

The overall shape of a particle cannot be unambiguously inferred from NMR when the protein is a homo-oligomer (*i.e.* consists of an unknown number of identical sub-units). In contrast, shape information is the forte of low-resolution techniques such as SANS and SAXS. SANS profiles of perdeuterated FKBP39 unambiguously confirmed a pentameric particle that matches the nucleoplasmin particle very well. SAXS data of a protiated protein confirmed this result for FKBP39, and also for the yeast protein Fpr4 which is even more unrelated to nucleoplasmin in sequence. Taken together, the SANS/SAXS studies strongly support the NMR structure and the evolutionary inferences drawn from sequence alone.

The team also investigated the structure of another protein expected to harbour a nucleoplasmin-like domain, the plant protein HD2, a putative histone deacetylase. Here, surprisingly, it was revealed that this protein assembled into a higher order structure, a decamer (two pentameric rings). The existence of a nucleoplasmin decamer had been long debated without any conclusive evidence, and this finding will therefore rekindle this discussion with respect to nucleoplasmin's well-documented biological role.

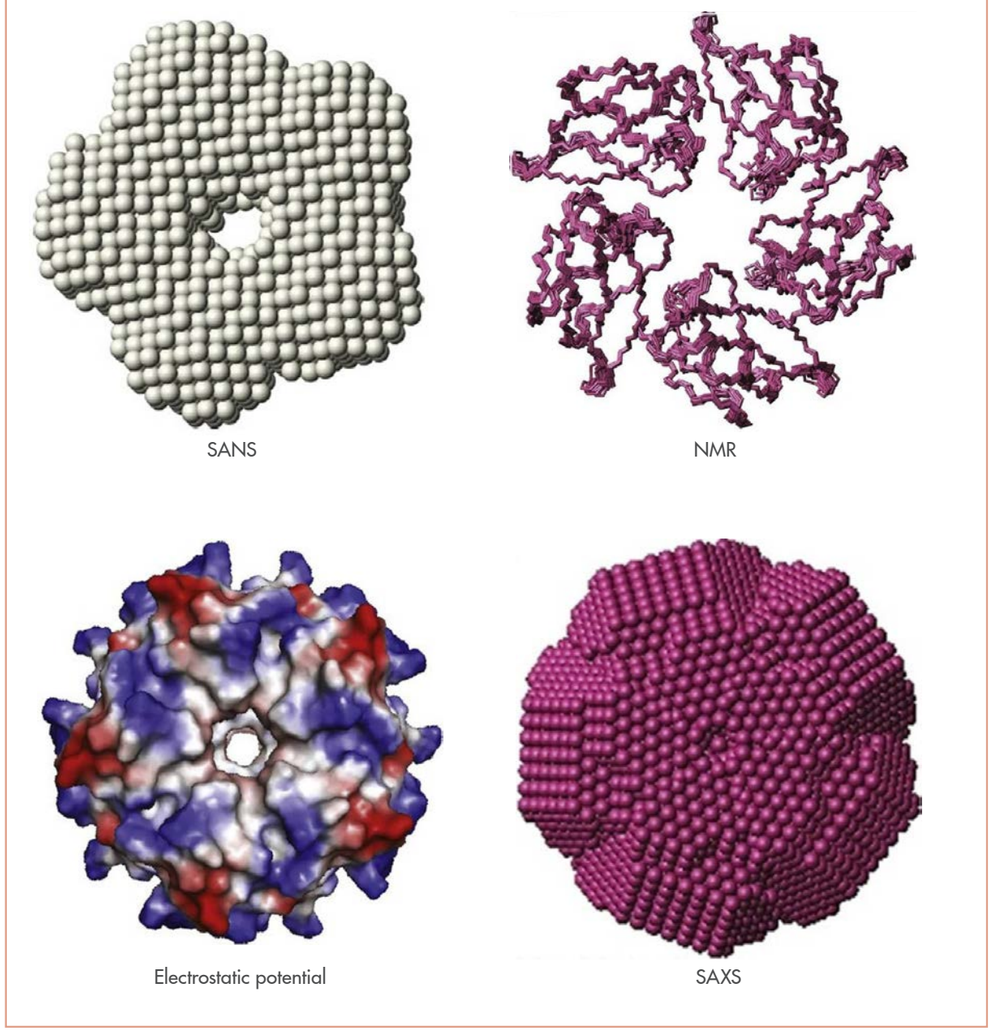

Figure 1
Solution state structures of the insect protein FKBP39 by SANS, NMR and SAXS.

BIOLOGY AND HEALTH

Neutron diffraction reveals the structure and water permeability of myelin from the central and peripheral nervous systems

Small momentum transfer diffractometer D16

Rapid nerve conduction in the central and peripheral nervous systems (CNS and PNS, respectively) of higher vertebrates depends on myelin, the tightly-packed, multi lamellar wrapping of lipid-rich membranes around nerve axons. The electrical insulation provided by myelin enables signal propagation to jump rapidly along the axon between electrically active myelin-free gaps (nodes of Ranvier). Conduction defects owing to disruption of the regular stacking of myelin membranes occur in demyelinating neuropathies such as multiple sclerosis (CNS) and Charcot-Marie-Tooth disease (PNS). Understanding the processes that govern myelin destabilisation requires knowledge of its structure which, owing to its paracrystalline order, makes it a particularly attractive target for diffraction analysis.

AUTHORS

A.R. Denninger and **D.A. Kirschner** (Biology Department, Boston College, USA)
G. Leduc (ESRF, Grenoble)
B. Demé and **V. Cristiglio** (ILL)

REFERENCES

[1] D.F. Parsons and C.K. Akers, Science 165 (1969) 1016
[2] D.A. Kirschner, D.L. Caspar, B.P. Schoenborn and A.C. Nunes, Brookhaven Symp. Biol. 27 (1976) III68
[3] S.C. Scott, K.R. Bruckdorfer and D.L. Worcester, Biochem. Soc. Trans. 8 (1980) 717
[4] B.C. Haywood and D.L. Worcester, J. Phys. E 6 (1973) 568
[5] A.R. Denninger, B. Demé, V. Cristiglio, G. LeDuc, W.B. Feller and D.A. Kirschner, Acta Cryst. D70 (2014) 3198
[6] A.R. Denninger, A. Breglio, K.J. Maheras, G. LeDuc, V. Cristiglio, B. Demé, A. Gow and D.A. Kirschner, Biophys. J. 109 (2015) 1387

Neutron diffraction (ND) from myelin was first reported over 45 years ago [1]. Few follow-up studies, however, have directly addressed questions of myelin biology [2-4], owing to limitations in early neutron technology which required large samples, multiple detector positions and exposure times up to several days. To be useful for myelin research today, ND must be rapid and compatible with small samples from mice and rats, which can provide numerous models of human demyelinating disorders.

We performed ND on the ILL instrument D16 to determine the distribution of lipids, protein and water, and the kinetics of water exchange, in myelinated tissue from mice and rats. Whereas X-ray diffraction can also be used to examine myelin, the ^{2}H-^{1}H contrast variation unique to ND allows localising D_2O and deuterated molecules. Data collection was carried out from fresh tissue during perfusion with different H_2O/D_2O solutions [5].

As previous ND experiments only used PNS tissue, we sought to determine whether CNS myelin could also provide meaningful neutron scattering data. Surprisingly, despite their small diameter (~ 0.5 mm), fewer layers of myelin and increased membrane packing disorder, rat optic nerves gave sufficiently strong diffraction for subsequent analysis, even at low contrast (low $\%D_2O$) (**figure 1**).

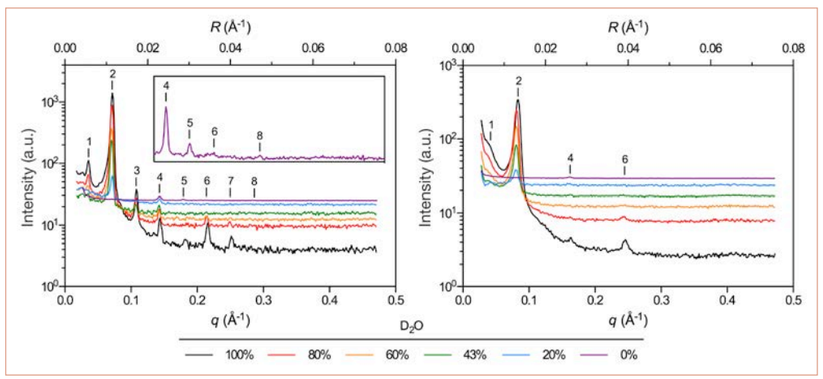

Figure 1

Neutron diffraction patterns from rat sciatic nerves (**left**) and rat optic nerves (**right**), equilibrated against 0 % to 100 % D_2O-saline. Scattering intensity is plotted against both the scattering vector *q* (Å^{-1}) and reciprocal co-ordinate R (Å^{-1}). Bragg orders are indicated with numerals above the reflections. The **inset** in the left panel is expanded along the *y*-axis to more clearly show the additional Bragg orders recorded in 100 % H_2O-saline.

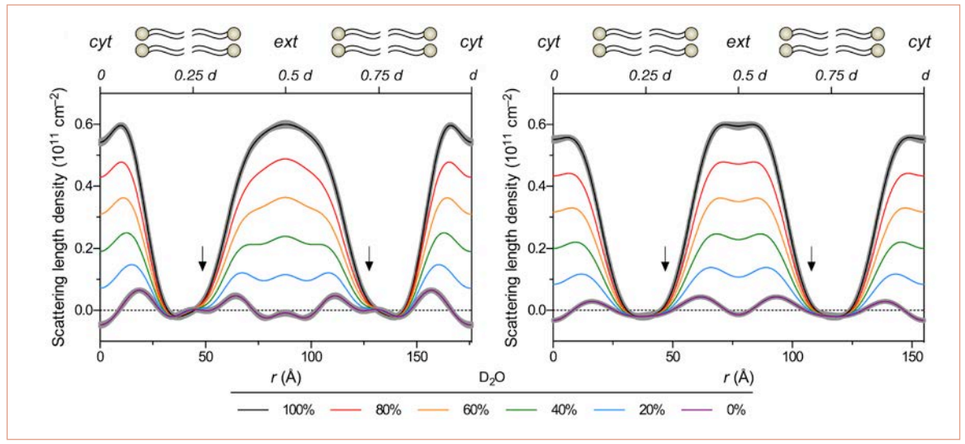

Figure 2

Neutron scattering length density profiles from rat sciatic nerves (**left**) and rat optic nerves (**right**) in 0 % to 100 % D_2O-saline. Scattering length density is plotted against radial distance, *r*, with the centre of the cytoplasmic (cyt) apposition at $r = 0$. The arrows indicate the higher level of neutron scattering density in the extracellular (ext) half of the bilayer, which is proposed to relate to an asymmetric distribution of cholesterol. For each panel, the upper *x*-axis indicates the positions of 0.25 *d*, 0.5 *d*, 0.75 *d*, and *d*.

Depending on D_2O content, Bragg orders 1, 2, 4, and 6 were visible and indexed to a period of 155.0 ± 1.1 Å, typical for CNS myelin. The 2nd order Bragg reflection dominated the patterns at high $\%D_2O$, indicating the presence—similar to PNS myelin—of two distinct water layers within the multi lamellar array. In contrast to the diffraction from PNS myelin, the absence of higher, odd-order reflections ($h = 3$, 5, and 7) from CNS myelin demonstrates that the extracellular and cytoplasmic appositions have similar widths (**figure 2**).

In a second study [6], we investigated the function of claudin-11 tight junctions (TJs) in CNS myelin. Ablation of claudin-11 results in slowed nerve conduction, which was thought to arise from a barrier defect in myelin. Although TJs are known to regulate paracellular diffusion, their barrier function in myelin has not been demonstrated. To investigate the function of claudin-11 TJs, we compared water-exchange kinetics in *Claudin 11*-null and control nerves by monitoring the intensity of the strong 2nd order Bragg reflection during H_2O-D_2O exchange. We found that this exchange was more rapid in the absence of claudin-11, indicating that interlamellar TJs serve primarily as a diffusion barrier. Moreover, these studies elucidate the mechanism by which TJs govern myelin function (**figure 3**).

In conclusion, our analysis not only reveals novel details about the dimensions, asymmetry and organisation of myelin's membranes and aqueous spaces, but also provides insight into the diffusion of water in myelin. We discovered differences in water-exchange kinetics between CNS and PNS myelin, and we found that mice lacking a component of the interlamellar TJs have different water permeability properties.

Beyond elucidating the structure of myelin, ND holds much promise in analysing the function of myelin. The monitoring over time of a simple exchange of deuterated and protonated material provides a direct and focused measure of myelin function and integrity, which could be exploited to measure the permeability of myelin from transgenic animals modelling human myelinopathies. Models of multiple sclerosis, like the experimental autoimmune encephalomyelitis (EAE) mouse, would be of particular interest.

Figure 3

Representative H_2O-D_2O exchange kinetics in spinal cords from control (+/-) and *Claudin 11*-null (-/-) mice. The extent of exchange was measured by following the intensity of the 2nd order reflection over time. The increase in exchange rate correlates in the absence of claudin-11 tight junction from the intramyelinic compartment (**inset**).

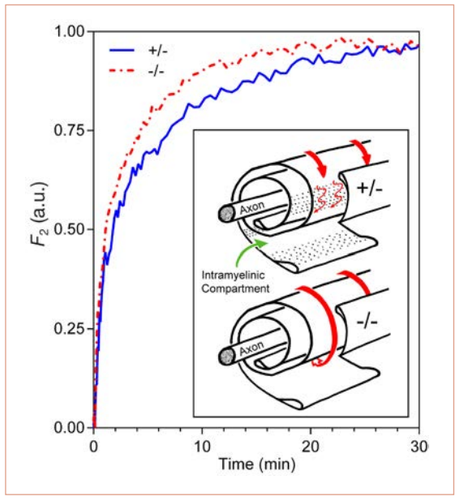

SCIENTIFIC HIGHLIGHTS

BIOLOGY AND HEALTH

Fast internal dynamics in alcohol dehydrogenase

Time-of flight spectrometer IN5
Backscattering spectrometer SPHERES
at the Heinz Maier-Leibnitz Zentrum

Proteins are true molecular machines acting on the nanoscale. They are very dynamic objects animated by a range of motions occurring on different time and length scales. Alcohol dehydrogenase is an enzyme that catalyses the breakdown of alcohol in different organisms. We used neutron spectroscopy to investigate the dynamics of alcohol dehydrogenase in solution on a broad range of time scales, to obtain a coherent picture of the molecular motions that bring the protein to life.

AUTHORS

M. Monkenbusch, A. Stadler, R. Biehl, M. Zamponi and **D. Richter**
(Jülich Centre for Neutron Science and Institute for Complex Systems, Forschungszentrum Jülich, Germany)
J. Ollivier (ILL)

REFERENCES

[1] S. Hammes-Schiffer and S.J. Benkovic, Annu. Rev. Biochem. 75 (2006) 519
[2] R. Biehl, B. Hoffmann, M. Monkenbusch, P. Falus, S. Préost, R. Merkel, and D. Richter, Phys. Rev. Lett. 101 (2008) 138102
[3] M. Monkenbusch, A. Stadler, R. Biehl, J. Ollivier, M. Zamponi, and D. Richter, J. Chem. Phys. 143 (2015) 075101

Proteins are dynamic objects that are animated by motions occurring on different length and time scales. It is seen more and more that molecular dynamics contributes to, and is even essential for, the biological function of a protein. In enzymes, flexibility and domain mobility are prerequisites for conformational changes that occur in the course of the enzymatic reactions [1]. In a previous neutron spin-echo spectroscopy study on alcohol dehydrogenase, the translational and rotational diffusion as well as slow large-scale domain motions could be determined [2]. The observed domain dynamics seen by neutron spin-echo spectroscopy imply a cleft-opening motion, indicating that they may pertain to biological function by opening the access to the catalytic region. Fast and localised internal motions in proteins are equally important for the biological function as they provide a source of conformational entropy that is, for example, relevant for ligand binding or protein-protein interactions.

In a recent study we have extended our investigation of the dynamics of alcohol dehydrogenase in solution by using high-resolution neutron time-of-flight and backscattering spectroscopy [3]. We have used the instruments IN5 at the ILL and SPHERES at the Heinz Maier-Leibnitz Zentrum. The properties of both neutron spectrometers allowed us to look at internal protein dynamics on time and length scales from atomic motions up to fluctuations of whole amino acid side-chains. In that way we have investigated the more localised, internal protein dynamics sitting on top of the global slower motions of translational-rotational diffusion and domain motions seen by neutron spin-echo spectroscopy.

To obtain a detailed theoretical understanding of the more localised dynamics of alcohol dehydrogenase we have developed an analytical model that allows a simultaneous description of the measured neutron time-of-flight and backscattering spectra (**figure 1**). Our model assumes that the protein performs translational and rotational diffusion as well as the previously observed large-scale domain motions [2]. A fast and localised diffusive process of parts of the protein is used to describe the additional fast internal protein dynamics. Analysis of the measured data shows

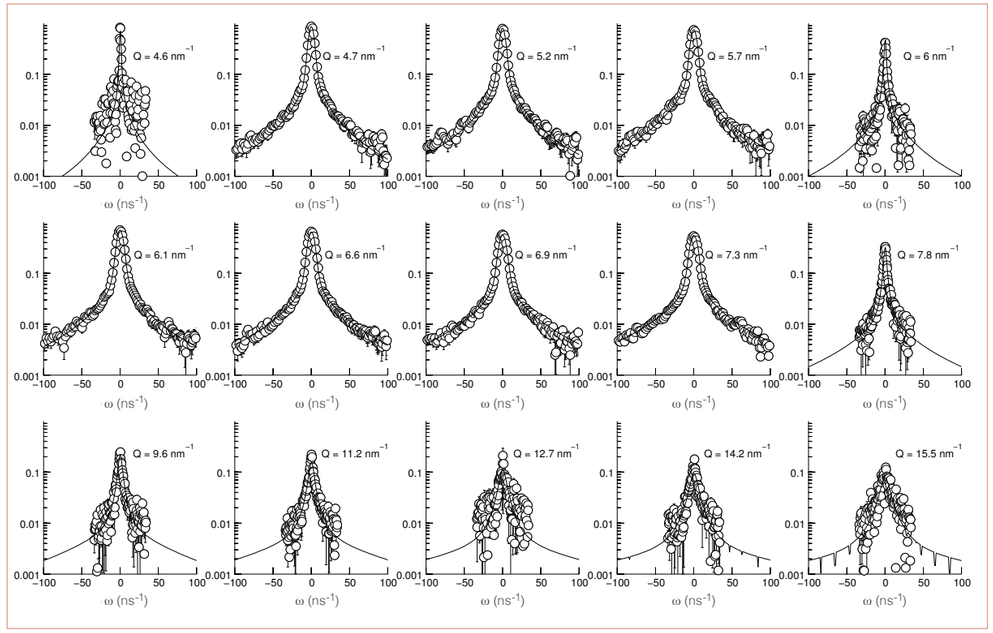

Figure 1

A compilation of neutron time-of-flight and backscattering (spanning $\omega = \pm$ 35 ns^{-1}) spectra measured with IN5 and SPHERES. The lines through the data represent a fit with the theoretical model consisting of global protein diffusion including a large-scale domain motion and internal localised protein dynamics. Note that the fit was simultaneous, describing all spectra recorded with both instruments.

that around one third of all hydrogen atoms in the protein participate in the fast internal process. The observed ratio suggests that mostly amino acid side-chains on the solvent-exposed protein surface contribute to the observed fast process, while residues in the hydrophobic core seem to have a significantly smaller contribution to the dynamics. **Figure 2** visualises the surface residues of alcohol dehydrogenase, which potentially contribute to the modelled fast internal process as, e.g. dangling side-chains.

Our present work demonstrates the potential of combining neutron spin-echo spectroscopy and high-resolution neutron time-of-flight and backscattering spectroscopy for a detailed understanding of molecular motions in proteins in solution. Our theoretical modelling approach opens new perspectives for systematic and coherent studies on the dynamics of protein in solution over a broad range of time scales.

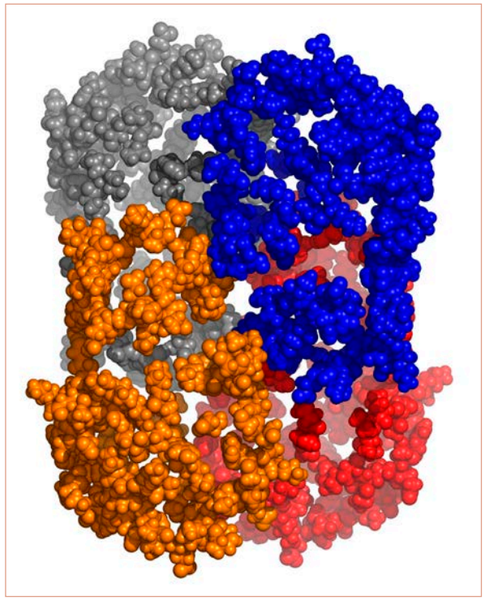

Figure 2

Surface residues of the alcohol dehydrogenase tetramer, possibly contributing to the fast internal motion observed by IN5 and SPHERES. The colour discriminates the four domains of the protein.

FUNDAMENTAL SCIENCE AND THEORY

Low spin structure of ^{86}Se: confirmation of γ collectivity at N = 52

Fission fragment spectrometer LOHENGRIN (PN1)

The evolution of nuclear properties far from stable nuclei is a key question in nuclear physics. Our recent study of ^{86}Se close to the ^{78}Ni magic core, performed at the LOHENGRIN separator of the ILL, indicates an onset of collective gamma vibrations there. The result was confirmed by large-scale, shell-model calculations. A further study is in progress that extends this evidence, following a recent campaign with the large array of germanium detectors EXILL at the PF1B cold neutron beam. This demonstrates the synergies between the decay spectroscopy of mass-separated beams at LOHENGRIN and prompt gamma-ray spectroscopy of fission products using large arrays of detectors, as in the upcoming ILL instrument FIPPS.

AUTHORS

T. Materna (CEA, DSM-Saclay, France)
W. Urban, M. Czerwiński and **T. Rząca-Urban** (University of Warsaw, Poland)
U. Köster and **H. Faust** (ILL)
K. Sieja (University of Strasbourg, France)
C. Bernards, C. Fransen, J. Jolie, J.-M. Regis, T. Thomas and **N. Warr** (University of Köln, Germany)

REFERENCES

[1] K. Sieja, T.R. Rodríguez, K. Kolos and D. Verney, Phys. Rev. C 88 (2013) 034327
[2] T. Materna, W. Urban, K. Sieja, U. Köster, H. Faust, M. Czerwiński, T. Rząca-Urban, C. Bernards, C. Fransen, J. Jolie, J.-M. Regis, T. Thomas and N. Warr, Phys. Rev. C 92 (2015) 034305
[3] M. Czerwiński, T. Rząca-Urban, K. Sieja, H. Sliwinska, W. Urban, A.G. Smith, J.F. Smith, G.S. Simpson, I. Ahmad, J.P. Greene and T. Materna, Phys. Rev. C 88 (2013) 044314
[4] T. Rząca-Urban, M. Czerwiński, W. Urban, A.G. Smith, I. Ahmad, F. Nowacki and K. Sieja, Phys. Rev. C 88 (2013) 034302
[5] A. Blanc, A. Chebboubi, G. de France, F. Drouet, H. Faust, M. Jentschel, G. Kessedjian, U. Köster, S. Leoni, T. Materna, P. Mutti, S. Panebianco, C. Sage, G. Simpson, T. Soldner, C.A. Ur, W. Urban and A. Vancraeyenest, EPJ Web of Conferences 93 (2015) 01015
[6] M. Czerwiński, T. Rząca-Urban, W. Urban, P. Bączyk, K. Sieja, B. Nyakó, J. Timár, I. Kuti, T.G. Tornyi, L. Atanasova, A. Blanc, M. Jentschel, P. Mutti, U. Köster, T. Soldner, G. de France, G. Simpson and C.A. Ur, Phys. Rev. C 92 (2015) 014328

Analogous to noble gas atoms, nuclei with so-called magic numbers (2, 8, 20, 28, 50 or 82) of protons or neutrons are particularly stable. Magic nuclei and their neighbours are spherical, while a common shape of most other nuclei is either prolate (like a rugby ball), oblate (disc-like) or triaxial (like a squashed rugby ball). The evolution of magic numbers far from stability is one of the current questions in nuclear physics and can be tested by studying the nuclear deformation. In the region of the doubly magic (Z = 28, N = 50) nucleus, ^{78}Ni, the appearance of deformation may also influence the path of the *r* - process in the astrophysical nucleosynthesis.

But for its lifetime no other information exists concerning the very exotic ^{78}Ni, which at present is barely accessible. However, one can learn about its properties by studying the neighbouring nuclei. A helpful tool here is the shell model. To overcome the presently unsolvable many-body quantum problem of heavy atomic nuclei, the shell model represents nuclei as valence nucleons (particles and holes) outside an inert core. Excitations in a nucleus are then described as excitations of the valence nucleons or – and here the shape of the nucleus comes into play – as a collective motion of the whole nucleus. The contemporary, large-scale, shell-model calculations can nowadays reproduce the spectra of both spherical as well as deformed nuclei, providing useful information on the properties of nuclei close to the core as well as the core itself.

The type of collectivity, which appears first when valence nucleons are added to a magic core, is a triaxial distortion, from gamma vibrations up to a triaxial shape. A characteristic signature of such a shape is the presence of positive-parity, excited states with odd spin values which appear low in excitation energy, as schematically shown in **figure 1**. It has been argued [1] that just four nucleons of one type outside the ^{78}Ni core are enough to drive a nucleus towards triaxiality.

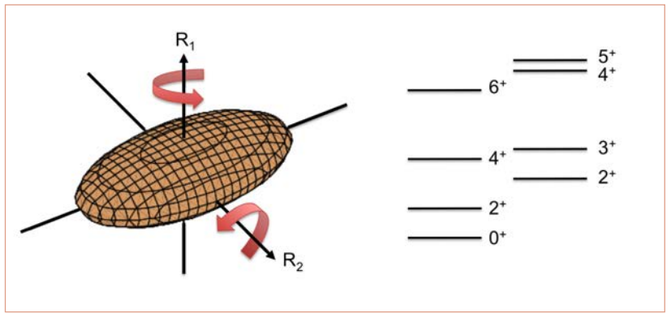

Figure 1
Simple picture of a rigid triaxial nucleus, which can be seen as a squashed rugby ball able to rotate around its main axes (**left**), with its theoretical level scheme (**right**). Positive-parity, odd-spin excited levels (3^+ and 5^+) appear from the coupling of both rotations.

The region in the nuclide chart northeast of ^{78}Ni is well fed by thermal-neutron-induced fission of ^{235}U, making the ILL a very competitive place for such studies. We produced ^{86}As by placing a ^{235}U target close to the core of the reactor. The fission-fragment mass separator LOHENGRIN, having a direct view on the target, was optimised to extract nuclei with mass A = 86, which were implanted at the focal point of the spectrometer, surrounded by a small array of germanium detectors. The setup measured gamma radiations emitted by A = 86 nuclei after their beta decay, here, following the decay of ^{86}As to ^{86}Se. The collected data allowed the construction of the excitation scheme of ^{86}Se, comprising information on energies, spins and parities as well as electromagnetic decays of excited levels [2]. The observed excitation pattern of ^{86}Se is characteristic of a gamma-soft nucleus, with tendencies to triaxiality. **Figure 2** shows the systematics of low-energy 3^+ excitations, characteristic of triaxial shape, observed in ^{86}Se and its N = 52 isotones.

The beta decay of ^{86}As populates only low-spin levels in ^{86}Se. A complementary method is required to access the high-spin states, which may tell us more about the triaxial band. These states are well populated in fission, but de-excite rapidly by gamma-ray emission. Therefore, gamma detectors have to be placed around the fission source. Initial studies of ^{86}Se [3] and ^{87}Se [4] were performed with a ^{252}Cf spontaneous fission source and GAMMASPHERE, a large array of germanium detectors at Argonne National Laboratory. Recently, an important experimental campaign (EXILL) has been performed at the ILL with the EXOGAM detector array [5]. Since thermal-neutron fission of ^{235}U populates the region of exotic nuclei close to ^{78}Ni much better than spontaneous fission sources, a wealth of new data was obtained. Initial results confirm the collectivity in the region, observed in the ^{88}Br nucleus [6], and work is in progress to identify more high-spin levels in the ^{86}Se and ^{87}Se nuclei. We note that the trend in **figure 2** suggests that the maximum effect will occur in ^{84}Ge, a nucleus with four valence protons. The study of this nucleus will, however, require a more sensitive detection system.

The above works nicely demonstrate the complementarity of both decay spectroscopy after an electromagnetic spectrometer and the prompt-gamma spectroscopy close to a fission target with a large germanium detector array. Ideally, one would like to combine both techniques to detect the prompt radiation with germanium detectors while using an electromagnetic separator to identify one of the recoiling fission fragments, thus firmly assigning weak gamma rays to a given nuclide. Our community is eagerly looking forward to the next generation, highly sensitive instrument FIPPS that is part of the ILL's Endurance Programme.

The small array of gamma-ray detectors installed at the focal plane of the LOHENGRIN spectrometer.

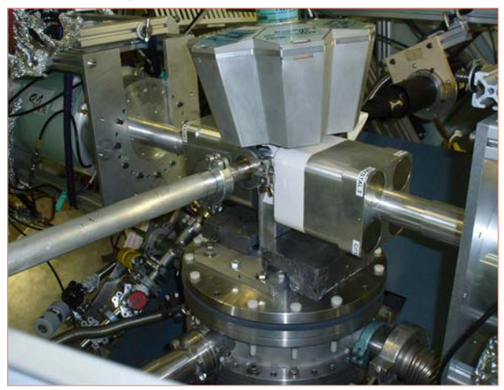

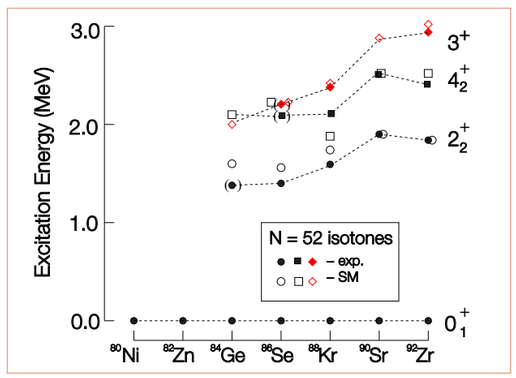

Figure 2
Comparison of experimental levels and shell model calculations for N = 52 isotones.

SCIENTIFIC HIGHLIGHTS

FUNDAMENTAL SCIENCE AND THEORY

Does the neutron lifetime depend on the method used to measure it?

Ultra-cold and very cold neutron facility PF2

As fundamental quantities, like the neutron lifetime, are measured with ever increasing accuracy and reliability, so the motivations for this research may evolve: to estimate the number of generations of elementary particles or parameters of the weak interaction needed in particular for designing large neutrino detectors and high-energy experiments; to verify stellar models or speculate on neutron stars; to explore physics beyond the Standard Model or simply investigate by-product physical effects. Sometimes experiments provide fundamental answers, sometimes they boost technology, but sometimes they raise more questions.

AUTHORS

S. Arzumanov, S. Chernyavsky, V. Morozov, Yu. Panin and **A. Strepetov** (KI, Moscow, Russia)
P. Geltenbort and V.V. Nesvizhevsky (ILL)

REFERENCES

[1] D. Dubbers *et al.*, Rev. Mod. Phys. 83 (2011) 1111
[2] A.T. Yue *et al.*, Phys. Rev. Lett. 111 (2013) 222501
[3] S. Arzumanov *et al.*, Phys. Rev. B 745 (2015) 79
[4] A. Serebrov *et al.*, Phys. Lett. B 605 (2005) 72

Neutrons are an important constituent of matter. More than half of the mass of a human body and more than half of the mass of its surrounding objects, are composed of neutrons. Although neutrons are everywhere, they are rarely available as isolated particles. The reason for this is that they get captured by other atoms and, more importantly, because free neutrons decay. Therefore nuclear reactors and spallation sources are used to provide the high neutron fluxes required in neutron research. For particle physics, the free neutron decay becomes an advantage since its decay rate is determined by the fundamental, so-called weak interaction. Since in the case of a neutron the decay rate – or in other words, the neutron lifetime – is practically unaffected by other fundamental interactions it allows us to extract rather clean information about the weak interaction. Knowledge of the neutron lifetime is also required in a variety of other important processes, in particular those described by the same Feynman diagram [1]. It determines the rate of weak nuclear reactions involved in the stellar cycle and notably in the sun; it plays its role in the hypothetical existence of neutron stars; and it is important for the design of huge, high-energy detectors and neutrino experiments, and the interpretation of their results.

Whatever the scientific motivation over the decades was, it has always been accompanied by demands for higher accuracy. Every endeavour has been made persistently to improve the measurement of the neutron lifetime, at the ILL and other research centres across the world. The best published results are based on two different techniques: 1) the so-called beam method, which measures the probability of the decay of a cold neutron (CN) during its passage over a well-defined distance in an experimental setup (absolute measurements of the neutron flux and spectrum as well as the flux of electrons or/and protons from the neutron β-decay); and 2) the storage method, which measures the number of surviving ultra-cold neutrons (UCNs) trapped in a closed volume as a function of storage time (relative measurements, nevertheless requiring good control of the theoretically poorly known losses of UCNs when interacting with the storage walls or fields).

Both approaches are very challenging, and a systematic comparison of all such experiments is periodically updated by the Particle Data Group (PDG). To date the best accuracy using the beam method was achieved in an impressive experiment at NIST [2]: $887.7 \pm 1.2_{stat} \pm 1.9_{syst}$ s.

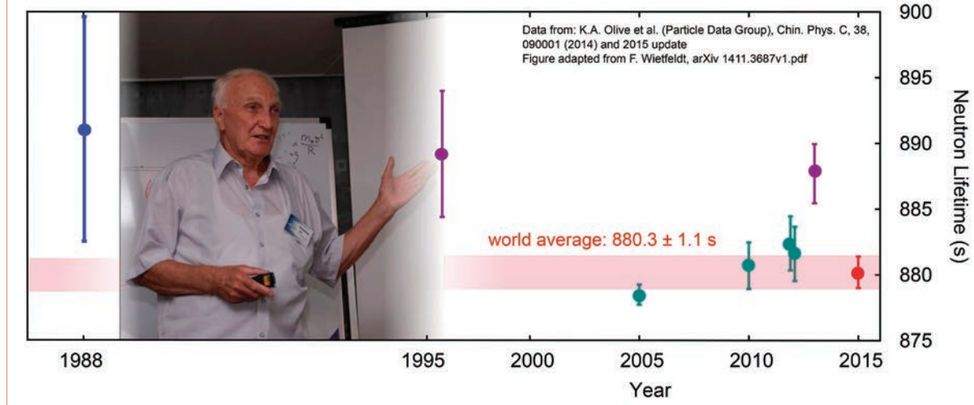

Figure 1

A comparison of recent neutron lifetime results obtained from beam (magenta) and storage (green) experiments. The most recent result [3] using the UCN storage technique is shown in red. The insert shows L.N. Bondarenko, who was one of the pioneers in the field, measuring the neutron lifetime with both the beam (blue) and storage (red) techniques.

The accuracy of the storage experiments has been dominated so far by a clever experiment led by a group from Petersburg Nuclear Physics Institute [4] and performed at the ILL's ultra-cold neutron installation PF2: $878.5 \pm 0.7_{stat} \pm 0.3_{syst}$ s. In its analysis the PDG takes into account the precision and scattering of all recent and updated experiments. Their recommended mean world value for the neutron lifetime is 880.3 ± 1.1 s.

The new experiment, under the guidance of a team from the Kurchatov Institute (KI) in Moscow, was again performed at PF2. It is based on the bottle method and measures not only the surviving UCNs after a certain storage time but also the inelastically up-scattered, and hence lost, UCNs during their storage [3].The recently published result (880.2 ± 1.2 s) is in line with those of other bottle experiments. Its accuracy is close to the world mean value's accuracy. The late Lev Nikolaevich Bondarenko (KI), one of the pioneers in neutron lifetime research and one of the first Russian users at the ILL, performed one of the first and at that time most precise neutron lifetime measurements using the beam method, and also participated in the experiment discussed here.

The results of the different neutron lifetime experiments are shown in **Figure 1**. It is evident that the results from the beam and storage methods contradict each other, while being self-consistent within their respective groups. The new experimental result [3] is important, particularly with regard to the contradictory results of the two methods. Efforts were focused on reliability and understanding systematic errors rather than on improving the absolute accuracy. A new experimental method was developed and a dedicated installation built for this experiment. Wherever possible, systematic effects were experimentally measured but not theoretically corrected for. The residual losses of UCNs, when colliding with the trap walls (inelastic scattering), were determined by measuring the flux of up-scattered neutrons. The efficiencies of the detectors for the up-scattered neutrons were measured experimentally using a specially developed neutron source at the end of a flexible UCN guide (commercial garden hose). The rate of the residual UCN losses was decreased significantly by keeping the temperature of the trap walls low. The effect of quasi-elastic UCN scattering was eliminated by the choice of a proper UCN trap geometry and dynamical shaping of the UCN spectra. The contributions of all UCN-spectrum-dependent uncertainties were strongly decreased by shaping the spectrum of the stored UCNs. Systematic uncertainties were summed up linearly to avoid any unknown interplay. The systemic studies were performed in three independent series of measurements at very different conditions, but always providing the same result. Only after careful experimental and theoretical analysis of all these effects, was the final result finally published [3].

As it happens sometimes, theory can accept the results of both techniques (beam and storage methods mentioned above), or even both simultaneously, but with different interpretations. Both measurements could be correct simultaneously, for instance, in an exotic case of so-called mirror neutrons, where "escape" does not mean "decay" or "up-scattering". Recent cosmological data, under the assumption of standard Big Bang Nucleosynthesis, seem to favour beam results. Weak interaction models in combination with other particle physics experiments seem to prefer UCN results.

What has been "in the air" is becoming evident: something is "hidden" in the field. Could it be new/unnoticed physics phenomena in one or both methods? Or do both techniques suffer from unknown systematic effects that need to be corrected for? What is certain, is that it is time to work hard towards another qualitative step in the field.

SCIENTIFIC HIGHLIGHTS

FUNDAMENTAL SCIENCE AND THEORY

Suppression of the spin Hall effect by spin glass order

AUTHORS

Y. Niimi (University of Osaka, Japan)
M. Kimata, Y. Omori and **Y. Otani** (University of Tokyo, Japan)
B. Gu and **S. Maekawa** (JAEA, Japan)
A. Fert (CNRS and Thales, Palaiseau, France)
T. Ziman (ILL)

REFERENCES

[1] N.F. Mott, Proc. Royal Soc. of London Series A (1929) 425; M.I. Dyakonov and V.I. Perel, ZhETF.Letters, 13 (1971) 657
[2] G-Y Guo, S. Maekawa and N.Nagaosa, Phys. Rev. Lett. 102 (2009) 036401
[3] D.H. Wei, Y. Niimi, B. Gu, T. Ziman and S. Maekawa, Nature Commun. 3, 1058 (2012)
[4] Y. Niimi, M. Kimata, Y. Omori, B. Gu, T. Ziman, S. Maekawa, A. Fert and Y. Otani, Phys. Rev. Lett. 115 (2015) 196602
[5] Y.J. Uemura, T. Yamazaki, D.R. Harshman, M. Senba and E.J. Ansaldo, Phys. Rev. B. 31 (1985) 546
[6] F. Mezei and A.P. Murani, J. Mag. Mag. Mat. 14 (1979) 211

Skew scattering and spintronics

One of the exciting areas in current condensed matter physics is the exploration of possibilities of transmitting and storing information *via* currents of spin rather than of charge. The idea is to replace current electronic devices with less noisy and more energy-efficient "spintronic" apparatus. One of the obstacles to this is that the creation of such spin currents, and their detection, relies on conversion from, and to, conventional charge currents that create measurable potentials. The most efficient mechanism in metals is that of spin-dependent skew scattering of electrons from impurities. Since the early days of quantum mechanics it has been known that skew scattering is a consequence of the Dirac equation [1] and it can be thought of as the correction in scattering theory caused by spin-orbit coupling, equivalent to the fine structure splitting in the spectroscopy of bound states. The problem with this is that as a relativistic correction, it will be small except in the heaviest elements. A subtler limitation to the strength of the effect is that in this skew scattering – where spins of one polarisation are preferentially scattered to, say, the left rather than right – the asymmetric probability depends on interference between at least two different scattering channels of opposite parity, making the effect even smaller. The challenge is to look for ways of enhancing the effect and thereby the efficiency of spintronic devices. One way is to look for scattering from resonances, for example from Kondo fluctuations [2] where, intuitively, the slowing down of the scattering process allows the electron to spend more time close to the strongest part of the potential, thus enhancing the effects of spin-orbit interaction.

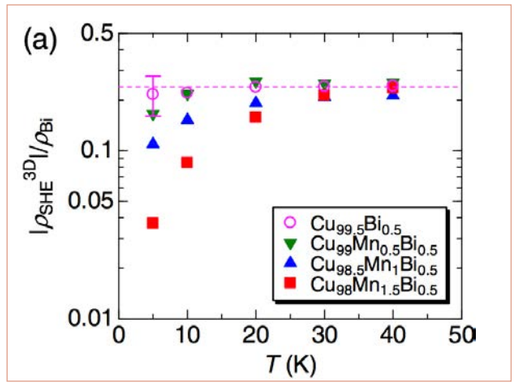

Figure 1
Transverse resistance as a function of temperature for CuBi alloys with and without Mn doping, that leads to spin glass order amongst the Mn moments and suppression of the spin Hall effect [4].

Skew scattering from co-operatively ordered magnets

Another possible enhancement with a long time scale could be skew scattering from collective excitations in magnetically ordered materials, where there can be a slowing down of the dynamics close to the ordering temperature. The first case considered was that of ferromagnets [3], where an anomaly in the spin Hall strength seen near the Curie temperature was related to higher order correlation functions. This motivated experimental consideration of an alloy with both Bi impurities for spin-orbit coupling and Mn moments ordering as a spin glass, where the power-law correlations should extend over a wider range of temperatures. In addition, higher-order correlation functions are known to be key to the ordering. In fact, experiments revealed a novel behaviour (**figure 1**): starting at temperatures well above the glass transition the relative strength of transverse scattering (the "spin Hall angle") decreases continuously, to as little as a third of its value in the paramagnetic region [4].

At these concentrations of magnetic manganese ions, the bismuth has relatively strong spin-orbit coupling and the Mn orders with glassy order. Our postulate is that what is happening is that the spin current exchanges with the Mn ions and this decreases the net skew-scattered charge current as it is the vector product of the injected spin current and the spin polarisation. In order to make a more quantitative theory, we need to know the time-dependence of the magnetic moments over a range of frequencies, wavelengths and temperatures. For this we returned to rather old experimental data of neutron scattering obtained by spin-echo techniques at the ILL soon after their invention and development. These are summarised in **figure 2**, and show that in such alloys with spin glass order, over a wide range of frequencies and wavelengths there is a common diverging time scale, independent of wave-vector. Exploiting this information, we have explained the decrease in the spin Hall angle by means of a model of motional narrowing, as is used in Nuclear Magnetic Resonance and muon spectroscopy [5], using the temperature dependence of the dynamical time scale for Mn moment fluctuation taken from the old neutron and muon data.

This work is illustrative of the way that relatively venerable, but unsurpassed, experimental results obtained from neutron scattering [6], especially combined with complementary techniques – spin resonance with muons or nuclei and bulk response measurements – and new theoretical models, continue to stimulate contemporary ideas in new devices fabricated on a nanometer scale.

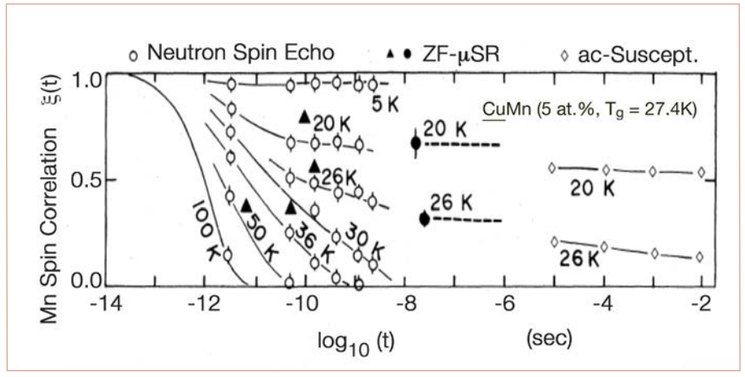

Figure 2
From [5]: Spin correlations as revealed by neutron spin-echo spectroscopy (IN11, 1979), zero-field muon spin resonance and AC susceptibility in CuMn spin glasses. The time scales taken from these experiments are used as input for the motional narrowing model explaining the suppression of the spin Hall effect [4].

MODERNISATION PROGRAMMES AND TECHNICAL DEVELOPMENTS

As the long-standing world leader in neutron science and technology, the ILL plays a key role in the progress made in this field. A multitude of techniques have been successfully developed at the institute since it was founded and we continue to break new ground, with the technical services of our Projects and Techniques Division currently at the forefront of technical innovation in many areas.

The Millennium Programme is coming to an end, with the commissioning of the majority of the instruments in guide hall ILL22 now completed. The improvements made to instrumentation over the past ten years have been spectacular. At the end of 2015 the next stage of our instrument upgrade programme, known as "Endurance", was formally approved by our Associates and Scientific Members. Phase I of Endurance will therefore be launched in 2016, with completion scheduled for 2020. We are confident that this new phase of our ambitious upgrade will not only prove to be yet another challenge for our competitors, but will also ensure that the ILL retains for many years to come its current status as the global benchmark for neutron science, a centre of excellence at the service of our users.

Charles Simon
Associate Director

A multitude of techniques have been successfully developed at the institute since it was founded and we continue to break new ground.

MODERNISATION PROGRAMMES AND TECHNICAL DEVELOPMENTS

MODERNISATION PROGRAMMES

Breakthrough technological advances

AUTHOR
C. Simon (ILL)

In 2015 the Millennium Programme continued to forge ahead, with the phasing in of various options on the instruments completed in 2014, namely ThALES, IN15 and D50. The final instrument of the programme, the wide-angle spin-echo spectrometer WASP, is currently under construction at the far end of the guide hall ILL22. At the same time, significant technological advances were made in many areas by the ILL's technical services.

The cold neutron triple-axis spectrometer **ThALES**, which was constructed in co-operation with Prague's Charles University, has now been operational for several reactor cycles and has enabled a gain in flux at the sample of a factor of 4 (depending on the wavelength) under background noise levels that are still perfectly acceptable. **ThALES** has now taken its rightful place alongside the world's best cold TAS instruments. Its final polarisation options (Heussler monochromator) are in the process of validation. The small-angle spectrometer **D22** has returned to the user programme with a completely overhauled collimator, a reduced-background detector and new control electronics (the first of the new generation). The reflectometer **SuperADAM**, which is operated by Sweden as a CRG (collaborating research group) instrument, is also operational, as is the diffractometer **D16**. Last but not least, **IN15**, the high-resolution spin-echo spectrometer, has been put back into user operation with new coils that allow the instrument to operate at a higher precession field. The same time resolution is now accessible with a shorter wavelength and hence a higher flux (typically a factor-10 increase), a success which confirms that the right technological choices were made on this instrument. The wide-angle spin-echo spectrometer **WASP** is currently under construction in the far end of the guide hall ILL22, and is due to be operational in 2017 as the replacement for IN11. Of the two remaining instrument positions in refurbished ILL22, one was recently occupied by **D50**, a reflectometer developed and operated by the Grenoble-based research and technology initiative IRT (*institut de recherche technologique*) for the microelectronics industry, while the other is planned to be taken up by a new ultra-cold neutron source, **SuperSUN**, financed by the French national research agency (ANR) and the ILL's Endurance Programme.

One of two of the ILL large helium 3 detectors built for LLB being installed in its vacuum tube.

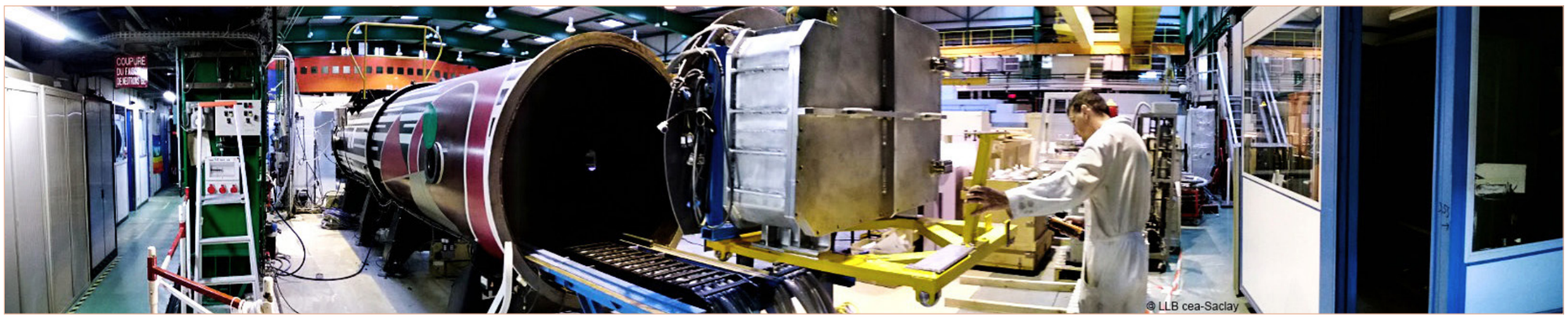

© LLB cea-Saclay

In parallel with the Millennium Programme, the ILL's various technical services have produced a host of technological advances that will benefit the international neutron user community as a whole.

- Let's begin with a look at neutron detectors. The recent achievements of the Neutron Detector Service in the area of large helium 3 detectors have been quite remarkable. They include the creation of three detectors for small-angle spectrometers (two for the Laboratoire Léon Brillouin and one for D33). The detector blocks, which were machined at the ILL, are made up of 128 tubes covering a surface area of 64 cm x 64 cm, drilled into the aluminium using a wire electrical discharge machine. Each of the tubes contains a resistive anode wire, allowing the position of the neutrons to be determined by charge division. The spatial resolution of the detectors is 5 mm in each direction and the count rate is 50 kHz per tube. The two detectors for the Laboratoire Léon Brillouin were inaugurated this year. Other ongoing projects include a multi-tube detector that is being developed for the Panther project (a time-of-flight instrument for thermal neutrons). Following the success of the IN5 detector, this type of detector is now considered almost as standard at the ILL. Prototyping has also begun in collaboration with FRM II in Munich of a detector for the future instrument XtremeD.
- Within the framework of collaboration contracts with the European Spallation Source (ESS) in Lund, the Neutron Detector Service is also very actively involved in the development of alternatives to helium 3, which continues to be a rare and therefore expensive commodity. These projects are the logical consequence of the patent taken out by the ILL a few years ago on the boron carbide-based multi-grid technology developed at the institute.

The ILL22 guide hall

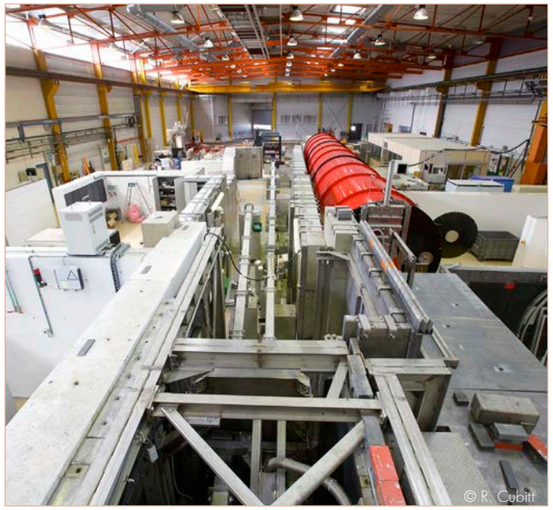
© R. Cubitt

- Moving on to neutron polarisation analysis, the "Tyrex" machine developed by the Neutron Optics Service produces a constant supply of polarised helium 3 for the production of spin-filter cells for polarisation analysis on ILL instruments. This machine has been replicated for use at ISIS in the UK and more recently at ANSTO in Australia.
- The Neutron Optics Service also produces monochromators, one of which was recently installed on an instrument at SNS in the United States.
- Improvements in neutron guide technology have meant that it has been possible to completely renovate a number of ILL guides under the Millennium Programme, upgrade work which is set to continue within the framework of Endurance. Thanks to these improvements, the flux gain on the instruments concerned has now reached a factor of 20. Of course, as the flux increases so do the difficulties in terms of radiation protection and background noise, bringing us new and more exciting challenges every day.
- Developed by the Instrument Control Service, NOMAD is instrument control software coupled with dedicated control electronics which now equips the majority of the ILL's instruments, much to the satisfaction of our users. The efficiency gains due to this standardisation of instrument control hardware and software have been spectacular.
- As for the ILL's IT Service, within the framework of a number of European projects it has successfully developed a revolutionary Scientific Data Policy that now serves as a model for other research infrastructures in Europe. Following the implementation of this policy, the ILL now generates bibliographic references for scientific data before the data are published, which represents a major change in the way scientific data are managed.

MODERNISATION PROGRAMMES

Endurance: the ILL's next instrument upgrade

AUTHORS
C.D. Dewhurst and C. Simon (ILL)

REFERENCES
[1] ILL 20/20 Endurance – The ILL's next instrument upgrade (http://www.ill.eu/quick-links/publications/)

The ILL is embarking on the next phase of its ambitious upgrade programme – Endurance – a suite of instrument, infrastructure and technical upgrades to help maintain the ILL's leading role in neutron science and materials research. The ILL has led the world in neutron science for more than 40 years – a remarkable record that has been achieved by offering best-in-class neutron scattering, particle and nuclear physics instruments, served by the world's brightest continuous neutron source. Such high pedigree has been maintained by attracting the most talented scientists and technical staff providing their collaboration and support to the scientific user community, as well as the continuous development of instrumentation and neutron technologies. As a result, the ILL's instrument suite has evolved continuously by exploiting new technologies and techniques, much of it developed in-house, and reacting to the ever-changing landscape of scientific problems and technology drivers. The ILL continuously offers new scientific opportunities, redefining the limits of what is measurable. This article details Endurance – the next phase of upgrade projects to be completed within two phases, Phase 1 (2015–2019) and Phase 2 (2019–2023).

From the Millennium Programme to Endurance

As a central hub for the European neutron scattering community the ILL provides efficient user access to its state-of-the-art instrument suite. It has never been more critical to sustain and underpin the European neutron scattering community, with the anticipated closures of the LLB (France) and HZB (Germany) neutron scattering centres in 2020. The Endurance Programme assures the timely development of new instrumentation concepts, techniques and capabilities. The ILL and Endurance will assure European access to advanced neutron instrumentation at least in the period until the ESS can offer a substantial instrument suite by 2030. The Endurance Programme will follow closely in the footsteps of the Millennium Programme (MP) – the ILL's latest round of such developments. Stretching over more than a decade, during periods 2001-2008 (M0) and 2008-2014 (M1), renewed or upgraded instrumentation from the MP delivered an increase by more than a factor of 25 in average instrument brightness, and added new capacity and scientific capabilities. To achieve the construction of world-leading instruments the MP also included renovation or replacement of critical infrastructure such as the replacement of neutron guides, expansion of neutron guide halls, instrument-control software and sample-environment equipment. A total budget of 75 M€ was dedicated to the MP – less than one year's budget.

Endurance: instruments and projects

Endurance, like the MP, will not only enable us to increase the number of experiments and users that we can support, but will open up new avenues of science in the directions of smaller samples, weaker signals, higher resolution or faster kinetic processes. It will provide new capabilities for currently emerging scientific areas, but equally will serve domains of science and technique that have not yet seen their full potential exploited under the MP.

The success of previous upgrade campaigns gives us pointers as to where next to develop our instrumentation and infrastructure. Currently, among the highest beamtime requests are those for instruments such as D33, FIGARO, IN16B, IN5 and LADI, all built or upgraded during the MP – a direct demonstration that we are building the right instruments with the required performance to address the scientific problems of today. Other highly demanded but older instruments include the powder diffractometers, D2B and D20, thermal single-crystal diffractometer D10, and the thermal and cold time-of-flight (TOF) spectrometers IN4, IN5 and IN6.

These instruments inspire the next generation of instrumentation at the ILL, such as the renewal or upgrade of the thermal and cold TOF spectrometers Panther (IN4), IN5$^+$ and Ramses with improved performance, increased flux, larger detector coverage and reduced background. At the same time the new and renewed instruments XtremeD and D10$^+$ will be powder and single-crystal diffractometers for small samples and magnetism at high magnetic fields and pressures. An upgraded D7$^+$ will provide the highest intensities for studies of magnetic liquids and glasses.
A relocated and upgraded IN13 (CRG) instrument, a unique spectrometer for studying the internal dynamics of biological macromolecules, will benefit from a new and dedicated neutron guide. Rainbows makes innovative use of refractive optics as an option to the D17 and FIGARO reflectometers, allowing the full, continuous white beam neutron flux for studying rapid kinetic processes. The instruments Fipps and SuperSUN will provide new tools for nuclear and particle physics studying the decay of neutron rich nuclei and providing an intense, latest generation source of ultra-cold-neutrons (UCN) respectively. Three neutron guide systems have to be rebuilt due to their age and technical performance and in order to provide intense and dedicated neutron beams to the new instruments. These are the H24 thermal neutron guides and the H15-H16 cold neutron guides, which date from 1972. The scheduled replacement of the in-pile H1-H2 beam-tube and primary beam extraction from the reactor is also considered under Endurance, as its detailed design can be optimised to best provide neutron beams for the new guide systems and instruments. Two parallel projects, Nesse and Bastille are proposed as part of the programme in order to provide state-of-the-art sample environment and software for data analysis. A summary of all Endurance projects is given in **table 1** (p.84).

Implementation and time scale

The aim of Endurance is to provide an upgrade path delivering ten instruments, three infrastructure projects and two user support projects over the eight-year period 2015 to 2023. Nevertheless recent budgetary issues have delayed the start of Endurance until funding contributions from associates and internal budget allocations can be assured. This delay has a direct impact on the most optimal implementation strategy, aside from any priorities that may be determined by the Scientific Council. For these reasons, Endurance can be broken down into modular sub-packages and dependencies in order to best adapt to the desired spending profile, construction manpower, logistics and reactor function while at the same time minimising downtime of the in-service instrumentation.

A natural division of projects and co-dependencies centres on instruments sharing the same guide renewal project, as highlighted in **table 1** – i.e. the Chartreuse H24 project involving the new, upgraded and relocated instruments XtremeD, D10$^+$, and IN13 (CRG), and the Vercors H15-H16 project involving instruments IN5$^+$, Ramses and D7$^+$, as well as those that are independent of significant infrastructure projects such as Panther, Rainbows, SuperSUN and Fipps. A crucial point to note is that the beam tube H1-H2 will reach end-of-lifetime and must be replaced for safety reasons in 2019. The association of this project with Endurance is crucial for the most effective planning of the various guide and instrument projects and for the minimisation of instrument downtime due to the associated works.

The construction and delivery of Endurance instruments will be split into two phases, 2015-2019 and 2019-2023. The various elements of Bastille and Nesse will be developed and delivered continuously between 2016 and 2023.

Phase 1	2017	Rainbows, Fipps (phase 1)
	2019	SuperSUN, Chartreuse side (XtremeD, D10$^+$, IN13 relocation, H24 projects) Panther (phase 1)
Phase 2	2023	Vercors side (D17$^+$, IN5$^+$, Ramses, H15-H16 projects) Panther (phase 2) and Fipps (phase 2)

MODERNISATION PROGRAMMES

Table 1 List and timescale of Endurance projects.

	Project	Description
Phases 1 & 2 (2016 -2023)		
	Nesse	A suite of new and upgraded sample environments for all scientific disciplines, soft, hard and bio.
	Bastille	Modern data analysis software to complement a modern ILL instrument suite.
Phase 1 (2016-2019)		
	XtremeD D10+ IN13+	New, high intensity powder and single crystal diffractometer optimised for extreme sample environments. This instrument will be operated as a Spanish CRG.
		Upgraded, more intense, single crystal diffractometer. Better adapted monochromators and non-magnetic sample stage for high magnetic field capability.
		Re-positioning of IN13 on the renewed H24 guide allows this CRG instrument to be upgraded to fully optimise the primary spectrometer.
	H24 (Guide)	Renewal of H24 thermal guide with m = 2 multi-branch guide serving the above instruments. Partial renovation of H23 for relocation of Laue and technical beamlines.
	Panther	New thermal spectrometer for studying dynamics in complex solids. Replaces and enhances the IN4 instrument with improved monochromators and position sensitive detector for single crystal studies (phase 1, new position sensitive detector).
Guide Independent	Rainbows	Upgrade option to the D17 and FIGARO reflectometers. Wavelength encoding using prisms allows white beam specular reflectivity measurements with more than one order magnitude flux gains.
	SuperSUN	New, world-beating source of ultra-cold neutrons for experiments in fundamental physics.
	Fipps	New, high-resolution fission fragment spectrometer for studying exotic nuclei (phase 1 germanium detectors and casemate).
	H1 / H2 (In-Pile Guides)	Necessary periodic renewal of the in-pile neutron guide extraction from the heart of the ILL reactor.
Phase 2 (2019-2023)		
	Ramses D7+ IN5+	New cold spectrometer for studying dynamics of advanced materials in extreme environments. Replaces and enhances the IN6 instrument.
		Upgraded primary spectrometer, monochromator, polariser and relocated on new H15 guide promises intensity gains on this diffuse scattering instrument with polarisation-analysis and TOF capabilities.
		An upgrade to the already outstanding IN5 cold spectrometer. Increased neutron flux due to guide renovation and extension of the energy range and resolution with a new chopper system.
	H15 / H16 (Guide)	Renewal of the H15 and H16 cold guides with m = 2 multi-branch guide serving the above instruments.
Guide Independant	Panther (pt 2)	New thermal spectrometer for studying dynamics in complex solids. Replaces and enhances the IN4 instrument with improved monochromators and position sensitive detector for single crystal studies (phase 2, new primary spectrometer).
	Fipps (pt 2)	New, high-resolution fission fragment spectrometer for studying exotic nuclei (phase 2 selector).

MODERNISATION PROGRAMMES AND TECHNICAL DEVELOPMENTS

Endurance: continued

Scientific case for Endurance

Studies on advanced magnetic and electronic materials: The projects, XtremeD and D10+, will develop new capabilities for investigating magnetic structures, including thin films and materials used in devices. Inelastic experiments on magnetic excitations will take advantage of the projects Panther, IN5+ and D7+. These instruments will provide not only outstanding performance in terms of flux and resolution, but also polarisation and spin analysis over the full spectral range, building on the long-standing experience of the ILL in this domain.

Exploring new materials and green energy applications: When it comes to atomic dynamics, instrumentation at the ILL covers a range in frequency and momentum that is unique in the world and not accessible to any other experimental probe. The instrument projects Ramses, IN5+ and Panther, aim to consolidate and develop these capacities further.

Analysing soft complex materials, life science and biology: To strengthen the instrument suite further, Rainbows will enhance capabilities for studying surfaces and interfaces, in particular allowing the study of kinetic processes on hitherto inaccessible timescales. For dynamics on molecular timescales the instruments Ramses and IN5+, with their dramatically improved signal quality, will open up routes for studying more complex and more dilute systems.

Tools for nuclear and particle physics: Using the high neutron flux available at the ILL it is possible to create very neutron-rich nuclei by neutron capture. The study of the decay of these exotic species provides key information about the structure and stability of atomic nuclei, and is both essential for understanding the nucleo-synthesis of elements in stars and relevant to advanced nuclear technology. The Fipps project will extend these experiments to more exotic nuclei by combining mass- and gamma-ray spectroscopy. Due to the absence of electromagnetic interactions, the neutron is the subatomic particle best suited for probing the gravitational force. Studies of its lifetime, decay and dipole moment explore the most fundamental theories in physics. The SuperSUN project aims to build the latest generation of ultra-cold neutron (UCN) source with densities of UCN's orders of magnitude greater than that available today.

Advanced sample environment (Nesse): The science that can be performed on instruments depends directly on the sample environments that are available in terms of capacity, capability (extreme conditions of temperature, magnetic field, humidity etc.) and efficiency. As sample environment (SE) increasingly becomes a limiting factor in neutron experiments it is timely that the ILL reinvests and modernises its SE in order to remain internationally competitive. The Nesse project will provide not only new capability and capacity but also increased efficiency in sample environment provision. In particular, small samples, soft matter, high pressures and low temperatures will be addressed.

Modern tools for data treatment (Bastille): Like Nesse, it will allow the ILL to make the most of its entire, state-of-the-art, current and future instrument suite. To this end, software is critical and Bastille will provide state-of-the art software for reduction and analysis, in collaboration with other neutron scattering facilities, allowing real-time production of scientific results and the most efficient use of beam time. New software, seamlessly integrated with data acquisition, will enable new ways of working and new science.

Phases 1 & 2 (2016-2023)
Phase 1 (2016-2019)
Phase 2 (2019-2023)

NEW EXPERIMENTAL TECHNIQUES

The H5 guide system – the latest innovative guide system at the ILL

AUTHORS

M. Kreuz, J. Beaucour, M. Böhm, R. Boffy, V. Cristiglio, B Demé, A. Devishvili, L. Didier, P. Falus, P. Fouquet, R. Gandelli, Y. Gibert, B. Giroud, M. Jacques, B. Jarry, P. Lachaume, A. Martel, L. Porcar, S. Roux, J. Segura, F. Thomas, A. Vorobiev (ILL)

As the world's leading centre for neutron science, the ILL provides scientists with a very high flux of neutrons. The transport of neutrons to the different instruments is continually being adapted to the latest technologies in order to maximise the useful neutron flux available. Even better, dedicated neutron guides can now be created with a geometry and wavelength spectrum that is optimised for individual instruments.

Under the old H5 guide system, three guides were available to deliver neutrons to seven instruments. With the new guide system, six individual guides have been created, supplying neutrons to eight instruments. The in-pile section of the three primary neutron guides – H51, H52 and H53 – includes a special component at the very beginning of the guide system, the so-called "separator". This is made of polished aluminium coated with a high-reflectivity neutron mirror.

H51 splits into two secondary guides, H511 and H512, which are optimised for the two instruments D22 (small-angle scattering) and IN15 (spin-echo spectrometer).

H52 splits into three secondary guides, H521, H522 and H523, which transport neutrons to the instruments on the southern side of the ILL22 guide hall. H522, with a radius of curvature of 4 000 m, will be used for the new spin-echo spectrometer WASP, which is due to be commissioned in 2016. H521, with a radius of curvature of 1 500 m, is shared in the conventional way between the three instruments D16 (diffractometer), SuperADAM (reflectometer) and D50 (industrial applications). The final guide, H523, has a smaller radius of curvature (800 m). It has been customised to feed neutrons to a cryostat containing liquid He^4 to produce ultra-cold neutrons (UCN).

Finally, the guide H53 is a fairly short (15 m), straight m = 3 guide, which is optimised to transport a high-divergence neutron beam to the three-axis spectrometer (ThALES) located in the reactor building.

figure 1 shows the layout of H5 from the reactor to the end of the guide hall.

Figure 1

The H5 layout from the reactor to the end of the western guide hall ILL22 showing the eight instrument positions.

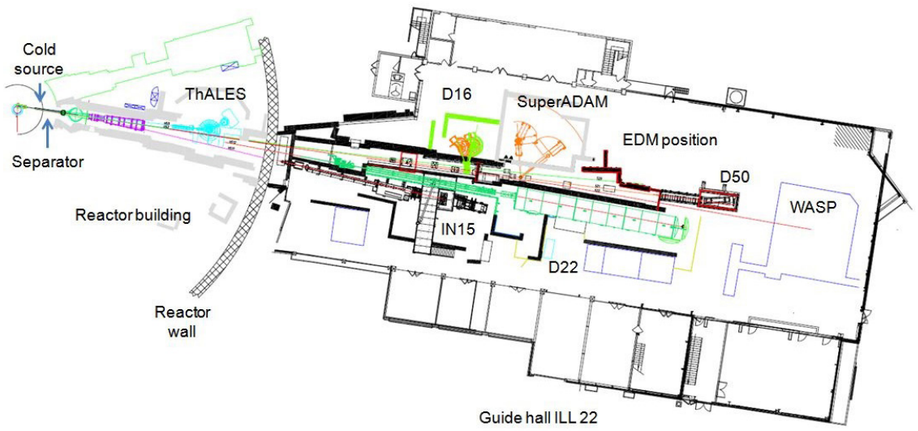

Neutron transport simulations and first results

Transport simulations were performed for the whole of the H5 guide system in the design phase. The design was then optimised taking into account the geometrical constraints of existing equipment and infrastructures.

The beam flux simulation results and first gold foil measurements of neutron capture flux (n/cm²/s) are shown in **figure 2** for various distances from the horizontal cold source. From the different values in **figure 2**, we can see that the simulations and experimental measurements are in reasonably good agreement, especially at a distance of more than 15 metres from the source, where neutron background from the core is low compared to the guided neutrons.

Concerning improvements to the flux at the entrance to the different instruments supplied by the H5 guide system, we observe an increase in neutron flux by a factor of 1.2 to 3.5 compared to the old guide system (see **table 1**). The real gain for the instruments is actually even greater since the instrument upgrades must also be taken into account. Thus the performance of the D16 spectrometer, for example, has increased overall by a factor of 10.

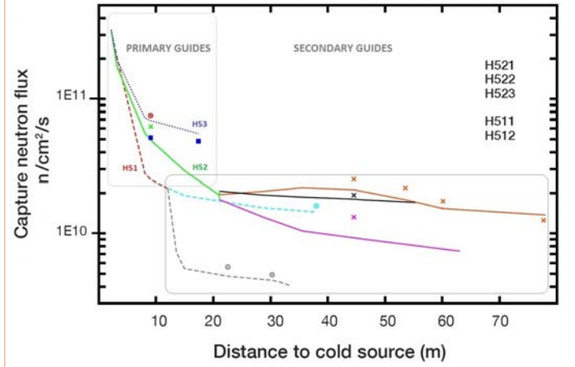

Figure 2

H5 beam flux simulations (lines) and corresponding gold foil measurements (dots)

In conclusion, the H5 project involving the complete rebuild of the guide system and the upgrade or renovation of all the related instruments has led to a tremendous increase in instrument performance. With the commissioning of the new spin-echo spectrometer WASP in 2016 the H5 project will be completed, representing a major improvement for the ILL instrument suite as a whole.

Table 1

Capture flux gain of the upgraded H5 instruments, as measured at the secondary guide exit (Sept. 2015) N.B.: The flux for the future UCN free position and WASP has not yet been measured. D50 is a new instrument and its flux cannot be compared with an old reference.

Measurements at the instrument end of the guide	Recent (10-year) best before renov.	H5 - 1988 commissioning	H5 - 2015 commissioning	GAIN	
				1988	10-year best
	(n/cm²/s)				
ThALES	2.00E+10 *2010 extrapol. @19m*	2.77E+10 19m	4.82E+10 17.4m	1.7	2.4
IN15	3.12E+09 2006 – 33.6m	1.64E+09 33.6m	4.95E+09 33.6m	3.0	1.6
D22	1.34E+10 2006 – 38m	1.60E+10 38m	1.61E+10 38m	1.0	1.2
D16	6.20E+09 2007 – 66.3m	1.14E+10 66.3m (EVA)	2.18E+10 53.5m	1.9	3.5
SuperADAM	4.90E+09 2004 – 71m	9.10E+09 71m	1.72E+10 60m	1.7	3.1
D50	–	–	1.23E10 77.7m	–	–

NEW EXPERIMENTAL TECHNIQUES

Neutron imaging using a conventional SANS instrument

AUTHORS
C.D. Dewhurst and I. Grillo (ILL)

REFERENCES
[1] For an topical overview see: Neutron News, Vol. 26, Issue 2 (2015)
[2] C. Dewhurst *et al.*, J. Appl. Cryst. Vol. 49 (2016) 1

Neutron imaging has enjoyed a flurry of activity and application in recent years with the construction of dedicated instruments at various neutron sources. The ILL, as yet, does not run a dedicated imaging facility despite significant interest among the science and engineering communities with particular relevance to industrial applications, non-destructive testing of components and imaging of archaeological artefacts. Here we demonstrate how scanning neutron imaging can be performed on a conventional small-angle neutron scattering (SANS) instrument, such as D33 at the ILL, giving access to transmission radiographic images as well as the dark-field or scattering-contrast and phase-contrast images with spatial resolutions down to about 100 µm.

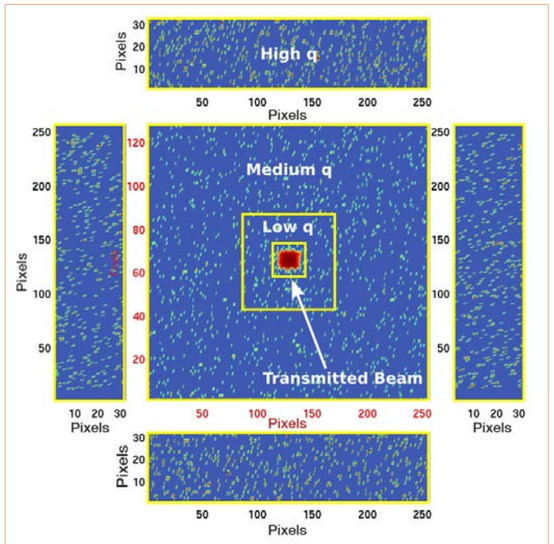

Figure 1
Typical raw data measured at one pixel position during the imaging scan. 9 486 such images of exposure time 5 seconds make up the scan over the object with images reconstructed from the transmitted beam intensity and scattering at low-, medium- and high-q (angles). Phase-contrast images were reconstructed from the pixel co-ordinates of the refracted beam centre position.

The use of neutrons for imaging is of particular interest due to their ability to penetrate bulk objects and their sensitivity to light elements providing high contrast of components, in particular those containing hydrogen. There are several high profile works detailing neutron imaging on examples such as running engines, lithium batteries, *in situ* studies of fuel cells, storage of hydrogen, water uptake in plants and non-invasive studies of cultural heritage objects [1].

Conventional neutron imaging uses a coaxial setup of neutron source of size D, beam collimation of length L, object to be imaged and detector placed as close as possible behind the object. The ratio L/D, the distance from object to detector, and the spatial resolution of the detector determine the spatial resolution that can be achieved and is typically of the order 10 µm to 100 µm. The measurements visualise the total attenuation cross-section, i.e. the sum of both absorption and scattering cross-sections. Small-angle neutron scattering, on the other hand, is a well-established and powerful technique used to study material or magnetic structures in the size range of about 10 Å to 10 000 Å. SANS instruments typically use a quasi-monochromatic and well collimated beam of neutrons on the sample in order to resolve scattering at the smallest angles. The measured scattering curve is not a real-space image but is effectively a Fourier transform of the real-space particle size distributions within the sample.

Neutron imaging can be performed on a conventional SANS instrument [2]. The method is rather straightforward and uses a fine beam in a raster-scan measurement over the area of interest, separating the absorption and scattering-based attenuation mechanisms and allowing identification of buried components in the object of different material composition and structural order. The sample chosen for these test measurements was the top 3 cm of a mechanical pencil, comprising multiple structures of dimensions between about 0.5 mm and several mm and made up of a variety of materials such as different plastics forming the body and mechanics of the pencil, a steel spring and the graphite pencil 'lead'. Measurements were made using a 200 µm circular sample aperture scanned over an area of 10 mm (horizontal) x 37 mm (vertical) in steps of 200 µm, thereby defining the spatial resolution of the resulting image. The instrument was configured with an incoming wavelength of 6 Å (δλ = 10 %), collimation length of 2.8 m, and front and rear detectors at 2 m and 3 m from the sample respectively. A total of 9 486 individual pixel SANS measurements were made [51 (horizontal) x 186 (vertical)] for 5 s at each position of the scan, with a further 1.5 s of dead time due to the movement of the sample and saving of the data, requiring a total measurement time of 17.1 hours.

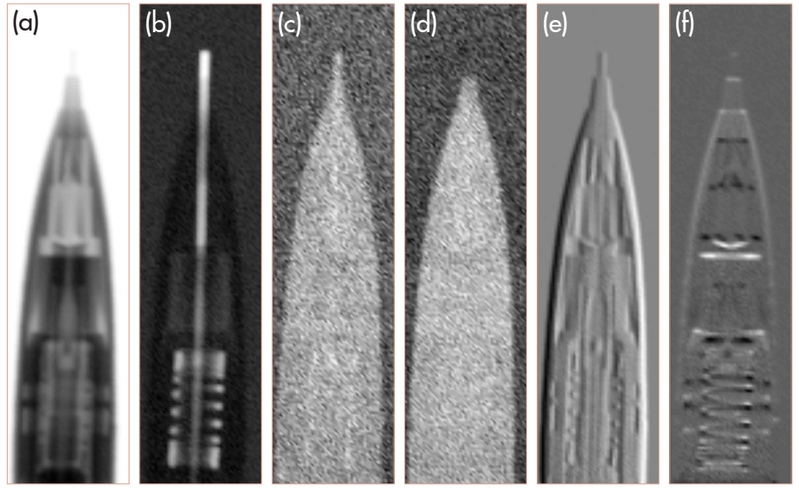

Figure 2
Scanning radiographic images of a mechanical pencil extracted from the transmission and scattering data depicted in **figure 1**: **(a)** Transmission radiograph; **(b–d)** Dark-field images based on small-angle scattering in the **(b)** Low-q, **(c)** Medium-q and **(d)** High-q regions indicated in **figure 1**; **(e–f)** Phase-contrast images given by the deflection of the transmitted beam due to refraction in the **(e)** horizontal and **(f)** vertical directions.

Figure 1 shows a typical transmission and SANS measurement at an individual pixel position over the sample. The number of counts in the direct beam varies from between ~2 400 counts for positions over the sample to ~50 000 counts with no sample giving a transmission of only ~5 % depending on the position over the sample. Outside of the main beam, sparse counts of ~1 300 counts and ~550 counts on the rear and front panel detectors due to scattering from the sample should be compared with the background of ~1 000 counts and ~500 counts for positions away from the sample.

Radiographic images can easily be reconstructed from the transmitted beam or from the rather arbitrarily defined low-, medium- and high-q (or angle) regions of scattering depicted in **figure 1,** by plotting the counts in a given window of the detector as a function of position across the sample. **Figure 2(a)** shows the image reconstructed from the transmitted beam and is similar to what might be expected from a conventional radiographic image, i.e. the bright-field image. **Figure 2(a)** shows particularly clearly the various plastic components due to attenuation of the beam, predominantly due to scattering. Despite the significant quantity of hydrogen-containing plastics, using a SANS instrument to separate the transmitted and scattered neutrons means that the image in **figure 2(a)** does not suffer from the 'fogging' or distortion of the image due to the background of incoherent scattering.

Figures 2(b-d) show images reconstructed from the scattering data in the low-, medium- and high-q regions of scattering, as indicated in **figure 1**, and reveal additional information about materials and structures within the sample. **Figure 2(b)** is particularly impressive whereby the steel spring and graphite pencil 'lead' are now clearly visible. This is due to the fact that while neither of these components attenuates the beam significantly, they scatter strongly in the lowest-q (smallest angle) regime. **Figures 2(c, d)** for the most part show only incoherent scattering due to the plastic components that give the transmission contrast in **figure 2(a),** with **figure 2(c)** in the medium-q regime still showing some evidence of the steel and graphite components.

Finally, additional images can be obtained from the so-called differential phase-contrast, measured here as the refracted position of the transmitted beam on the detector due to the combined shape and refractive index of the buried components. A centre of mass calculation across the transmitted beam reveals small deflections in the beam position of a maximum +- ~1 (~2) pixel(s) in the vertical (horizontal) direction corresponding to a physical shift in the beam centre on the detector of ~5 mm or ~0.1°. **Figures 2(e, f)** show these images reconstructed from the beam centre position in the horizontal and vertical directions respectively, due to the differential phase-contrast in the sample. **Figure 2(e)** shows clearly vertical boundaries in the sample, such as the edges of the pencil, whereas **figure 2(f)** shows, for example, the thin, but nearly horizontal windings of the steel spring.

In conclusion, scanning SANS imaging is a rather simple but powerful technique, requiring nothing more than a conventional SANS instrument equipped with a small, resolution defining sample aperture ~100 µm and precision movement stages for sample scanning. The time required for imaging samples not only depends on the incident beam flux but also scales with the required resolution and desired image area. Scanning imaging using a SANS instrument allows the different contrasts due to absorption (bright-field), scattering (dark-field) and phase-contrast to be separated, with each giving their own unique information and highlighting different components within the sample.

NEW EXPERIMENTAL TECHNIQUES

Stroboscopic experiments with sub-ms time resolution

Neutrons offer unique advantages for the study of matter, such as high penetration power, isotopic and magnetic sensitivity, as well as low radiation damage. Consequently, they are a vital tool for answering essential scientific questions in a broad range of fields, such as soft matter science, biology, pharmacy, engineering science and magnetism. However, even with the most modern neutron sources, neutron flux limitations are a significant drawback. This is particularly true for the study of kinetic processes, when only a very short period of time is available to collect data. Ideally, time resolutions below one second (or even a millisecond) are needed to study processes such as particle precipitation, shear alignment and the formation of hierarchical structures. One possibility for overcoming these limitations is to study repeatable processes and integrate the neutron signal over many cycles.

Figure 1

Stroboscopic effect illustrated by a picture of a bouncing basketball.

M. Maggs, Edit by R. Bartz – Creative Commons Attribution – Share Alike 3.0 unported license.

AUTHORS

F. Adlmann and **M. Wolff** (Uppsala University, Sweden),
P. Gutfreund (ILL, Grenoble, France)

REFERENCES

[1] D. Kipping, R. Gähler and K Habicht, Phys. Lett. A 372 (2008) 1541

[2] A. Wiedenmann, U. Keiderling, K. Habicht, M. Russina and R. Gähler, Phys. Rev. Lett. 97 (2006) 057202

[3] M. Wolff, P. Kuhns, G. Liesche, J.F. Ankner, J.F. Browning and P. Gutfreund, Combined neutron reflectometry and rheology, J. Appl. Cryst. 46 (2013) 1729

[4] J. Jiang, C. Burger, C. Li, J. Li, M.Y. Lin, R.H. Colby, M.H. Rafailovich and J.C. Sokolov, Macromolecules 40 (2007) 4016

[5] K. Mortensen, E. Theunissen, R. Kleppinger, K. Almdal and H. Reynaers, Macromolecules 35 (2002) 7773

[6] F.A. Adlmann, P. Gutfreund, J.F. Ankner, J.F. Browning, A. Parizzi, B. Vacaliuc, C.E. Halbert, J.P. Rich, A.J.C. Dennison and M. Wolff, J Appl Cryst 48 (2015) 220

This can be achieved by phasing the neutron beam with the excitation and is used, for example, in the TISANE technique [1,2], where each neutron is recorded in a histogram presenting its scattering event at a certain time during the duty cycle of the excitation. However, this technique is limited by the need for total synchronisation, meaning that the relative phase of the neutron pulse and the excitation must be known and constant at all times. In reality, this is almost impossible to achieve for longer measurement times or for any sample-dictated response, such as oscillatory shear.

This challenge can be overcome by storing all neutron events regarding their arrival at the detector with respect to a universal clock. The same clock is used simultaneously to store either the signal of the excitation, for example the strain on a sample or an electric or magnetic field, or a trigger marking the beginning of a duty cycle. The approach is similar to taking photographs with a high-speed camera. **Figure 1** shows the example of a bouncing basketball. The only difference in our case is that several identical photographs must be superimposed in order to achieve good enough contrast to resolve the image in reciprocal space. This approach offers the particular advantage that the data can be binned to any time resolution once the experiment is finished during the post-processing. This paves the way for data mining as well as the tracking of instrument or source failures, since no information is lost when storing the data. The theoretical limit regarding time resolution is similar to TISANE and mainly determined by the sample-detector distance. For typical neutron instruments, time scales below 1 ms become easily accessible.

In order to demonstrate the capabilities of our approach, we conducted combined neutron reflectivity and rheology measurements on the instrument FIGARO (**figure 2**) [3]. An oscillatory mechanical load was applied to a micelle-forming aqueous block polymer solution. This type of sample is known to be highly sensitive to shear, and structural reorientations have been shown previously by transmission SANS (small-angle neutron scattering) in a Couette geometry [4,5]. Technically, we applied a repeatable, oscillating mechanical excitation with the stress-controlled rheometer (Anton Paar-MCR 501) available at the ILL, and fed a triggering signal in the neutron event stream allowing stroboscopic time-binning during data analysis. We demonstrated, by analysing the (111) Bragg reflection of the face-centred cubic (FCC) crystal structure formed by the micellar solution under large amplitude oscillatory shear (LAOS), that we could follow the structural reorganisation during shear with a time resolution of at least 500 µs (**figure 3**) [6].

In summary, we have shown the feasibility of time-resolved reflectivity measurements on FIGARO with time resolutions below a millisecond. This paves the way for time-resolved experiments at the ILL, since our approach can easily be transferred to any neutron scattering technique. For the first time, we have successfully used event-mode-based data acquisition combined with a trigger signal to extract time-resolved neutron scattering data. The latest detector acquisition cards at the ILL support this mode of operation and the option to collect the event stream is available as standard in the NOMAD control system. Possible applications of the approach, other than rheology, are magnetic relaxation, the dynamics of nematic crystals, piezoelectric behaviour and mechanical hysteresis, to name but a few.

Figure 2

Experimental set-up and geometry of the experiment.

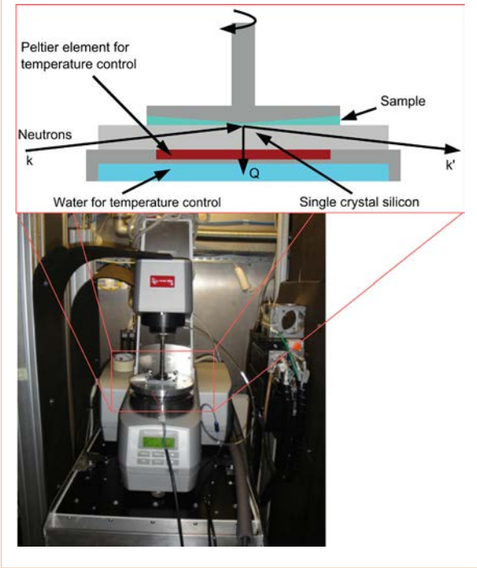

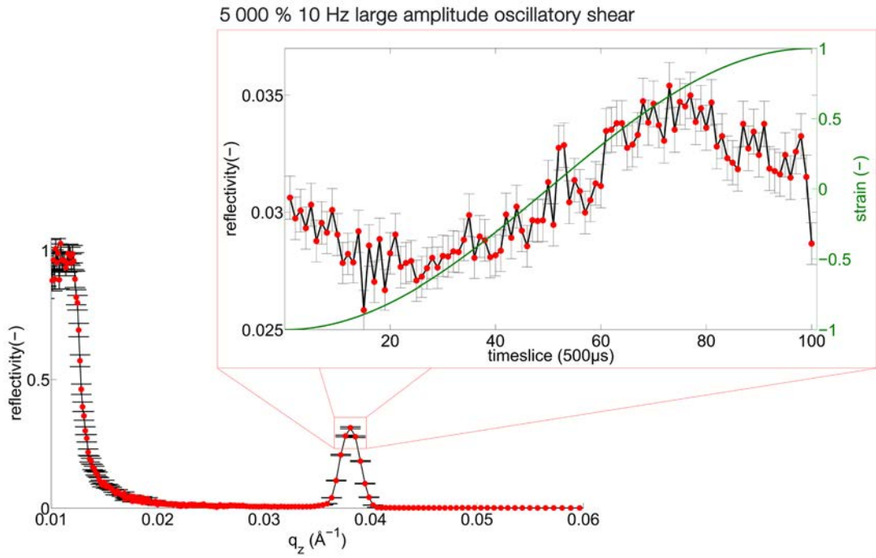

Figure 3

Reflectivity curve of our model sample F127 in D20. The inlay shows the dependence of the 111 peak over the half-period of the sinus duty cycle of oscillatory shear (5 000 % strain and 10 Hz). To better illustrate the feature a static data set with a more visible peak was chosen.

TECHNICAL AND COMPUTING DEVELOPMENTS

Paving the way for even better neutron guides

AUTHORS

R. Boffy, J. Beaucour, M. Kreuz and **R. Schwein**s (ILL)
S. Peuget (CEA, DEN, DTCD, SECM, LMPA-Marcoule, France)
F.J. Bermejo (Instituto de Estructura de la Materia, Consejo Superior de Investigaciones Cientificas, Madrid, Spain)

The mechanical rupture of neutron guides due to irradiation ageing is an issue that neutron institutes throughout the world have been facing for many years. Thanks to fast-ageing experiments and a set of characterisation techniques, we have unveiled some of the reasons why glass guides made of certain types of borosilicate (Borofloat or N-ZK7) may degrade and even break under operating conditions.

Guides are used to transport neutrons to scientific instruments located several tens of metres from the neutron source. The instruments located at the end of these guides benefit from a higher flux intensity and a much lower background compared with instruments located close to the reactor. Neutron guides usually have a rectangular cross-section and are made of an assembly of mirror-coated glass plates (see **figure 1**). The plates are made of a borosilicate glass, such as Borofloat, N-ZK7, N-BK7 or S-BSL7. These materials combine two interesting features: first, they produce a surface quality that allows a certain type of coating to be used that increases neutron reflectivity; and second, they absorb the non-reflected neutrons through $^{10}B(n, \alpha)^{7}Li$ reactions within the first hundred microns from the reflective surface. This second property provides neutron radiation shielding to the surrounding environment and reduces self-activation.

However, this can turn into a drawback. The α particle and the recoil lithium ion share around 2.5 MeV of kinetic energy that will be deposited less than 5 µm from the neutron capture point. The direct consequence of this is that the glass is modified by irradiation – this phenomenon was quickly identified as the origin of the splintering of neutron guides made of Borofloat or N-ZK7 glass. While a similar degradation process could also be expected to occur in N-BK7 and S-BSL7, these glasses actually resist a neutron fluence that is orders of magnitude higher. We also found that a mirror coating on the irradiated surface does not influence the radiation hardness of the glass substrate below. **Figure 1** shows the inside of a splintered guide due to irradiation ageing. If degradation of this kind occurs on an evacuated guide, it may cause the guide to implode suddenly and thus damage surrounding equipment.

To understand the root causes of such a failure mechanism, we performed a set of test irradiations and characterisation experiments.

Figure 1

Glass neutron guides:
(left) H5: a brand new triple guide;
(right) inside of H113, mirror peeling off due to the splintering of the glass below (credits S-DH, SMAE).

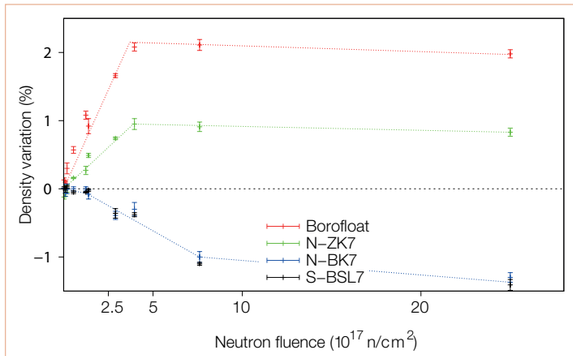

Figure 2

How the density of Borofloat, N-ZK7, N-BK7 and S-BSL7 changes as a function of received fluence. Dotted lines added to facilitate reading.

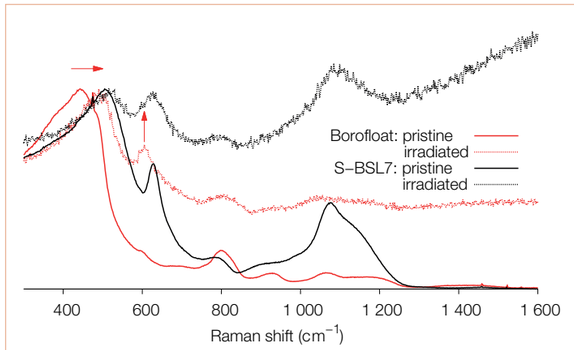

Figure 3

Raman intensity of Borofloat and S-BSL7 glass, before and after irradiation. Borofloat: shifting of Si-O-Si band (around 450 cm^{-1}) and growth of three-membered silicon ring (around 600 cm^{-1}). The higher background and the ramp at high frequency for the irradiated specimens are due to the experimental set-up in a hot cell and the luminescence, respectively.

The first thing we found was that mirrors break due to the heterogeneous shrinking of the substrate. Of the different glasses tested, the ones that break the quickest are those that become the most compact under irradiation. Borofloat and N-ZK7 mirrors, which break at around 2×10^{15} and 2.8×10^{16} n/cm^2 respectively, are very reactive in this fluence range, while N-BK7's density is stable and does not splinter (**figure 2**). In practical terms, the heterogeneous irradiation encountered in the ILL's guides under the typical grazing incidence of neutrons creates a gradient of shrinkage within the plate which in turn generates stresses. Once these stresses exceed the fracture toughness of the glass, the mirror splinters.

In the light of these findings, we tried to understand what could explain the differences in radiation hardness between the different glasses studied, given their similar boron content. The combination of Raman and NMR spectroscopy highlighted important structural differences between the glasses studied. On the one hand, Borofloat and N-ZK7 have a relatively low content of BO_4 units together with silicon- and boron-rich areas. Their behaviour under neutron flux is dominated by their silica domain, which shrinks and incorporates boron atoms into it (see **figure 3**). On the other hand, N-BK7 and S-BSL7 are characterised by a homogeneous borosilicate network made up primarily of BO_4 units bonded with four silicon atoms. The macroscopic density stability of these materials stems from the fact that they are relatively resistant to irradiation. In any case, during measurements at the ILL on the small-angle scattering instrument D11, no phase segregation was detected under flux. The deposited energy and the ballistic mixing tend to create a rather more homogeneous glass.

Thanks to this study, we were able to understand why neutron guide breakup may occur under irradiation and to devise a set of material design rules applicable to ILL guides. On the one hand, Borofloat should be used solely for low-flux guide sections, for example those located behind a monochromator or a velocity selector, and under vacuum housing to avoid catastrophic failures. On the other hand, N-BK7 and S-BSL7 appear to be resistant to irradiation and could be used all along the guide, although vacuum housing is nonetheless recommended.

More generally speaking, the irradiation devices developed at the ILL are now available to characterise future substrates. Current research is investigating the use of metallic and composite materials which should allow innovative geometries and eliminate the risk of brittle breakage.

MODERNISATION PROGRAMMES AND TECHNICAL DEVELOPMENTS

TECHNICAL AND COMPUTING DEVELOPMENTS

New software tools emerging from the ILL Scientific Data Policy

AUTHOR

J.F. Perrin (ILL)

REFERENCES

[1] http://www.ill.eu/users/ill-data-policy
[2] https://www.datacite.org
[3] https://www.epsrc.ac.uk/about/standards/researchdata
[4] http://journals.plos.org/plosone/s/data-availability

Central facilities for neutron scattering and synchrotron X-rays in Europe are increasingly working together to develop and share infrastructure for the data they collect. Such co-operation should not only make it easier and more efficient for users to access and process their data but also to be recognised for their experimental work. It should also help to increase the scientific value of the data by opening it up to a wider community for further analysis, thus fostering new collaborations between scientific groups. Ultimately, this should improve the quality and quantity of publications from such data. However, with these developments comes a need to define how such data and any associated metadata are stored and made accessible, and for this a common data policy has been established to provide a suitable working framework. This article presents the ILL's rationale for such a project and the new software tools that have been developed for scientists.

Since its first neutrons were delivered, the ILL has strived to archive the experimental data files generated by experiments. In the 1990s, with the emergence of the Internet, those files were freely and openly available on the ILL web servers immediately upon completion of experiments, but without the necessary organisational structure or metadata information to allow data processing or data analysis to be done properly by scientists outside of the experimental team. Sometimes this lack of structured information created data-processing problems even for the experimental team itself. Too often the tools and methods for data processing were precarious or "fragile", and relied upon individual know-how and organisation (for instance, the data file names corresponding to an experiment were recorded in a single paper notebook).

The initial idea driving this "Data Policy" effort was to increase the impact of the work done at the ILL by trying to improve the usability and hence the usage of the data. The project focuses primarily on the preservation of all types of metadata and the structuring of this information in a way that makes the data both understandable and shareable within the scientific community. Of course, it was also obvious that any changes had to be compatible with measures to protect our users. In other words, they had to be given sufficient time to publish their research before sharing the data so that they could avoid being "scooped".

In 2008, together with the other European synchrotron and neutron facilities, we started discussions on this topic. After three years of active internal discussions, the ILL decided, with the approval of its Scientific Council, to publish the ILL "Scientific Data Policy" in November 2011, just before the opening of the December 2011 proposal round. The text came into force in October 2012, and prescribed a default non-disclosure period of three years during which access to data is restricted to the experimental team; in cases where no request for data has been made, this period would be extended to five years [1].

Following the publication of the ILL Scientific Data Policy, a working group was set up. Its purpose was to prepare the ensuing organisational changes and steer development of the necessary software tools with a clear focus on usability and functionality (especially during experiments), as well as data security. The new data portal (**data.ill.eu**) created to implement the changes brought about by the Scientific Data Policy was released in 2014: it provides a global search engine for all textual metadata related to an experiment, making it possible to quickly retrieve all data of interest related to the search criteria, while restricting access to data that are not yet public.

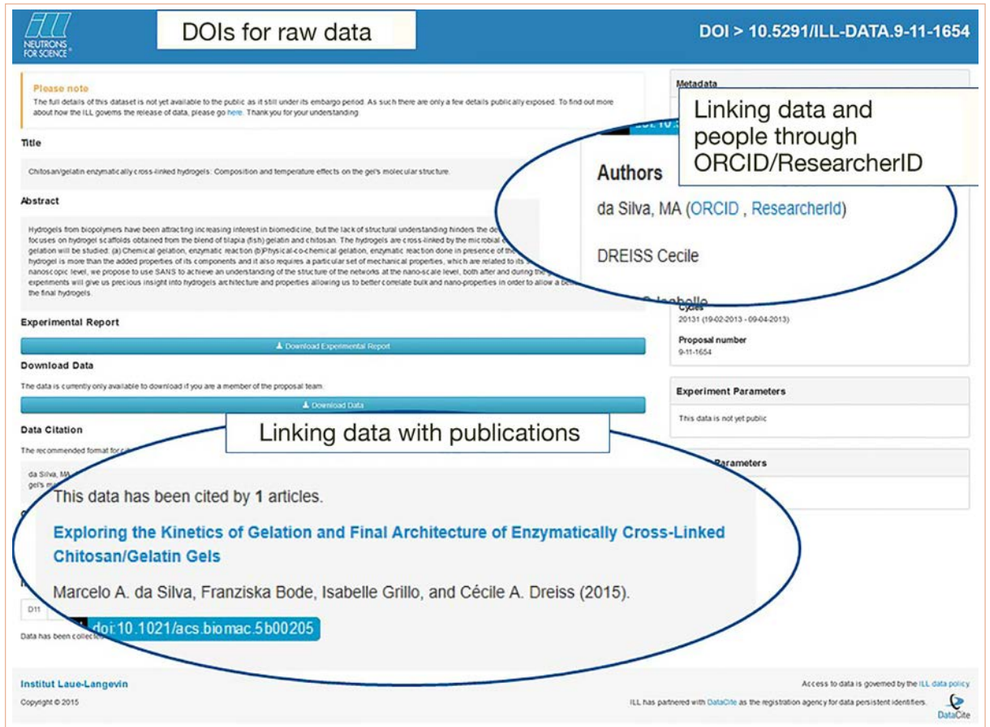

Thanks to this tool, experimental teams now have some control over the visibility of and access to their data. They can, if they wish, decide to give access to certain individuals, for example if they want to widen the collaboration or respond to access requests from publication peer reviewers. They can also make their data public before the end of the non-disclosure period, once their corresponding articles have been published and they no longer need the data. Similarly, a user who has identified data of interest for his/her research can contact the experimental team and ask for access authorisation.

In order to link publications with the corresponding data over a long time period, the ILL "mints" a Digital Object Identifier (DOI) for each dataset using the services of DataCite [2]. DOI is a standard solution for creating a unique and persistent identifier – it has already been widely adopted by the publishing sector. The experimental team receives the DOI as soon as it is generated and is strongly encouraged to cite it in the reference section of its published articles. This DOI citation allows readers to obtain more information about the referenced experiments, access the data via **data.ill.eu** and even request access if the data are not yet publicly available. DOIs also facilitate the finding and collection of relevant publications and hence the generation of scientific-output statistics; these are of the utmost importance nowadays not only for scientists but also for the ILL, and therefore contribute to the recognition of the work accomplished. Experimenters can also register their ORCID or ResearcherID, which is then automatically associated with the data they have generated, thus reducing the risk of ambiguity.

We are delighted to announce that, following the publication of the first scientific articles by users citing data DOIs, we have just reached a new milestone: for the first time we have users who have made their experimental data public before the end of the non-disclosure period.

At a time when funders (such as EPSRC [3]) and publishers (such as PLOS [4]) are increasingly requesting that data be publicly accessible and preserved for a long period of time after publication of associated articles, the work achieved within the framework of the ILL Scientific Data Policy, and the tools now available, represent an important asset for the ILL's users, helping them to meet such requirements easily and at no extra cost.

EXPERIMENTAL AND USER PROGRAMME

Neutron beams and instrument facilities are free of charge for proposers of accepted experiments. Scientists affiliated to the institute's member countries will also, in general, be assisted with necessary travel and daily subsistence for a limited period. The User Support team makes all arrangements for accommodation and will process claims for expenses after users have completed their experiments.

The ILL User Support team is dedicated to helping all visiting researchers to make the most of its facilities. If you are coming to the ILL to carry out experiments, the User Office is here to give you the organisational and administrative support you need to successfully perform your experiments.

For further information about the institute's facilities, applications for beamtime, user support and the experimental programme, please visit our website: **http://www.ill.eu/users**.

In order to maintain their ranking on the international scene, European research institutes must optimise their resources and develop synergies at every level.

The ILL is firmly committed not only to building high-performance instruments but also to offering the best scientific environment to the user community. We have established successful collaborations with neighbouring institutes over the years, and launched many successful scientific and support partnerships.

In parallel, the ILL and the ESRF have been working on plans to transform our joint site into a research campus – the "European Photon and Neutron science campus", or EPN-campus for short – with a truly international reputation.

The ILL is firmly committed not only to building high-performance instruments but also to offering the best scientific environment to the user community.

INSTRUMENT LIST

EXPERIMENTAL AND USER PROGRAMME

INSTRUMENT LIST

ILL INSTRUMENTS		
D2B	powder diffractometer	operational
D3	single crystal diffractometer	operational
D4 (50 % with IN1-LAGRANGE)	liquids diffractometer	operational
D7	diffuse-scattering spectrometer	operational
D9	single crystal diffractometer	operational
D10	single crystal diffractometer	operational
D11	small-angle scattering diffractometer	operational
D16	small momentum-transfer diffractometer	operational
D17	reflectometer	operational
D19	single crystal diffractometer	operational
D20	powder diffractometer	operational
D22	small-angle scattering diffractometer	operational
D33	small-angle scattering diffractometer	operational
FIGARO	horizontal reflectometer	operational
IN1-LAGRANGE (50 % with D4)	three-axis spectrometer	operational
IN4	time-of-flight spectrometer	operational
IN5	time-of-flight spectrometer	operational
IN6	time-of-flight spectrometer	operational
IN8	three-axis spectrometer	operational
IN11	spin-echo spectrometer	operational
IN16B	backscattering spectrometer	operational
IN20	three-axis spectrometer	operational
PF1	neutron beam for fundamental physics	operational
PF2	ultra-cold neutron source for fundamental physics	operational
PN1	fission product mass-spectrometer	operational
PN3 – GAMS	gamma-ray spectrometer	operational
SALSA	strain analyser for engineering application	operational
ThALES	three-axis spectrometer	operational

CRG INSTRUMENTS		
BRISP	Brillouin spectrometer	CRG-B operational
D1B	powder diffractometer	CRG-A operational
D23	single crystal diffractometer	CRG-B operational
GRANIT	gravitation state measurement	CRG operational
IN12	three-axis spectrometer	CRG-B operational
IN13	backscattering spectrometer	CRG-A operational
IN22	three-axis spectrometer	CRG-B operational
SuperADAM	reflectometer	CRG-B operational
S18	interferometer	CRG-B operational

JOINTLY FUNDED INSTRUMENTS		
LADI (50 %)	Laue diffractometer	operated with EMBL
IN15	spin-echo spectrometer	operated with FZ Jülich and HZB Berlin
GRANIT	gravitation state measurement	operated with LPSC (UJF, CNRS)

TEST AND CHARACTERISATION BEAMS	
CT1, CT2	detector test facilities
CYCLOPS	Laue diffractometer
TOMOGRAPHY	neutrography
OrientExpress	Laue diffractometer
T3	neutron optics test facility
T13A, C	monochromator test facility
T17	cold neutron test facility

INSTRUMENT LAYOUT – JANUARY 2016

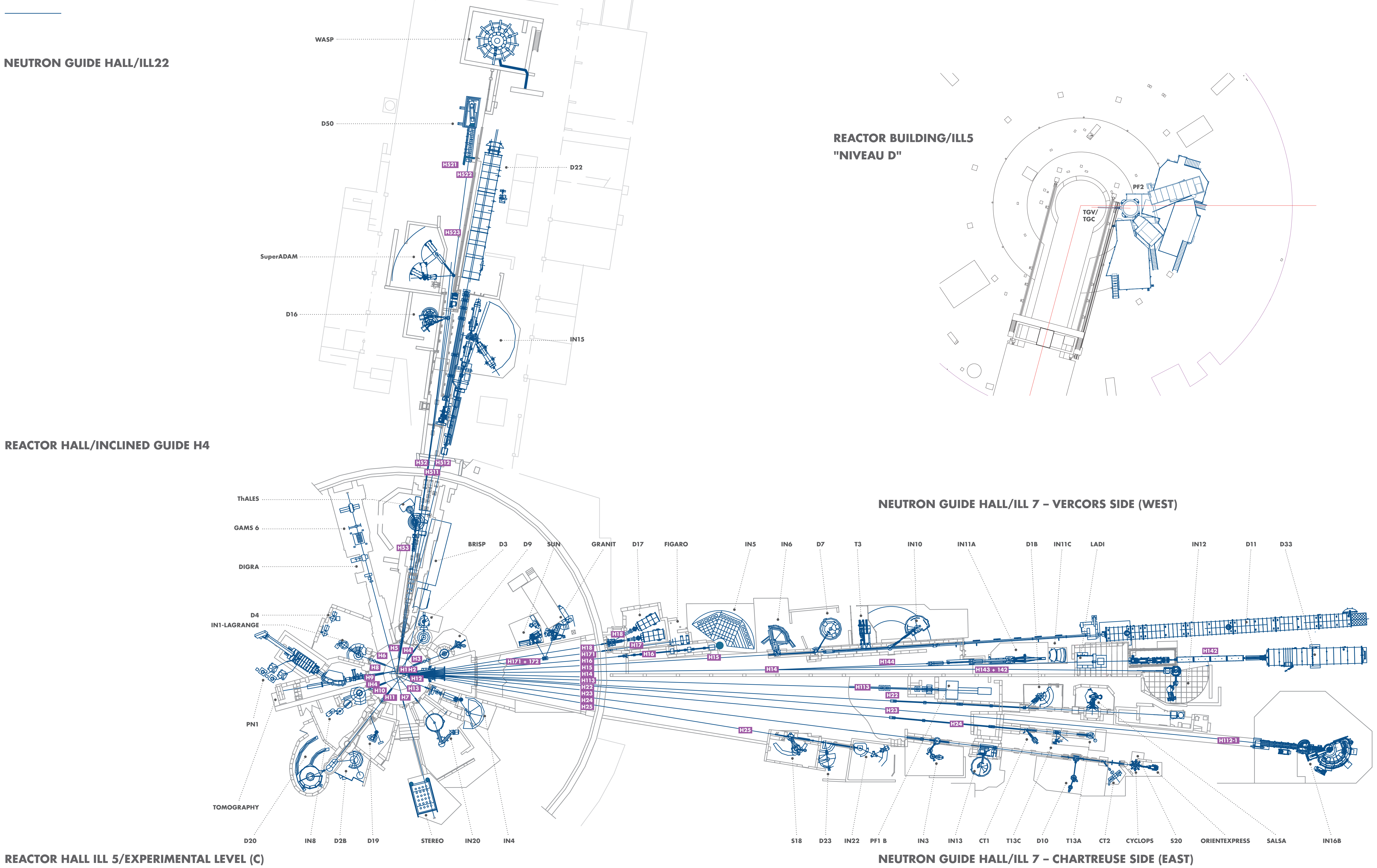

INSTRUMENT LAYOUT 2015

EXPERIMENTAL & USER PROGRAMME

USER PROGRAMME

THE ILL USER CLUB

All administrative tools and information for our scientific visitors are grouped together and directly accessible on the web, courtesy of our user-friendly, online User Club. Club members can log on using their own personal identification to gain direct access to all the information they need. Users with particular responsibilities have privileged access to other tools, according to their role. The ILL User Club includes the electronic proposal and experimental reports submission procedures, as well as electronic peer review of proposals. Additional electronic services have also been put in place: acknowledgement of proposals, subcommittee results, invitation letters, user satisfaction forms and so on.

PROPOSAL SUBMISSION

There are different ways of submitting a proposal to the ILL:

- Standard submission – twice a year – via the Electronic Proposal Submission system (EPS)
- Long-Term Proposals (LTPs) – once a year – via the EPS system
- Easy access system (EASY) – throughout the year – via our User Club website
- Director's Discretion Time (DDT) – throughout the year – via the Head of Science Division
- Special access for proprietary research and industrial users.

Submission of a standard research proposal

Applications for beamtime should be submitted electronically, via our Electronic Proposal Submission system (EPS) available on the User Club website. Proposals can be submitted to the ILL twice a year, usually in February and in September. The web system is activated two months before each deadline. Submitted proposals are divided amongst the different colleges (**see box below**) according to their main subject area.

THE ILL SCIENTIFIC LIFE IS ORGANISED INTO 10 COLLEGES:

College 1	Applied Metallurgy, Instrumentation and Techniques
College 2	Theory
College 3	Nuclear and Particle Physics
College 4	Magnetic Excitations
College 5A	Crystallography
College 5B	Magnetic Structures
College 6	Structure and Dynamics of Liquids and Glasses
College 7	Spectroscopy in Solid State Physics and Chemistry
College 8	Structure and Dynamics of Biological Systems
College 9	Structure and Dynamics of Soft-condensed Matter

Proposals are judged by a Peer Review Committee of the subcommittees of the ILL Scientific Council. Subcommittee members are specialists in relevant areas of each College. Two proposal review rounds are normally held each year, approximately eight weeks after the deadline for submission of applications. Before each meeting, the subcommittee receives a report from the appropriate College on the technical feasibility and safety of a proposed experiment. The subcommittee evaluates the proposals for scientific merit and recommends that the ILL Management award beamtime to the highest-priority proposals.

There are normally four reactor cycles a year, each of which lasts 50 days. Accepted proposals submitted by February will receive beamtime in the second half of the year and those submitted by September, in the first half of the following year. More detailed information on application for beamtime and deadlines is given on our website, at **http://www.ill.eu/users/applying-for-beamtime/**.

Easy access system

The easy access system (EASY) grants diffraction beamtime to scientists from ILL member countries who need a rapid structural characterisation of samples and data analysis. Access is open all year long and allows applicants to bypass the ILL's standard proposal round and consequent peer review process.

The system offers applicants one neutron day per cycle, on two instruments (D2B and D16), in which to perform very short experiments at room temperature. The users are not invited to the ILL but send their samples to one of two designated ILL scientists who are responsible for the measurements and sample radiological control. The ILL ships back the sample once the measurement is finished. Interested parties can apply for EASY beamtime through the User/Visitors' Club. More information is available at **http://club.ill.eu/cvDocs/EASY_Guidelines.pdf**.

Long-Term Proposals

Users from ILL member countries can also apply for extended periods of beamtime by submitting a Long-Term Proposal (LTP). The purpose of this process is to facilitate the development of instrumentation, techniques or software – that could be beneficial to the ILL community as a whole – through the award of beamtime over several cycles. The total amount of beamtime that may be allocated to LTPs on any particular instrument is capped at 10 %, and beamtime is not awarded to LTPs to perform science beyond essential testing.

LTPs can be submitted once a year at the autumn proposal round, using the specific LTP application form. The primary criterion for acceptance of an LTP is the excellence of the science that it will ultimately enable. The length of LTP projects is expected to be three years typically, with continuation approved at the end of each year, based on an annual report; a final report is also required at the end of the project. More details are given at **http://www.ill.eu/users/applying-for-beamtime/**.

Submission of a proposal to the Director's Discretion Time

This option allows a researcher to obtain beamtime quickly, without going through the peer-review procedure. Director's Discretion Time (DDT) is normally used for 'hot' topics, new ideas, feasibility tests and to encourage new users. Applications for DDT can be submitted to the Head of the Science Division, Prof. Helmut Schober, at any time.

Experimental reports

Users are asked to complete an experimental report on the outcome of their experiments. The submission of an experimental report is compulsory for **every** user who is granted ILL beamtime. Failure to do so may lead to the rejection of any subsequent continuation proposals.

All ILL experimental reports are archived electronically and searchable via the web server as PDF files (under **http://club.ill.eu/cv/**).

COLLABORATIVE RESEARCH GROUP INSTRUMENTS

The ILL provides a framework in which Collaborative Research Groups (CRGs) can build and manage instruments at the ILL to carry out their own research programmes. CRGs represent a particularly successful form of long-term international scientific collaboration. They are composed of scientists from one or two research disciplines, are often multinational and involve carrying out a joint research programme centred around a specific instrument. CRGs enjoy exclusive access to these instruments for at least half of the beamtime available. The CRGs provide their own scientific and technical support, and cover the general operating costs of these instruments. If there is demand from the user community and the resources are available, the beamtime reserved for the ILL can be made accessible to users via the subcommittees.

There are currently three different categories of CRG instruments.

- In the **CRG-A** category, external groups lease an instrument owned by the ILL. They have 50 % of the beamtime at their disposal and for the remaining 50 % they support the ILL's scientific user programme.
- In the **CRG-B** category, groups own their instrument and retain 70 % of the available beamtime, supporting the ILL programme for the other 30 %.
- Finally, in the **CRG-C** category instruments are used full time for specific research programmes by the external group, which has exclusive use of the beam.

Support laboratories

The opportunities we offer to our users extend beyond the privilege of access to the world's leading suite of neutron instruments. The ILL – in collaboration with the European Synchrotron Radiation Facility (ESRF) and other institutes – is actively responding to the needs of scientists unfamiliar with neutron techniques and in need of training and support facilities. New support facilities have been already set up on the ILL site. For more information see p.106.

ACCESS FOR INDUSTRIAL USERS

The ILL's instruments are used by a wide range of industries besides academic research, from pharmaceutical and chemical companies to materials and process engineering, energy and environment sectors. Neutron techniques are of particular interest in the industrial context as they provide unique and essential information at the atomic and molecular level.

The Business Development Office (BDO) is the single point of contact for industry looking to use the ILL's neutron scattering instruments. The Business Development Office matches the needs of industrial customers, directs them towards the best technique and scientists, and takes care of the administrative procedures. It provides industrial customers with fast, proprietary access and confidentiality under specific contract to any of the world-leading scientific instruments of the ILL. The BDO may also set up dedicated research and development partnerships for technological research with consortia including academic and industrial partners.

Contact: Jérôme Beaucour, **beaucour@ill.eu**.

USER AND BEAMTIME STATISTICS

THE ILL USER COMMUNITY

The ILL welcomed 1 386 users in 2015, including 316 from France, 245 from Germany and 257 from the UK (**figure 1**). Many of our visitors were received more than once (giving a total of 1 923 user visits).

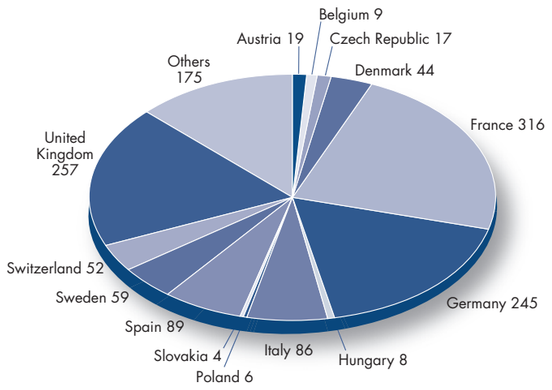

Figure 1: National affiliation of ILL laboratories users in 2015.

We value feedback from our users as an indicator of how well our facility is fulfilling their needs and to initiate action when this is not the case (**figure 2**). The *User Satisfaction Form* is a means of finding out what our users think of the facility. Users who have just finished an experiment at the ILL are asked to share their views on different topics by completing the questionnaire through the User Club. User comments are made available to managers for their information and action when appropriate. User feedback rate was about 66 % in 2015.

INSTRUMENTS

The instrumental facilities at the ILL are shown in the schematic diagram on page 98. The list of instruments as of December 2015 is summarised below. Besides the 28 ILL instruments there are nine Collaborative Research Group (CRG) instruments (marked with an asterisk *):

- powder diffractometers: D2B, D20, SALSA, D1B*
- liquids diffractometer: D4
- single-crystal diffractometers: D3, D9, D10, D23*
- large-scale structures diffractometers: D19, LADI, D16
- small-angle scattering diffractometers: D11, D22, D33
- reflectometers: D17, FIGARO, SuperADAM*
- diffuse scattering and polarisation analysis spectrometer: D7
- three-axis spectrometers: IN1-LAGRANGE, ThALES, IN8, IN20, IN12*, IN22*
- time-of-flight spectrometers: IN4, IN5, IN6, BRISP*
- backscattering and spin-echo spectrometers: IN11, IN15, IN16B, IN13*
- nuclear physics instruments: PN1, PN3
- fundamental physics instruments: PF1, PF2, S18*

IN15 has special status since it is a joint venture of the ILL with FZ Jülich. GRANIT* is not listed above because as a CRG-C instrument (p.101) it is not available as a 'user' instrument. Details of the instruments can be found on our website at **http://www.ill.eu/instruments-support/instruments-groups/**.

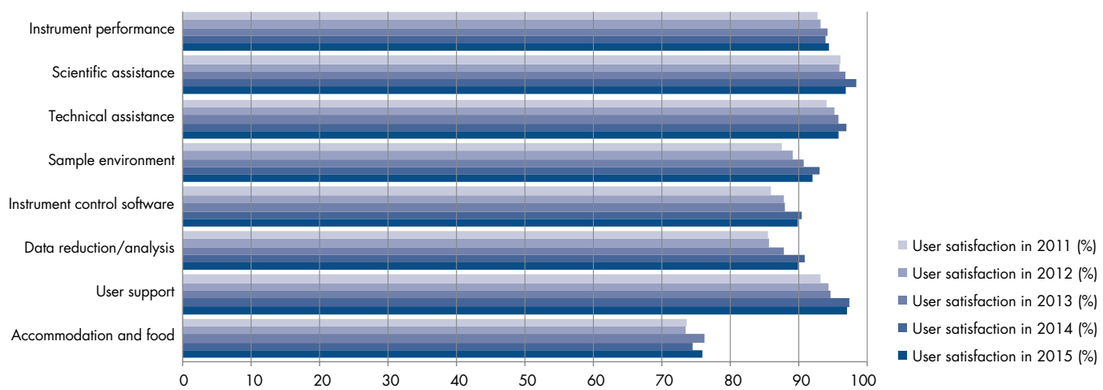

Figure 2 : User satisfaction survey results for 2015, compared with those obtained in previous years.

BEAMTIME ALLOCATION AND UTILISATION FOR 2015

During 2015 the reactor operated for 3 cycles (one split in two), representing 158 days of neutrons. The last cycle of the year lasted longer (60 days) and was operated at lower power (42 MW) (see § Reactor Operation, p.108).

Overall, the subcommittees of the Scientific Council examined 1 188 proposals requesting 7 412 days in 2015. Of these 775 proposals received beamtime, requiring the allocation of 4 184 days of beamtime on the different instruments. A total of 834 experiments were scheduled. The distribution of accepted proposals amongst the different research areas and colleges is given in **figure 3**.

In 2015, the member countries of the ILL were as follows: France, Germany, UK, Austria, Belgium, the Czech Republic, Denmark, Hungary, Italy, Poland, Slovakia, Spain, Sweden and Switzerland.

Table 1 gives the beamtime distribution amongst the different **member** countries (request and allocation in 2015). In calculating the statistics of beamtime per country, the attribution is based on the location of the laboratory of the proposers, not their individual nationality. For a proposal involving laboratories from more than one member country, the total number of days is divided amongst the collaborating countries and weighted by the number of people from each.

Figure 3: Beamtime allocation in 2015: distribution amongst the different research areas **(a)** and colleges **(b)**.

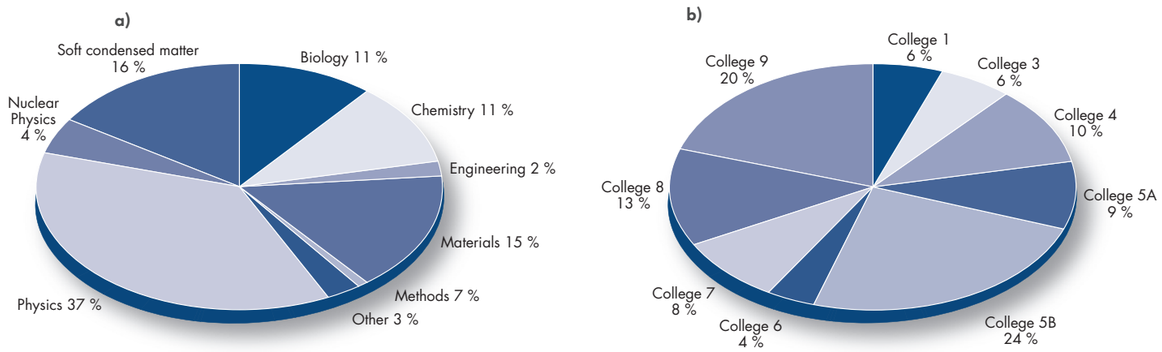

Table 1: Distribution amongst the Associate and Scientific Member countries of beamtime requested and allocated in 2015 during the subcommittees of the Scientific Council. *Proposals from purely non-member countries and from purely ILL or ESRF proposals do not appear in this table, therefore the total request and allocation is different in Table 2.*

	Request days	Request %	Allocation days	Allocation %	Allocation days	Allocation %
Member countries only			Before national balance		After national balance	
AT	211.88	2.87	187.63	4.46	159.57	3.83
BE	39.92	0.54	23.73	0.56	23.70	0.57
CH	437.96	5.93	222.63	5.30	207.83	4.99
CZ	107.84	1.46	75.90	1.81	75.87	1.82
DE	1 741.62	23.60	1 011.32	24.07	1 007.84	24.18
DK	130.71	1.77	86.58	2.06	86.54	2.08
ES	291.89	3.95	181.53	4.32	183.40	4.40
FR	1 733.56	23.49	1 016.56	24.19	1 018.79	24.45
GB	1 574.62	21.33	872.93	20.77	871.16	20.90
HU	46.70	0.63	13.23	0.31	22.95	0.55
IN	273.57	3.71	68.27	1.62	68.21	1.64
IT	358.78	4.86	205.46	4.89	205.27	4.93
PL	76.17	1.03	37.34	0.89	37.32	0.90
SE	328.25	4.45	187.68	4.47	187.48	4.50
SK	27.51	0.37	11.50	0.27	11.38	0.27
Total	**7 380.99**	**100.00**	**4 202.29**	**100.00**	**4 167.29**	**100.00**

EXPERIMENTAL AND USER PROGRAMME

USER AND BEAMTIME STATISTICS

Local contacts are not counted as proposers except when they are members of the research team. The beamtime requested by and allocated to scientists from the ILL, ESRF or EMBL is allocated to the member countries according to a weighting system based on the fractional membership of the country of the institute concerned. When a proposal involves collaboration with a non-member country, the allocated time is attributed entirely to the collaborating member country (or countries), and weighted by the number of people from each member country. Proposals in which all proposers are from non-member countries therefore do not appear in this table. This explains why the total number of allocated days differs from that in **table 2**.

A more complete view of beamtime use is given in **table 2**. Requests for and allocation of beamtime, as well as the number of scheduled experiments, refer to standard submissions to the subcommittee meetings. The effective number of days given to our users also takes into account Director's Discretion Time and CRG time for CRG instruments.

INSTRUMENT PERFORMANCE

Table 2 also gives a summary of instrument performance for 2015. For each cycle a record is kept of any time lost from the total available beamtime and the reasons for the lost time analysed, for all the instruments. The table gives a global summary for the year.

Overall 4 536 days were made available to our users in 2015 on ILL and CRG instruments, which represents about 78 % of the total days of operation. A total of 212 days were used by ILL scientists to carry out their own scientific research. About 12 % of the total beamtime available on the ILL instruments was allowed for tests, calibrations, scheduling flexibility, recuperation from minor breakdowns and student training.

Beam days given to science in 2015 amounted to 4 748 (used for users and internal research).

In 2015, 313 out of 5 784 days were lost as a result of various malfunctions, which represents about 5 % of the total available beamtime. The breakdown by reason for beamtime losses is shown in **figure 4b**.

Of the total 313 days, 158 were lost for reasons other than more classic failure. Detailed comments on the larger beamtime losses (more than 20 days) are as follows:

- PF2 lost about 50 days because of the earthquake safety measures and work at the PF2 turbine.
- On PN1, 23 days were lost because a problem – which could only be repaired during a reactor shutdown – prevented target changes during the entire cycle. An additional 15 days were lost because of a broken motor.
- GAMS lost 24 days because that target changer was out of order.

Figure 4: (a) Use of ILL beamtime **(b)** Reason for beamtime losses.

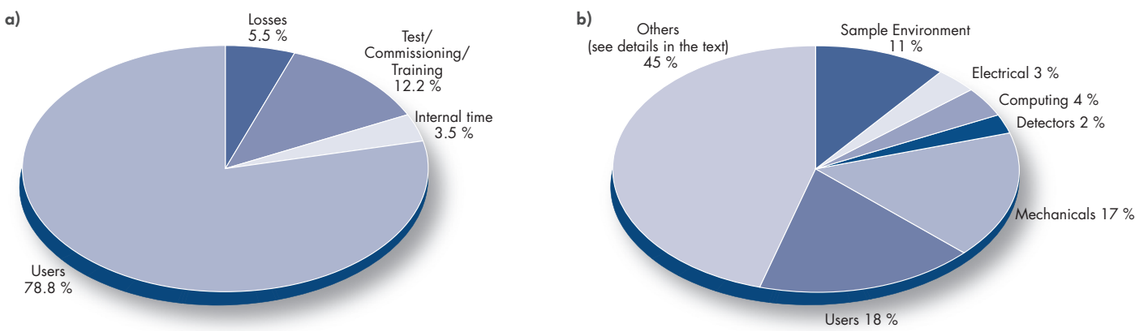

Table 2: Beamtime request/allocation (via standard subcommittees and Director Discretion Time – DDT together) by instrument and instrument performance. CRG instruments are in blue.
* 'days allocated' refers to only those days reviewed by the subcommittees (i.e. excluding CRG days and DDT) – allocation based on the originally planned 4 cyles.
**'days used' refers to the total number of days given to users (i.e. including CRG days for CRGs and DDT).
PF2 consists of different set-ups where several experiments are running simultaneously. The values given are averages for these positions.
D4 and IN1 share the same beam port and cannot be run simultaneously.

Instrument	Days requested	Days allocated*	Number of scheduled experiments	Available days	Days used for users**	Days lost	Days for commissioning /test/training	Days for internal research
BRISP	8	8	1	127	12	26	64	25
D1B	76	83	30	158	139	3	10	6
D10	298	163	24	158	152	3	3	0
D11	223	116	60	158	119	3	35	1
D16	139	92	18	158	118	4	28	8
D17	229	132	40	158	133	5	10	10
D19	190	138	20	158	127	5	20	6
D2B	239	138	60	158	146	1	4	7
D20	270	136	53	158	143	3	5	7
D22	218	86	42	158	106	4	41	7
D23	101	62	10	158	146	2	10	0
D3	129	116	15	158	138	6	12	2
D33	309	144	48	158	123	2	18	15
D4	121	60	12	77	65	2	3	7
D7	259	145	22	158	136	1	21	0
D9	194	140	17	158	139	4	13	2
FIGARO	241	154	47	158	131	4	17	6
IN1	139	58	12	81	59	1	13	8
IN11	133	100	11	158	111	18	22	7
IN12	160	29	4	158	136	2	16	4
IN13	138	71	10	158	115	3	19	21
IN15	211	41	9	158	57	4	93	4
IN16B	280	131	34	158	108	12	36	2
IN20	163	108	16	158	135	6	12	5
IN22	187	58	9	158	156	2	0	0
IN4	229	146	33	158	131	7	14	6
IN5	316	166	37	158	145	4	8	1
IN6	136	134	29	158	145	0	8	5
IN8	251	143	23	158	118	20	20	0
LADI	438	170	22	158	143	4	6	5
PF1B	255	186	7	158	142	12	4	0
PF2/5	182	185	4	158	119	23	16	0
PN1	287	159	10	158	107	40	7	4
PN3 - GAMS 6	227	146	10	158	94	59	5	0
SALSA	162	94	17	158	110	3	29	16
SUPERADAM	119	36	7	158	138	0	20	0
S18	155	54	2	158	114	11	30	3
ThALES	86	56	9	127	80	4	15	12
Total	**7 412**	**4 184**	**834**	**5 784**	**4 536**	**313**	**707**	**212**
Percentage of the total available beamtime					78.42 %	5.41 %	12.22 %	3.67 %

EXPERIMENTAL AND USER PROGRAMME

SCIENTIFIC SUPPORT LABORATORIES

PARTNERSHIP FOR SOFT CONDENSED MATTER

The Partnership for Soft Condensed Matter (PSCM) offers on-site sample preparation and characterisation facilities located in a new laboratory building that is physically connected to both ILL and ESRF experimental halls. The collaborative development of specialised sample environments and instruments enables cutting-edge experiments for the investigation of the structure and dynamics of bulk and interfacial soft matter systems.

In the year 2015 the ILL-PSCM hosted about 160 ILL users and 10 visiting scientists and students.

A number of research institutes have requested to join the initiative and we are happy to welcome the groups of K. Huber (Paderbon, Germany) and M. Gradzielski (TU-Berlin, Germany) as new collaborative partners in the year 2015.

The PSCM is located on the 2nd floor of the Science Building, along with the Soft Matter Science and Support group.

Users wishing to use the PSCM laboratories and equipment in conjunction with neutron measurements should indicate this when submitting their request for beamtime.
Further details can be found at
http://www.epn-campus.eu/pscm/.
Equipment can be booked online at
https://pscm.epn-campus.eu/.

PARTNERSHIP FOR STRUCTURAL BIOLOGY

The Partnership for Structural Biology (PSB) contains a powerful set of technology platforms that are contributed by the various partner institutes (ILL, ESRF, EMBL, IBS, and the unit for host-pathogen interactions). These platforms include advanced capabilities that strongly complement the neutron scattering facilities available to ILL users: synchrotron X-rays, electron microscopy, nuclear magnetic resonance (NMR), high-throughput methods (e.g. soluble expression and crystallisation), and a range of biophysical techniques such as isothermal calorimetry and surface plasmon resonance. The PSB inlcudes the Deuteration Laboratory (see below) as a user platform. It also includes the joint SANS/SAXS platform and there is also strong connectivity and collaboration between the ILL and ESRF life sciences/ structural biology and industry groups. The aim of the PSB is to enhance the interdisciplinary capabilities of each of the facilities co-located on the site. Further details are provided on its website **http://www.psb-grenoble.eu/**. The Carl-Ivar Brändén building (CIBB) is the principal site for the PSB and its partner organisations.

DEUTERATION LABORATORY

The ILL's Life Science Group (**http://www.ill.eu/lsg**) is located within the CIBB building and contains the Deuteration Laboratory (D-Lab) platform as well as a developing platform for large protein crystal growth (funded as part of the new SINE2020 programme). Of particular importance is the D-Lab user programme which uses *in vivo* recombinant expression approaches to provide deuterated analogues of proteins and lipids for the study of structure (crystallography, SANS, fibre diffraction) and dynamics (EINS) using neutron scattering. The platform is therefore of central importance to the activities of biological work relating to all of the ILL instrument groups. The group is involved in a wide variety of externally funded programmes that exploit the capabilities of the PSB as well as promoting interdisciplinary structural biology. It also interacts strongly with industry.

Each year the group takes a small number of undergraduate placement students that are trained in many of these techniques and contribute to method development activity.

Access to the D-Lab platform is through a rapid peer-review proposal system (**http://www.ill.eu/deuteration**). Successful applicants from ILL member state countries are provided with deuterated material without charge if the neutron experiment is carried out using ILL facilities. Other applicants are expected to contribute to the costs involved.

CHEMISTRY LABORATORIES

The Chemistry Laboratories, together with the PSCM Laboratories, are run by the Soft Matter Science and Support Group. The main facilities are based in the Science Building; in addition three smaller sample preparation labs can be found in the guide halls ILL7 and ILL22.

The laboratories offer ILL users various possibilities for sample preparation for their neutron experiments, but also support the in-house research conducted by instrument scientists and PhD students.

A variety of basic lab equipment and chemicals are available, but also equipment such as (vacuum) ovens, high temperature furnaces or a glove box can be found in the different laboratories. In order to securely handle nanomaterials in powder form, a special safety cabinet is going to be installed in co-operation with the ESRF Chemistry Laboratories. It should be operational from the beginning of 2016.

Besides the equipment for sample preparation, additional equipment for sample characterisation including light scattering, UV-Vis, FTIR or DSC is offered *via* the PSCM laboratories.

Further information on the Chemistry Laboratories can be found on **http://www.ill.eu/instruments-support/labs-facilities/chemistry-laboratories/home/**.

MATERIALS SCIENCE SUPPORT LABORATORY

The joint ILL-ESRF Materials Science Support Laboratory (MSSL) provides a range of support to our users, from advice with experiment proposals through sample preparation to the performance of the experiment. We provide equipment for tensile testing, hardness testing and microscopy as well as the fabrication of specialised sample holders. In particular, the Laboratory works with users to optimise the experimental methodology before the start of an experiment. This takes the form of standardised specimen mounting, digitisation of samples and definition of measurement macros. It is recommended that users contact us well in advance and arrive at the ILL a day or two prior to the start of an experiment to enable these off-line preparations to be performed. More information may be found on the MSSL's website **http://www.ill.eu/sites/mssl/**.

C-LAB

The Computation Lab (C-Lab) offers support to ILL users for atomistic simulations such as molecular and lattice dynamics using classical (force field) and *ab initio* (DFT) methods. Typical applications for simulations are structure, phonons and (some) magnetism in crystals, and structure and dynamics in (partially) disordered systems ranging from liquids and glasses to macro/bio-molecular systems. As samples become more complex, simulations can provide key, complementary information that will help to interpret experimental data and understand how systems behave. Scientists and thesis students at the ILL benefit from the software, hardware and expertise of the C-Lab, while users can benefit *via* their local contacts. In order to improve access to simulations for users, they are able to request simulation support for their neutron scattering experiments on the first page of the ILL proposal forms by ticking the appropriate box. Since autumn 2007, 495 proposals were submitted to the C-Lab.

Featured images © W. Burat

REACTOR OPERATION

The ILL High Flux Reactor (HFR) produces the most intense neutron flux in the world: 1.5 x 10^{15} neutrons per second per cm^2, with a thermal power of 58.3 MW. The reactor operates 50-day cycles, with each cycle of operation followed by a shutdown period during which the fuel element is changed and a number of checks are carried out. Occasional longer shutdowns allow for equipment maintenance. There are normally 4 reactor cycles per year, supplying 200 days of neutron flux for scientific use.

Following the nuclear disaster at Fukushima, Japan, the French nuclear safety authority (ASN) decided to launch additional safety assessments on all French nuclear bases (INBs), including the ILL. This additional safety review had an impact on the institute and affected its budget over the past years, and will continue to in the future. The studies performed by the reactor division teams analysed the behaviour of the ILL reactor under extreme conditions: the earthquake scenarios envisaged would have caused major damage to a town like Grenoble and would have led to the failure of all the dams on the river Drac, leaving the centre of town under 10 metres of water.

We have been putting the plans into operation since 2012. You will probably know that a major seismic reinforcement programme (the so called REFIT programme) has already been carried out at the ILL, ending in 2007. The 2011 studies demonstrated the robustness of the reactor against the maximum physically expectable earthquake, cumulated with the possibility of the loss of the 4 dams upstream on the river Drac. This implies reinforcement of elements traversing the reactor containment and the construction of a new emergency reactor control room for the crisis management teams from which all the emergency safety circuits can be controlled. The civil work of building that will house the emergency control room is already achieved. The whole work is scheduled to be carried out over 5 years (from 2012 to 2016), with no major perturbation to the ILL user programme.

The ILL High Flux Reactor (HFR) produces the most intense neutron flux in the world.

REACTOR OPERATION

Reactor operation in 2015

4 reactor cycles were completed in 2015 using 3 fuel elements. As the first cycle had to be interrupted, the remainder of the fuel element from this cycle was reloaded into the reactor for the third cycle. A total 158 days of scientific activity were provided.

Cycle n°	Start of cycle	End of cycle	Number of days of operation	Number of days scheduled	Power in MW	Number of unscheduled shutdowns
174	16.04.15	17.05.15	31.5	45	58.3	1
175	17.06.15	06.08.15	50	50	52.5	1
176	08.09.15	23.09.15	15	0	51.0	0
177	13.10.15 15.12.15	12.12.15 16.12.15	60 1.5	47	42.0 58.3	0 0
Total			**158**	**142**	**50 MW on average**	**2**

In compliance with a temporary instruction, the first cycle was interrupted when the flow rate on the heat exchanger of the shutdown and control rod cooling system fell below the minimum threshold. Authorisation to operate without this heat exchanger (by switching the cooling system to the two main heat exchangers) was obtained in time for the start of the second cycle. The 2015 reactor cycle schedule was optimised to take into account the number of fuel elements available. As a result, a final cycle of 47 days originally scheduled in 2015 was postponed until 2016. There will therefore be 3 cycles in 2016, instead of 2 cycles as originally planned.

The last cycle of the year lasted longer (60 days) and was operated at lower power (42 MW). This was the first time in the ILL's history. After the Xenon "poisoning" period of about 48 hours the reactor was then restarted and ran at nominal power for more than a day and a half; this additional time can be used in the future for internal experimental work on the instruments, and for commissioning and testing.

THE KEY REACTOR COMPONENTS (KRC) PROGRAMME

The aim of the KRC programme is to upgrade or replace some of the reactor's most important components in order to guarantee the safety and reliability of the reactor for the coming years of operation. The programme was launched in 2005 and will continue until 2017, the date of the next ten-year safety review of our installations.

The main work still to be completed under the KRC programme includes:

- the replacement of beam tubes
- the upgrade of the out-of-pile part of the horizontal cold source, including its instrumentation and control system
- the manufacture of safety rods made of hafnium; the prototype of these safety rods was delivered at the end of 2015
- the procurement of replacement cells for the cold sources.

MAIN WORK CARRIED OUT IN 2015

Maintenance operations:

- Modification of the new shutdown cooling pumps; the material which the bearings are made of was showing signs of premature wearing and therefore had to be replaced
- Implementation of in-service monitoring of nuclear pressure equipment
- Heavy maintenance of main diesels.

Work on the Key Reactor Components:

- Delivery of a prototype safety rod made of hafnium (safety rods are currently manufactured using a silver-indium-cadmium alloy)
- Replacement of beam tube H12.

Work following the post-Fukushima safety assessment:

- Digging of wells and laying of pipework for the groundwater circuit
- Implementation of the seismic depressurisation system (CDS) in passive mode at the beginning of the first cycle
- Implementation of almost all the instrumentation needed in an extreme emergency situation
- Full commissioning of the emergency reactor control room, which is designed to withstand a 7.3-magnitude earthquake along the Belledonne fault and the breach of the 4 dams on the river Drac. The use of the emergency reactor control room was validated during the emergency response exercise carried out in January 2015 to test the ILL's Internal Emergency Plan (PUI – *Plan d'Urgence Interne)*
- Installation of containment wall penetrations and cableways for the laying of cables and circuits for the "hardened safety core" components.

WORK PLANNED DURING THE LONG 2015/2016 WINTER SHUTDOWN

A very ambitious programme of work is planned for this scheduled shutdown from 17 December 2015 to 17 May 2016. It includes work on the Key Reactor Components, work required by the safety authority (ASN) in the light of the post-Fukushima safety assessment, and numerous maintenance operations. In particular, the shutdown will be used to implement in active mode the seismic depressurisation system (CDS), which is part of the "hardened safety core" and contributes to the reactor containment function, together with the GAS (seismic annular space pressurisation) system.

RADIOACTIVE WASTE AND EFFLUENTS

The ILL's activities in 2015 generated waste and effluents respecting the regulatory limits applicable to our installation, as follows:

Evacuation of radioactive waste	Quantity
Decay bins (60 l)*	0
5 m³ pre-concreted crates (low and intermediate-level waste)	0
5 m³ crates (low and intermediate-level waste)	6
200 l drums of "incinerable" waste	144
120 l HDPE drums (laboratory waste)	7
30 l cylinders (liquid)	2

**Waste stored in decay bins must be held in interim storage before opening the deep.*

Gaseous effluents	Released in 2015 (TBq)
Tritium	7.2
Noble gases	1.1
Carbon-14	0.2
Iodine	0.0000011
Aerosols	0.000000071

Liquid effluents	Released in 2015 (TBq)
Tritium	0.043
Carbon-14	0.0001
Iodine	0.00000051
Other activation products	0.000033

Part of the reactor's outer shell with the new seismic depressurisation circuit, shell penetrations, and cableways linking the reactor to the new seismically resistant electronics room.

WORKSHOPS AND EVENTS

ILL WORKSHOPS AND SCHOOLS IN 2015

16-18 FEBRUARY
Local FullProf School

2-6 MARCH
FullProf School-2015

18-22 MAY
EMBO 2015 – Workshop on small-angle neutron and X-ray scattering from proteins in solution

26-28 MAY
CCP-SAS 2015 – Atomistic Modelling for Small-Angle Scattering

6 SEPTEMBER – 3 OCTOBER
XRAY 2015 – X-ray and Neutron Science – International Student Summer Programme

14-18 SEPTEMBER
HSC18, organised with ESRF – Hercules Specialised Courses

28-30 SEPTEMBER
NDS2015 – 4th International Workshop on Neutron Delivery Systems

29 SEPTEMBER – 2 OCTOBER
MECASENS 2015, organised with ESRF – 8th International Conference on Mechanical Stress Evaluation by Neutron & Synchrotron Radiation

21-23 OCTOBER
LiQ2015 – International Workshop on Liquid-Liquid Interfaces

24-26 NOVEMBER
Characterisation of Soft Functional Materials for Industry – Training workshop for Industrial R&D Scientists and Engineers

7-8 DECEMBER
CARAC' 2015 – *La caractérisation au service de l'industrie*

14-18 DECEMBER
FullProf School-2015 2nd session

Short reports on the ILL workshops can be found on the ILL News for Reactor Users (December 2015 issue) –
http://www.ill.eu/top-links/publications/ill-news/
Workshop websites can be found at
http://www.ill.eu/news-events/past-events/

ILL CHRONICLE 2015

15 JANUARY
Visit by UK representatives of the Harwell Campus to GIANT

9 MARCH
UK Press visit

11 MARCH
STFC Directors' meeting with ILL and ESRF

21-24 APRIL
Meetings of the ILL Scientific Council and its Subcommittee meetings

29-30 APRIL
Meeting of the Subcommittee on Administrative Questions (SAQ)

12 MAY
Visit by National Academy of Sciences from USA at ILL

9 JUNE
Visit of Prof. Victor Aksenov, Director of the PNPI (Russia)

10 JUNE
Visit by Swedish Governor of Stockholm and delegation to EPN Campus

23 TO 25 JUNE
Associates' meeting, Scientific Partners' Meeting and Steering Committee meeting in Dusseldorf and Vals (NL)

28 AUGUST
Delegation from Pernambuco, Brazil to GIANT campus

30 AUGUST – 4 SEPTEMBER
ECNS 2015 Zaragoza

8 SEPTEMBER
Visit by Philippe Baptiste, Gabriel Chardin and Alain Schuhl (CNRS)

13-14 OCTOBER
Meeting of the Subcommittee on Administrative Questions (SAQ)

5 NOVEMBER
Visit by Prof. Marquardt, Chairman of the Board of Directors (FZJ)

19-20 NOVEMBER
Meetings of the ILL Scientific Council

2-3 DECEMBER
Meeting of the Steering Committee

10 DECEMBER
ASN visit (the French Nuclear Safety authority)

A YEAR IN PHOTOS

Visits and events

1

2

3

4

5

1. Prof. W.G. Stirling (Director of the ILL) and Prof. V.L. Aksenov (Director of the PNPI, Russia) sign a MoU to strengthen the mutual technical and scientific cooperation. (On the back, from left: M. Walter, C. Simon and M. Rodriguez-Castellano).
2. Hannu Mutka (ILL) giving a tour of the experimental hall during the visit of Governor of Stockholm, Mrs Chris Heister, and a Swedish delegation.
3. Participants to the 2015 edition of HERCULES school (Higher European Research Course for Users of Large Experimental Systems) which celebrated its 25th anniversary this year.
4. Visit from a group of Swedish students that won a competition to increase the number of girls studying scientific subjects after high school.
5. EPN campus staff gather to pay homage to Paris terrorist attack victims of 13th November.

Science Festival

1

2

3

4

5

1–4. The staff welcomed the Grenoble public to the EPN campus common stand during the French science festival week on 9 and 10 October.

5. Françoise Vauquois (ILL Communication Unit) awarding the first prize to the QUIZ winner, Theano Wilhem.

WORKSHOPS AND EVENTS

A YEAR IN PHOTOS

Happy users

1

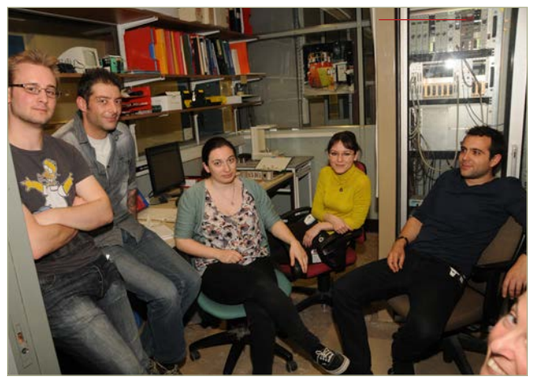

2

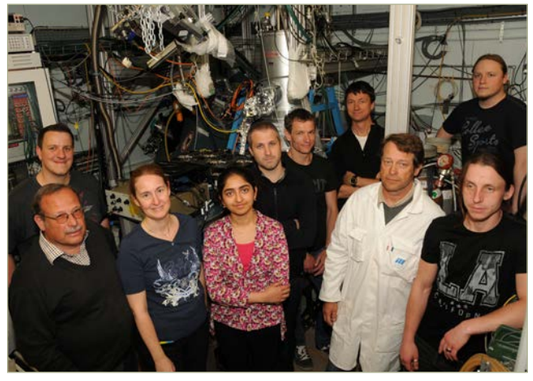

3

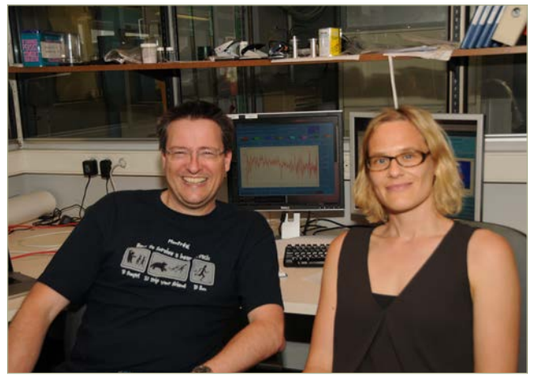

4

5

1. From left: Mathieu Morin (CNRS Grenoble), Rosanna Ignazzi (Niels Bohr Institut, Copenhagen), Irina Piazza (ILL), Nicolas Martinez (UJF Grenoble), Gaëtan Inidjel and Francesca Natali (ILL), during their experiment on IN13.
2. First campaign with a set up of calorimetric low temperature detectors at LOHENGRIN. From left: Pascal Scholz (Giessen University, back), Peter Egelhof (GSI Darmstadt and Mainz University, front), Saskia Kraft-Bermuth (Giessen University), Santwana Dubey (Helmholtz Graduate School Frankfurt), Aurélien Blanc (ILL), Artur Echler (Giessen University), Ulli Köster (ILL), Norbert Laurens (ILL), Patrick Grabitz (GSI, front) and Stefan Stolte (Mainz University, back).
3. Paul Henry and Pascal Deen from the European Spallation Source (ESS Lund).
4. Isabelle Mirebeau from the LLB Saclay.
5. Norman Kretzschmar, Michael Wulff, and Martin Nors Pedersen, ESRF.

6

7

8

9

10

6. From left: William Stirling (ILL Director) searching for anisotropic thermal conductivity in UO_2 with Jean-Christophe Griveau (ITU Karlsruhe), Frédéric Bourdarot (CEA Grenoble), Roberto Caciuffo (ITU Karlsruhe) and Louis-Pierre Regnault (ILL).
7. From left: Yoann Calzavara (ILL), Meriem Alaoui, Pr. Gilles Despaux, Ghita Zaz (Université Montpellier) and Pierre Jimenez (ILL), measuring possible irradiaton effects on fuel plates within the PERSEUS project.
8. From Left: Jacques Bossy (CNRS/Inst. Néel), Bachir Ouladdiaf (ILL), Jean-Claude Marmeggi (CNRS/UJF), Alain Filhol (ILL) and Pierre Bastie (UJF).
9. From left: Pascal Scholz (Giessen University), Santwana Dubey (Helmholtz Graduate School Frankfurt), Artur Echler (Giessen University) and Patrick Grabitz (Mainz University).
10. Many thanks to Serge Claisse for all the hours spent in the guide hall taking nice pictures of our happy users!

FACTS AND FIGURES

STAFF ON 31/12/2015

464.5 people including 65 experimentalists in the scientific sector and 35 thesis students.

329 French, 43.5 German, 40.5 British, 40 scientific participating countries and 11.5 others.

Country		%
French	329.0	70.83 %
German	43.5	9.36 %
British	40.5	8.72 %
Member countries	40.0	8.61 %
Others	11.5	2.48 %
Total	**464.5**	**100 %**

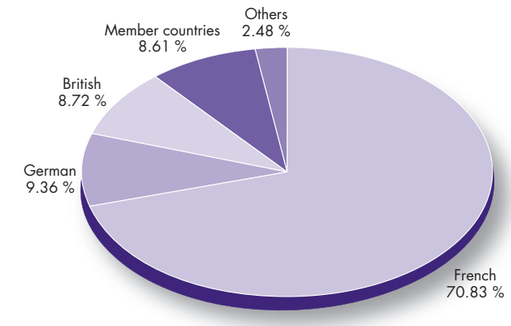

REVISED BUDGET 2015: 81.180 M€ (excluding taxes)

Income	M€	%
Income from Associates (incl. Fukushima & Millennium Progamme & add. nuclear tax)	62.618	77.13 %
Income from Scientific members	19.383	23.88 %
Own income	3.064	3.77 %
Carry forward from 2014	4.584	5.65 %
Reserve	-7.238	-8.92 %
Cashflow	-1.231	-1.52 %
Total	**81.180**	**100.00 %**

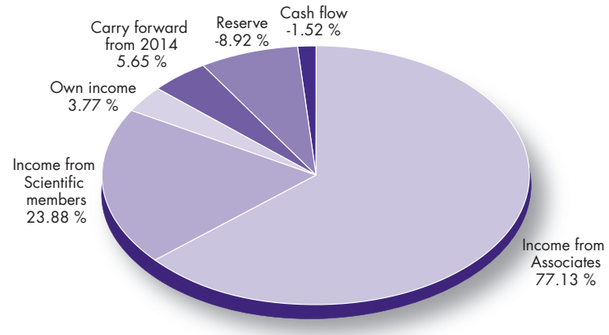

Expenditure	M€	%
Staff costs	45.650	56.23 %
Operating costs	16.242	20.01 %
Investment costs	13.369	16.47 %
Fuel cycle	5.919	7.29 %
Total	**81.180**	**100.00 %**

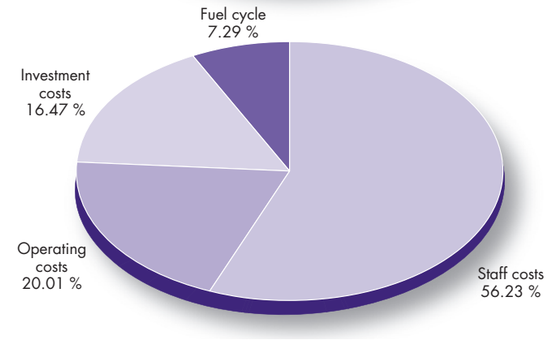

PURCHASING STATISTICS (Figures 2015 to end of November 2015)

	M€	%
France	12.197	69.10 %
Germany	3.182	18.03 %
United Kingdom	0.681	3.85 %
Scientific members	0.731	4.14 %
Others	0.861	4.88 %
Total	**17.652**	**100.00 %**

France captif market	7.558	
Total captif/non captif	**25.210**	

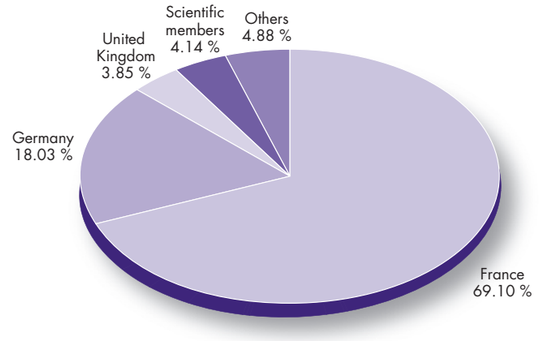

FACTS AND FIGURES

FACTS AND FIGURES

NAME

Institut Max von Laue-Paul Langevin (ILL).

FOUNDED

17 January 1967.

Intergovernmental Convention between France, Germany and United Kingdom (19/07/1974).

ASSOCIATES

France

Commissariat à l'Energie Atomique et aux Energies Alternatives (CEA).

Centre National de la Recherche Scientifique (CNRS).

Germany

Forschungszentrum Jülich (FZJ).

United Kingdom

Science & Technology Facilities Council (STFC).

COUNTRIES WITH SCIENTIFIC MEMBERSHIP

Spain

MINECO Ministerio de Economia y Competitividad.

Switzerland

Staatssekretariat für Bildung, Forschung und Innovation (SBFI).

Italy

Consiglio Nazionale delle Ricerche (CNR).

CENI (Central European Neutron Initiative)

Consortium composed of:

- Austria: Österreichische Akademie der Wissenschaften.
- Czech Republic: Charles University of Prague.
- Hungary: Research Institute for Solid State Physics and Optics (RISP) / Budapest on behalf of the Hungarian Academy of Sciences (MTA).
- Slovakia: Comenius University Bratislava.

TRANSNI

(Belgian-Danish-Swedish Transnational Neutron Initiative Consortium)

- Belgium: Belgian Federal Science Policy Office (BELSPOL).
- Sweden: Swedish Research Council (VR).
- Denmark: Danish Agency for Science, Technology and Innovation (DASTI).
- Poland: ILLPL Consortium of Polish Scientific and Research Institutions (first half of 2015).

SUPERVISORY AND ADVISORY BODIES

- Steering Committee, which meets twice a year.
- Subcommittee on Administrative Questions, which meets twice a year.
- Audit Commission, which meets once a year, and statutory auditor.
- Scientific Council with 9 Subcommittees, which meets twice a year.

REACTOR

Operating 3 cycles in 2015 (one split in two).
158 days in total, average power 50 MW (p.110).

EXPERIMENTAL PROGRAMME

- 834 experiments (allocated by Subcommittees) on 28 ILL-funded and 9 CRG instruments.
- 1 386 visitors from 43 countries.

Publications in 2015

In 2015, the ILL received notice of 556 publications by ILL staff and users.

They are listed on the ILL website:
www.ill.eu/science-technology/scientific-publications/list-of-publications/

THE DISTRIBUTION BY SUBJECT IS AS FOLLOWS

Applied Physics, Instrumentation and Techniques	36
Biology	53
Crystallography	79
Liquids and Glasses	34
Magnetic Excitations	45
Magnetic Structures	73
Materials Science and Engineering	50
Nuclear and Particle Physics	46
Theory	14
Soft Matter	88
Spectroscopy in Solid State Physics and Chemistry	29
Other	5

ILL PHD STUDENTSHIPS

PhD students at ILL in 2015*	44
PhD theses completed in 2015*	15
PhD theses completed in 2015**	5

* *Receiving a grant from ILL.*
** *Receiving an external grant.*

ORGANISATION CHART IN 2015

REVIEW PANELS

(Chairs)

APPLIED METALLURGY, INSTRUMENTATION AND TECHNIQUES
D.J. Hughes (WMG, Warwick University, UK)

NUCLEAR AND PARTICLE PHYSICS
W. Heil (University of Mainz, Germany)

MAGNETIC EXCITATIONS
T.G. Perring (ISIS, UK)

CRYSTALLOGRAPHY
C. Masquelier (CNRS Amiens, France)

MAGNETISM
F. Damay (CEA Saclay, France)

STRUCTURE AND DYNAMICS OF LIQUIDS AND GLASSES
N. Clarke (Sheffield University, UK)

SPECTROSCOPY IN SOLID STATE PHYSICS AND CHEMISTRY
D. Djurado (CEA Grenoble, France)

STRUCTURE AND DYNAMICS OF BIOLOGICAL SYSTEMS
A.D. Podjarny (University of Strasbourg, France)

STRUCTURE AND DYNAMICS OF SOFT CONDENSED MATTER
O. Sandre (CNRS Pessac, France)

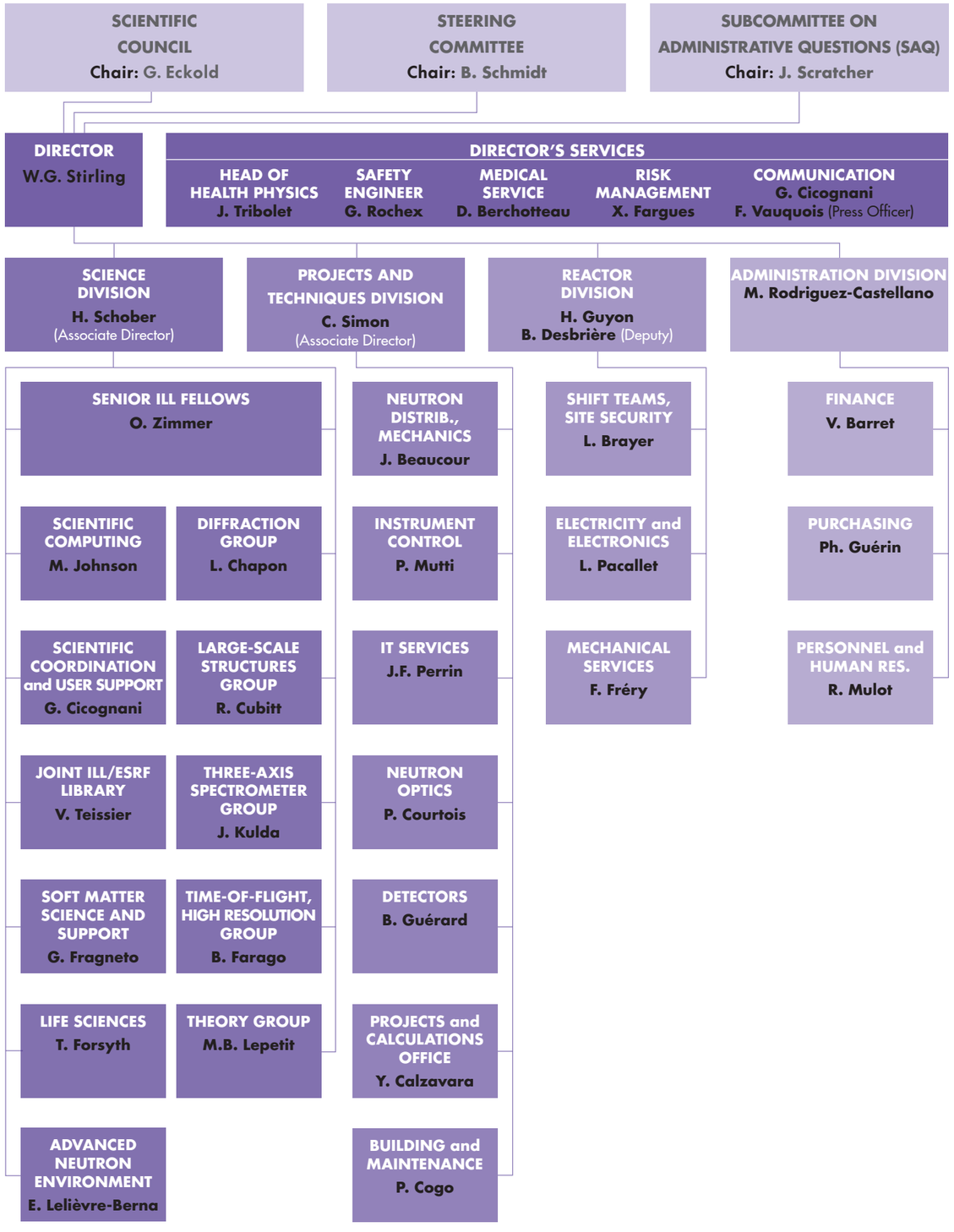

71, avenue des Martyrs
38000 Grenoble
France
www.ill.eu

This report has been printed using FSC certified paper **www.fsc.org**